ENGAGEMENT OF MAP KINASE AND mTOR SIGNALING BY THE TSC-2 TUMOR SUPPRESSOR IN RENAL CANCER

By

Jennifer Diane Cohen

A Dissertation Submitted to the Faculty of the

DEPARTMENT OF PHARMACEUTICAL SCIENCES

In Partial Fulfillment of the Requirements
For the Degree of

DOCTOR OF PHILOSOPHY

WITH A MAJOR IN PHARMACOLOGY & TOXICOLOGY

In the Graduate College

THE UNIVERSITY OF ARIZONA

2009

THE UNIVERSITY OF ARIZONA
GRADUATE COLLEGE

As members of the Dissertation Committee, we certify that we have read the dissertation prepared by Jennifer Diane Cohen

entitled "ENGAGEMENT OF MAP KINASE AND mTOR SIGNALING BY THE TSC-2 TUMOR SUPPRESSOR IN RENAL CANCER"

and recommend that it be accepted as fulfilling the dissertation requirement for the Degree of Doctor of Philosophy

_____ Date: 11/06/09
Dr. Serrine S Lau

_____ Date: 11/06/09
Dr. Terrence Monks

_____ Date: 11/06/09
Dr. Timothy Bowden

_____ Date: 11/06/09
Dr. Richard Vaillancourt

_____ Date: 11/06/09
Dr. Georg Wondrak

Final approval and acceptance of this dissertation is contingent upon the candidate's submission of the final copies of the dissertation to the Graduate College.

I hereby certify that I have read this dissertation prepared under my direction and recommend that it be accepted as fulfilling the dissertation requirement.

_____ Date: 11/06/09
Dissertation Director: (Dr. Serrine S Lau)

STATEMENT BY AUTHOR

This dissertation has been submitted in partial fulfillment of requirements for an advanced degree at the University of Arizona and is deposited in the University Library to be made available to borrowers under rules of the Library.

SIGNED: Jennifer Diane Cohen

ACKNOWLEDGEMENT

I would first like to thank my advisor, Dr. Serrine Lau, for her support, guidance, and patience throughout my graduate career. She pushed me to my limits, which was instrumental in my growth both as a scientist and as an individual. I am thankful to have had her as my mentor, and it has been a great opportunity for me to conduct my graduate studies under her supervision.

I would also like to thank my dissertation committee members, Dr. Terrence Monks, Dr. Timothy Bowden, Dr. Richard Vaillancourt, and Dr. Georg Wondrak, for their continuous advice, and guidance. Thank you for challenging me to think more critically about my data and the scope of my project. Also, I would like to thank Dr. Nagle for his collaboration, inspiring the direction of my project, and for making his lab available to me. I would like to thank the staff and faculty of the Department of Pharmacology and Toxicology at The University of Arizona for their advice and assistance over the years.

I am grateful to all the members of the Lau and Monks laboratories for their friendship, support, guidance, and motivational words; especially Matt and Ashley. I am also thankful for the many scientific collaborations within the group that helped me progress as a scientist. In addition, thank you to Doug Cromey for his time and assistance on the confocal microscope.

Lastly, I would like to thank my parents, brothers, sister, and friends for their love and faith in me. I am truly grateful for your unwavering support, pushing me to follow my dreams, and encouragement through the difficult times.

TABLE OF CONTENTS

TABLE OF CONTENTS -- CONTINUED

TABLE OF CONTENTS -- CONTINUED

TABLE OF CONTENTS -- CONTINUED

LIST OF FIGURES

LIST OF FIGURES -- CONTINUED

LIST OF FIGURES -- CONTINUED

LIST OF ABBREVIATIONS

AMPK	AMP-activated protein kinase
cAMP	cyclic adenosine monophosphate
CDK	Cyclin dependent kinase
CKI	Cyclin dependent kinase inhibitor
ERK	extracellular-signal-regulated kinase
GAP	GTPase-activating protein
GSK3β	glycogen synthase kinase 3 β
γ-GT	γ-glutamyl transpeptidase
GSH	glutathione
GST	glutathione-S-transferase
HEK293	human embryonic kidney cells
HIFα	Hypoxia-inducible Factor α subunits
HQ	Hydroquinone
IKK β	inhibitory κB kinase β
IP	immunoprecipitation
IARC	International Agency for Research on Cancer
LOH	loss of heterozygosity
mTOR	mammalian target of rapamycin
mTORC1	mammalian target of rapamycin complex 1
mTORC2	mammalian target of rapamycin complex 2
MAPK	mitogen-activated protein kinase
MEF	mouse embryonic fibroblasts

OSOM	outer stripe of the outer medulla
PBS	phosphate-buffered saline
QTRRE	quinol-thioether rat renal epithelial cells
RCC	renal cell carcinoma
RSK	p90 ribosomal protein S6 kinase
ROS	reactive oxygen species
RTK	receptor tyrosine kinase
SCF^{SKP2}	Skp-Cullin-F-box
TGF-α	transforming growth factor alpha
TGHQ	2,3,5-*tris*-(glutathion-S-yl)hydroquinone
TCL	total cell lysate
Tsc-2	tuberous sclerosis-2
TSC	tuberous sclerosis complex
4EBP1	eukaryotic translation initiation factor 4E binding protein 1
eIF4E	eukaryotic translation initiation factor 4E
VEGF	vascular endothelial growth factor
VHL	von Hoppel-Lindau disease

ABSTRACT

The tuberous sclerosis-2 (*Tsc-2*) gene functions as a renal tumor suppressor, and loss of heterozygosity (LOH) at the *Tsc-2* locus has been noted in tumors of both tuberous sclerosis and sporadic patients. In both rats and mice, *Tsc-2* is a major target for spontaneous renal cell carcinoma (RCC); but only in rats *Tsc-2* is a target for chemically induced RCC as well. Treatment of Eker (*Tsc-2*$^{EK/+}$) rats with 2,3,5-*tris*-(glutathion-S-yl) hydroquinone (TGHQ) results in loss of the wild-type allele of *Tsc-2* in renal preneoplastic lesions and tumors. Furthermore, TGHQ transformation of primary renal epithelial cells derived from *Tsc-2*$^{EK/+}$ rats (QTRRE cells) also results in LOH at the *Tsc-2* allele, and cells are tuberin null. Additionally, subcutaneous injection of QTRRE cells in athymic nude mice promotes tumor formation. Mechanistic studies in these three RCC models have been carried out to determine how the tumor suppressor tuberin negatively regulates the Raf/MEK/ERK MAPK cascade. Analysis of kidney tumors formed in *Tsc-2*$^{EK/+}$ rats following 8-months of TGHQ treatment reveals increases in B-Raf, Raf-1, pERK, cyclin D1, p27^{Kip1}, 4EBP1, p-4EBP1(Thr70), p-4EBP1(Ser65), and p-4EBP1(Thr37/46) protein expression. These data establish the involvement of mTOR and MAPK signaling cascades in tuberin null tumors. Similar increases in 4EBP1 and p4EBP1 are observed in renal tumor xenografts derived from subcutaneous injection of QTRRE cells in nude mice. Concomitant with increases in expression of these proteins in TGHQ-induced renal tumors, similar changes are observed in QTRRE cells, which also exhibit high ERK, B-Raf and Raf-1 kinase activity; and increased expression of cyclin D1, p27, p-4EBP1 (Thr70), p-4EBP1 (Ser65), and p-4EBP1 (Thr37/46). Manipulation of the Raf/MEK/ERK kinase cascade in QTRRE cells, with kinase

inhibitors and siRNA, indicates that Raf-1/MEK/ERK participates in crosstalk with 4EBP1 to regulate translation of cyclin D1.

Cyclin D1 and p27 protein levels are increased in the cytoplasm of all three RCC models. In normal human proximal tubule cells (HK-2), p27 and cyclin D1 are localized to the nucleus. Due to the instability of the cyclin D1-CDK4 complex, p27 interaction is necessary for complex assembly and stabilization. Therefore, the cyclin dependent kinase inhibitor p27 has been the focus of our studies, in an effort to determine the mechanism for cytoplasmic mislocalization and stabilization of cyclin D1. Manipulation of p27 protein levels in QTRRE cells with phosphodiesterase inhibitors, dibutyryl cAMP, and the proteosome inhibitor MG132, all result in a parallel increase in p27 and cyclin D1. Furthermore, p27 siRNA and sorafenib treatment both cause a decrease in p27 and cyclin D1. Further manipulation of cAMP, Rap1B, and B-Raf proteins, revealed that cAMP/PKA/Rap1B/B-Raf activation and B-Raf//ERK MAPK inhibition both modulate p27 expression and compartmental localization in tuberous sclerosis renal cancer. Phosphodiesterase inhibitors play a role in regulating the expression, degradation, and cytoplasmic localization of p27. Therefore, cytoplasmic p27-cyclin D1 mislocalization and stabilization may have an oncogenic role in the cytosol and play a crucial role in tumor formation.

CHAPTER 1: INTRODUCTION

1.1. General Comments

Cancer is the second leading cause of death in the United States, and over 1.2 million Americans are diagnosed with cancer annually. Cancer is the uncontrolled proliferation of cells leading to tumor formation and invasion of surrounding tissues, resulting from a combination of genetic and environmental factors. These factors initiate mutations in tumor suppressor genes or activation of oncogenes, which results in disregulation of signaling cascades, uncontrolled growth, and eventual tumor formation. This work investigates how genetic predisposition and chemical exposure affect signaling of the tumor suppressor gene tuberous sclerosis 2 (*Tsc-2)* during renal tumor formation in the Eker ($Tsc\text{-}2^{EK/+}$) rat. In the rat, *Tsc-2* is the primary genetic target for both spontaneous and carcinogen-induced mutations

Hydroquinon (HQ) is found ubiquitously in the environment and is commonly utilized in the chemical industry. The hydroquinone glutathione (GSH) conjugate, 2,3,5-*tris*-(glutathion-S-yl) HQ (TGHQ), is metabolized by enzymes in the brush border membrane of proximal tubules located within the outer stripe of the outer medulla (OSOM) of the kidney. The resultant HQ-cysteine conjugates are recognized by amino acid transporters in the OSOM and transported into proximal tubule cells. In renal epithelial cells, these conjugates redox cycle, adduct macromolecules, and form reactive oxygen species (ROS). This produces a selective nephrotoxicity and nephrocarcinogenicity in the OSOM of rats. Treatment of $Tsc\text{-}2^{EK/+}$ rats with TGHQ results in loss of the wild-type allele of *Tsc-2* in renal preneoplastic lesions and tumors. TGHQ transformation of primary renal epithelial cells derived from $Tsc\text{-}2^{EK/+}$ rats

(QTRRE cells) also results in LOH at the *Tsc-2* allele, and cells are tuberin null. Additionally, subcutaneous injection of QTRRE cells in athymic nude mice promotes tumor formation. Mechanistic studies utilizing these three models of renal carcinogenesis will permit a better understanding of how the tumor suppressor tuberin modulates the mTOR and MAPK signaling cascades. Elucidation of intricate networks of protein signaling cascades perturbed during tumor formation may be relevant in numerous disease states and tissue types.

1.2. Kidney Physiology

The kidney is comprised of three distinct sections: the cortex, medulla, and papilla; which each play a vital role in total body homeostasis. The utility of the kidney is dependent on blood flow through each distinct section of the kidney, which is considerably disproportionate, with the cortex receiving approximately 90%, medulla 8%, and papilla 2% . Functionally, the kidney is involved in the excretion of metabolic wastes, the regulation of extracellular fluid volume, electrolyte composition, acid-base balance, and synthesis and release of hormones (Klaassen 2001). The functional unit of the kidney that carries out these tasks is the nephron, which is comprised of a vascular element, a tubular element and the glomerulus. The rat kidney contains approximately 35,000 nephrons, compared to the human kidney that consists of around 1 million nephrons (Seldin 1985).

The afferent arterioles are innervated by the sympathetic nervous system to supply blood to the glomerulus. The glomerulus is comprised of an intertwined group of capillaries that filters nutrients, wastes, electrolytes, water, and small molecules. The

glomerular capillary wall provides a barrier to the passage of macromoleules, as well as restricted filtration of anionic molecules (Klaassen 2001). Blood leaves the glomerular capillaries via the efferent arteriole, allowing for passage of the ultrafiltrate to the tubular element.

The tubular element consists of the proximal tubule, loop of Henle, and distal tubule. The proximal tubule is separated into segments S1, S2, and S3. The S1 (pars convoluta) segment is the initial portion of the proximal convoluted tubule, and is distinguished by its tall brush border, highly-developed vacuolar lysosomes, interdigitated basolateral membrane, and densely packed mitochondria (Klaassen 2001). The high concentration of mitochondria drives the reabsorption of Na^+ through the epithelial N^+ transporters. Cells within the S2 segment possess a shorter brush border, fewer mitochondria, and less basolateral interdigitation than cells in the S1 segment (Klaassen 2001). The distal portion of the proximal tubule constitutes the S3 segment and extends into the outer stripe of the outer medulla (OSOM). These cells have a highly developed brush border, fewer lysosomes and mitochondria than S1 or S2 segments, and contain the highest concentrations of gamma-glutamyltranspeptidase and dipeptidase. Following filtrate passage through the proximal tubule, water is then reabsorbed in the loop of Henle. The distal tubule, the final component of the tubular element, further reabsorbs any remaining ions and water to concentrate the urine.

Of all the tubular elements, the proximal tubule is the workhorse of the nephron. It reabsorbs about 60-80% of solute and water filtered by the glomerulus. It is also responsible for the reabsorption of K^+, HCO_3^-, Cl^-, PO_4^{3-}, Ca^{2+}, and Mg^{2+}; as well as numerous transport systems that reabsorb amino acids, glucose and citric acid cycle

intermediates (Klaassen 2001). Therefore, injury to the proximal tubule will severely disturb the water and solute balance, as well as critically impair whole-kidney function. Furthermore, the proximal tubule is most affected by toxicant-mediated injury, due to its high metabolic capacity, high concentration of transporters, and its ability to concentrate xenobiotics. GSH-conjugated xenobiotics or metabolites are transported to the kidney for detoxication and excretion. Systemic GSH-conjugates are transported to the kidney in high concentrations. Due to the high concentration gamma-glutamyltranspeptidase in the S3 segment of proximal tubule, this segment has the highest apical transport of GSH. The selective transport and accumulation of GSH-conjugates in the proximal tubule causes cytotoxicity, acute renal failure, and possible nephrocarcinogenicity.

1.3. Renal Carcinogenesis

The American Cancer Society estimates that there will be about 54,000 new cases of kidney cancer in the United States in the year 2009, and about 13,000 people will die from the disease. Renal cell carcinoma (RCC) accounts for 80-85% of all malignant kidney tumors. RCC occurs at nearly twice the frequency in men than in women (Jemal et al. 2004). Additionally, studies show that women have a less severe prognosis, as well as higher survival rates after RCC recurrence than men (Onishi et al. 2002). The decreased severity of RCC in women has been linked to specific protective factors, such as oral contraceptive use and moderate alcohol consumption (Dhote et al. 2004). The main risk factors for RCC are tobacco consumption and severe obesity (Dhote et al. 2004). Renal carcinomas lack early warning signs, which results in a higher proportion of patients with metastases at the time of diagnosis (Schoffski et al. 2006). Since RCC is

highly resistant to chemotherapy or radiation, surgical resection is often used as a first line therapy.

Renal cell tumors display a variety of different cytomorphological characteristics and cellular origins. Histological classification of epithelial renal tumors include clear cell (~75% of all kidney cancer), types I and II papillary (~15%), chromophobe (~5%) and oncocytoma (~5%) (Linehan et al. 2003). Several congenital diseases, such as von Hoppel-Lindau disease (*VHL*), autosomal dominant polycystic kidney disease, and tuberous sclerosis (*TSC*) are associated with the development of RCC. Mutations in the *VHL* tumor suppressor gene occur in approximately 80% of all clear cell tumors, and the most common site for mutation is a chromosome 3p deletion (Gnarra et al. 1996). Loss of heterozygosity on the *VHL* gene locus is an early event in human RCC, and its tumorigenic inactivation is strictly associated with the kidney (Walker 1998). *VHL*s protein product is an E3 ubiquitin ligase for Hypoxia-inducible Factor α subunits (HIFα), which is crucial for the maintenance of oxygen homeostasis (Maxwell et al. 2001). pVHL has a variety of functions in the kidney: it regulates cell cycle arrest through stabilization of $p27^{Kip1}$ (Pause et al. 1998), and negatively regulates the expression of vascular endothelial growth factor (VEGF) thus inhibiting angiogenesis (Siemeister et al. 1996).

The *VHL* tumor suppressor gene is a primary target for mutations in human RCC (Gnarra et al. 1994; Shuin et al. 1994) but has not been found to contribute to rodent renal tumorigenesis (Kikuchi et al. 1995; Walker et al. 1996). *VHL* knockout mice do not develop spontaneous RCC (Gnarra et al. 1997; Haase et al. 2001), and in addition, *VHL* mutations in rat RCC are very uncommon (Shiao et al. 1997). Loss of heterozygosity

(LOH) at the *Tsc-2* locus has been demonstrated in renal tumors in humans (Yu et al. 1986; Wagner et al. 1996), and in the development of spontaneous RCC in both rats and mice (Yeung et al. 1994; Kobayashi et al. 1995; Kobayashi et al. 1999; Onda et al. 1999). Therefore, *Tsc-2* is the primary target for RCC in rodents. The Eker rat (*Tsc-2*$^{EK/+}$) carries a single autosomal mutation that predisposes them to the development of spontaneous renal cell tumors at a very high incidence. A germline insertion of an endogenous retrovirus in the Tsc-2 gene, on rat chromosome 10q (syntenic with human chromosome 16p) is responsible for the predisposing "Eker" mutation (Eker et al. 1981) Spontaneous or chemically induced tumors in the Eker rat express wild-type *VHL* (Walker et al. 1996). But the majority of renal cell tumors observed in the Eker rat originate from the renal proximal tubules and are histologically similar to renal tumors in humans (Everitt et al. 1992; Walker 1998). Furthermore, the *Tsc-2* gene shares a number of common downstream effectors with the VHL gene in renal tumor development; such as p27 (Soucek et al. 1997); VEGF (Brugarolas et al. 2003; Rebuzzi et al. 2007), and HIFα (Brugarolas et al. 2003; Liu et al. 2003) . These data suggest that the Tsc-2$^{EK/+}$ rat exhibits many similarities to the human counterpart, and therefore, is an excellent animal model with which to study mechanisms of chemical-induced renal carcinogenesis.

1.4. Hydroquinone Metabolism and Nephrocarcinogenicity

Hydroquinone (HQ; 1,4-benzenediol; $C_6H_4(OH)_2$; CAS Registry Number: 123-31-9), the reduced form of 1,4-benzoquinone, is the simplest quinone. It is found ubiquitously in nature, and is commonly utilized in the chemical industry. In 1994 the annual production of HQ was over 35,000 tons (Westerhof et al. 2005). Industrially, HQ has been used as an antioxidant in food preservation, a polymerization inhibitor in the rubber industry, a depigmenting agent in cosmetics and skin-care products, a developer in photography, and a component of non-filtered cigarette smoke (Monks et al. 1992; Pryor 1997). In produce and products for consumption, HQ is a natural component of coffee beans, wheat-based products, tea leaves, as well as specific fruits and vegetables (Deisinger et al. 1996; DeCaprio 1999).

1.4.1. Absorption, Distribution, Metabolism, and Excretion of HQ

The rate of HQ absorption is highly dependent on a number of factors; including, the route of exposure, concentration, and duration of exposure. Oral ingestion of radiolabeled HQ by rats was readily absorbed into most tissues, with the highest amount of accumulation in the liver and kidney (Divincenzo et al. 1984). Similarly, intraperitoneal injection of ^{14}C-HQ in mice resulted in accumulation in the liver and kidney, as well as increased levels in the blood and bone marrow (Subrahmanyam et al. 1990). Whereas intravenous injection of HQ resulted in concentration in the bone marrow, thymus, and spleen (Greenlee et al. 1981). HQ is also rapidly absorbed via inhalation; in contrast to the least rapid route being dermal absorption/permeability (Bucks et al. 1988).

Following absorption, HQ is metabolized in the liver by phase II metabolic enzymes to hydrophilic conjugates, such as HQ-monoglucuronide and HQ-monosulfate, which are rapidly excreted via the urine (English 1988). Another minor product excreted through the urine is *N*-acetyl-[*L*-cystein-*S*-yl]-HQ (English 1988). HQ can also be oxidized by cytochrome P450 (1A1, 2E1, and 3A4) (Hill et al. 1993), prostaglandin H synthase (Lau et al. 1987), or myeloperoxidase (Subrahmanyam et al. 1990) enzymes to 1,4-benzoquinone; which can chemically react with GSH to form 2-(glutathion-S-yl)HQ and a multitude of substituted GSH adducts (Lau et al. 1988; Monks et al. 1992). **Figure 1.1** illustrates the proposed pathway for HQ metabolism. Increasing addition of GSH conjugates leads to the formation of TGHQ, which is the most potent nephrotoxic adduct (Lau et al. 1988). The formation of the quinone-thioether adduct results in targeting to the kidney, where its further bioactivated to mediate its nephrotoxicity.

GSH is comprised of γ-glutamyl-L-cysteinylglycine, which plays an important role in the detoxication of xenobiotics by reacting with electrophiles to form thioethers (Dekant 1996). GSH conjugates are targeted to the kidney via the bloodstream for clearance. However, GSH-HQ transportation to the kidney results in further bioactivation within the brush border of proximal tubule epithelial cells in the S3 segment of the OSOM (Monks et al. 1992). Proximal tubule cells within the OSOM have increased levels of γ-glutamyl transpeptidase (γ-GT) and cysteinylglycine dipeptidase metabolic enzymes. These enzymes cleave the γ-glutamate and glycine moieties respectively, forming highly reactive HQ-cysteine conjugates. The HQ-cysteine conjugates are recognized by the L-amino acid transporter in the proximal tubule brush border, allowing for rapid reuptake (Monks et al. 1997; Monks et al. 1998). To complete

the formation of mercapturic acid synthesis, cysteine-thioether N-acetyltransferases catalyzes the transfer of an acetyl group to the cystein-S-yl-HQ conjugates (Duffel et al. 1982). The resultant mercapturic acids can be excreted into the urine. Alternatively, the HQ-cysteine conjugates are capable of redox cycling, resulting in the formation of ROS, as well as conjugate adduction to macromolecules (Whysner et al. 1995). Therefore, the GSH conjugates enhance the biological reactivity of HQ to produce a selective nephrotoxicity in the OSOM of rats.

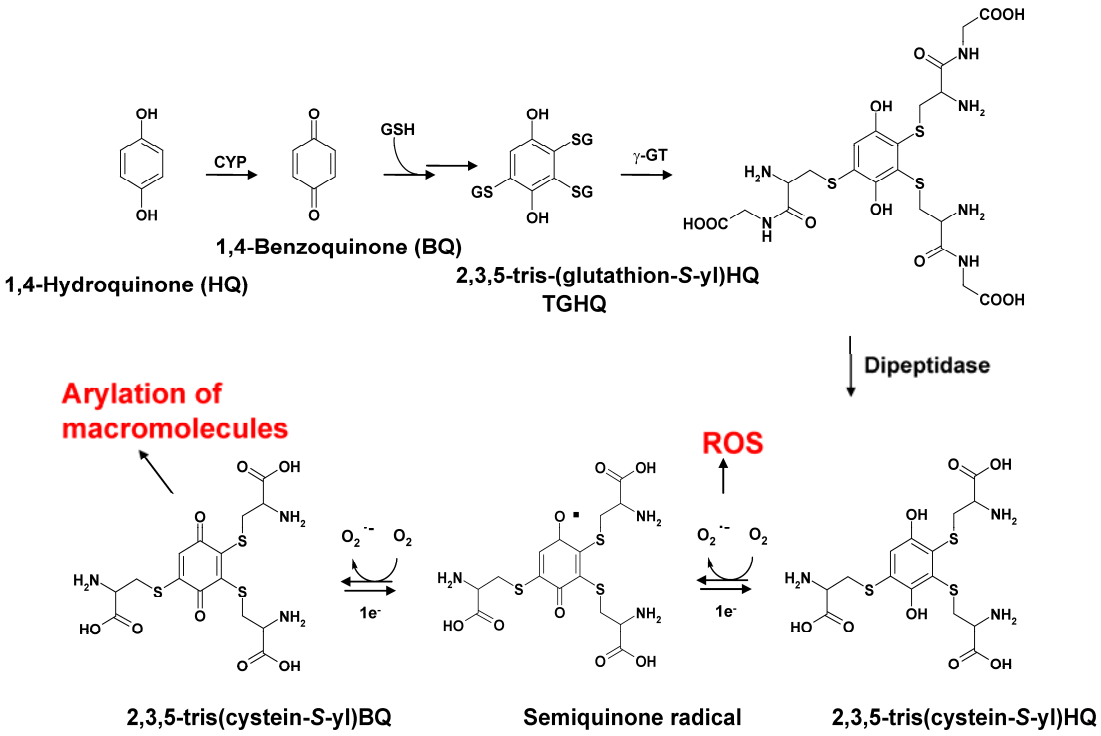

Figure 1.1. Formation and bioactivation of 2,3,5-tris-(glutathion-S-yl) hydroquinone (TGHQ).

Hydroquinone is conjugated to GSH in liver. GSH conjugates are targeted to the kidney for clearance. GSH-HQ is further metabolized by γ-glutamyl transpeptidase (γ-GT) and cysteinylglycine dipeptidase enzymes in the S3 segment of the OSOM. HQ-cysteine is recognized by amino acid transporters in proximal tubules in the OSOM. Following re-uptake, the highly reactive HQ-cysteine conjugates are capable of redox cycling, resulting in the formation of reactive oxygen species (ROS), as well as conjugate adduction of macromolecules.

1.4.2. Nephrotoxicity HQ and TGHQ

Each sequential GSH substitution leads to an increasing degree of proximal tubular necrosis, with TGHQ (10-20 μmol/kg, i.v.) resulting in the most severe renal necrosis in Sprague Dawley rats (Lau et al. 1988). This severe renal necrosis is localized to proximal tubules within the S3 segment of the OSOM (Lau et al. 1988). As described above, this is due to the localization and abundance of γ-GT and dipeptidase enzymes with this segment of the cortico-medullary junction. Identification of TGHQ, as well as other GSH conjugates, in the urine and bile of rats treated with HQ (1.82 mmol/kg, i.p.) further supports a role for GSH-HQ in HQ-mediated nephrotoxicity (Monks et al. 1992).

In another study, Fischer 344 rats were treated with HQ and TGHQ, which resulted in site-selective cytotoxicity and cell proliferation in proximal tubules within the OSOM (Peters et al. 1997). Nephrotoxicity levels were determined by measuring blood urea nitrogen, urinary γ-GT, alkaline phosphatase, glutathione-S-transferase (GST) and glucose levels, which were elevated following treatment with HQ and/or TGHQ (Peters et al. 1997). Histological analysis established the presence of tubular necrosis and sustained regenerative hyperplasia (BrDU incorporation) in the S3 segment of the proximal tubule (Peters et al. 1997). Furthermore, pretreatment with acivicin, an irreversible inhibitor of γ-GT, inhibits the nephrotoxicity of HQ (Peters et al. 1997). Taken together, these studies have established a role for GSH-HQ mediated nephrotoxicity in rats.

Interestingly, factors in addition to γ-GT activity contribute to species susceptibility to TGHQ nephrotoxicity, as both mice and guinea pigs have similar levels of renal γ-GT activity but only guinea pigs are susceptible to TGHQ mediated

nephrotoxicity (Lau et al. 1995). A possible explanation for this species difference may be attributed to N-deacetylation:N-acetylation ratio dissimilarity between mice and guinea pigs (Lau et al. 1995). Regardless of this dissimilarity, TGHQ has proven to be a potent nephrotoxic (Peters et al. 1997) and nephrocarcinogenic (Lau et al. 2001) metabolite of HQ, as described in further detail below.

1.4.3. Nephrocarcinogenicity of HQ and TGHQ

HQ has been classified in the Group 3 category by the International Agency for Research on Cancer (IARC), as it is not classifiable as to its carcinogenicity to humans (1999). The document states that there is inadequate evidence in humans and limited evidence in experimental animals for the carcinogenicity of HQ (1999). Early studies of HQ in Fisher 344 rats reported increases in renal tubular hyperplasia and adenomas (Shibata et al. 1991; Kari et al. 1992). A number of studies have demonstrated that HQ is clastogenic (Tsutsui et al. 1997), causes single-strand breaks in hepatocytes (Walles 1992), and induces *in vitro* formation of 8-oxo-deoxyguanosine (Lau et al. 1996). Although there are a number of studies that have confirmed HQ exposure can result in DNA adduct formation *in vitro* (Kalf et al. 1985; Jowa et al. 1990), studies have yet to identify these DNA adducts in vivo.

The most probable mechanism involved in HQ-mediated nephrotoxicity and nephrocarcinogenicity is the generation of ROS and covalent binding of electrophilic metabolites to macromolecules (Monks et al. 1992; Monks et al. 1997). HQ is highly reactive and can undergo a one-electron oxidation to 1,4-benzosemiquinone, which can subsequently undergo another one-electron oxidation to 1,4-benzoquinone, with the

reverse reaction occurring simultaneously. This redox cycling allows for the transfer of electrons to molecular oxygen to form superoxide anions ($O_2^{\bullet -}$). Further enzymatic reactions with $O_2^{\bullet -}$ results in the formation of hydroxyl radical (•OH), which may be the reactive species responsible for HQ-mediated oxidative damage (Monks et al. 1997).

Similarly, following enzymatic metabolism of TGHQ to 2,3,5-tris(cystein-*S*-yl)HQ, it then redox cycles within the proximal tubule to a semiquinone radical and then to 2,3,5-tris(cystein-*S*-yl)BQ; which results in increased oxidative stress (Lau et al. 1996). TGHQ is the most potent nephrotoxic and nephrocarcinogenic GSH conjugate of HQ (Lau et al. 1988). *In vivo*, TGHQ is capable of forming ROS, as well as adducting tissue macromolecules (Kleiner et al. 1998). Treatment of Fischer 344 rats and guinea pigs with TGHQ resulted in 2-bromo-N-(acetyl-L-cystein-S-yl)HQ protein adduct formation within the S3 segment of proximal tubules (Kleiner et al. 1998). Therefore, the mechanisms by which TGHQ induces nephrotoxicity and nephrocarcinogenicity are quite complex and numerous. Based on these studies, the combination of redox cycling induced ROS generation, protein adduct formation, sustained regenerative hyperplasia, and enhanced cell proliferation are responsible for the nephrocarcinogenicity of TGHQ (Lau et al. 1996). Although each of these mechanisms is crucial for TGHQ induced nephrocarcinogenicity, my focus will be on TGHQ induced disregulation of the tumor suppressor gene *Tsc-2* and the possible proto-oncogene (p27), in our established models for tuberous sclerosis renal cell carcinoma (described below).

1.5. Tuberous Sclerosis Complex

Tuberous sclerosis (TSC) is an autosomal dominant hereditary disease with a high rate of spontaneous mutation in *Tsc-1* (human 9q34) and *Tsc-2* (human 16p13) genes (Kida et al. 2005). The disease has a prevalence of approximately 1 in 10,000 new births (Osborne et al. 1991) and about 65% of TSC patients have no familial history (Sampson et al. 1989). TSC is characterized by the development of hamartomous or cystic lesions in the brain, heart, lungs, skin, and kidney (Gomez 1991). The syndrome is also associated with seizures, mental retardation, and autism. Loss of heterozygosity (LOH) at either the *Tsc-1* or *Tsc-2* gene locus has been identified in preneoplastic lesions and tumors of TSC patients (Carbonara et al. 1994; Green et al. 1994; Henske et al. 1996). In comparison, the mutation frequency of *Tsc-2* is much higher than *Tsc-1* in tumors; and *Tsc-2* mutations result in a more serious syndrome than *Tsc-1* (Cheadle et al. 2000). Therefore, the focus of our studies is on *Tsc-2* as a genetic target for RCC, and the TGHQ-Eker rat ($Tsc\text{-}2^{EK/+}$) model is greater than 70-fold more susceptible to the induction of RCC than their homozygous wild-type litter mates ($Tsc\text{-}2^{+/+}$) (Walker et al. 1992).

1.5.1. The Tuberous Sclerosis 2 (*Tsc-2*) Tumor Suppressor Gene

The *Tsc-2* gene encodes the 1784 amino acid protein tuberin, which is highly expressed in the brain, heart, and kidney tissue (Wienecke et al. 1996). Mutations in TSC genes have been demonstrated in human renal tumor formation (Bernstein et al. 1991; Bjornsson et al. 1996), and LOH at the *Tsc-2* locus has been noted in tumors of TSC patients and sporadic patients as well (Henske et al. 1995; Carbonara et al. 1996). *Tsc-2*

has been shown to be a major target for spontaneous (in both rats and mice) and chemically (rats only) induced RCC (Yeung et al. 1994; Kobayashi et al. 1995; Urakami et al. 1997; Kobayashi et al. 1999; Onda et al. 1999). The well established rat model we used in our laboratory for studying *Tsc-2* related RCC is the Eker rat (*Tsc-2*$^{EK/+}$) (Kubo et al. 1994; Yeung et al. 1995; Kobayashi et al. 1997).

1.5.2. Signal Transduction of *Tsc-2*

Tsc-2 signal transduction cascades have been shown to modulate vascular permeability, cell survival, cell proliferation, and metastasis in the progress of a variety of cancers (Pantuck et al. 2007; Rosner et al. 2008; Inoki et al. 2009). Therefore, it is crucial to further dissect the *Tsc-2* signaling cascade in *Tsc-2*$^{EK/+}$ rat renal tumor formation, in order to better understand the biology of the disease and to identify potential drug targets.

The gene products of *Tsc-1* (harmartin) and *Tsc-2* (tuberin) form a heterodimeric protein complex that is a central hub of signal transduction in the cell (**Figure 1.2**). There are sixteen known phosphorylation sites on tuberin, and regulation of tuberin by upstream kinases results in stabilization or de-stabilization of the tuberin/harmartin complex (Martin et al. 2005; Huang et al. 2008). The AMP-activated protein kinase (AMPK) is activated by energy deprivation and AMPK phosphorylation of tuberin enhances the stability of the tuberin/harmartin complex (Martin et al. 2005). Other proteins which act to enhance complex stability are REDD1 and glycogen synthase kinase 3 β (GSK3β) (Huang et al. 2008). REDD1 is capable of reversing AKT-mediated inhibition of the complex through modulation of 14-3-3 adapter proteins; and following

activation by Wnt signaling pathway, GSK3β phosphorylates tuberin in an AMPK-dependent manner (Huang et al. 2008). Whereas, AKT/PKB phosphorylation results in destabilization of tuberin and disruption of the tuberin/harmartin complex (Martin et al. 2005). Other kinases involved in the destabilization of the complex are inhibitory κB kinase β (IKK β), p90 ribosomal protein S6 kinase (RSK), and extracellular-signal-regulated kinase (ERK) (Huang et al. 2008). Stabilization of the complex is necessary for the restriction of growth upstream of mTOR.

Inhibition of mTOR by tuberin occurs through the GTPase-activating protein (GAP) activity of tuberin toward the small G protein Rheb, which acts upstream of the mammalian target of rapamycin (mTOR) (Inoki et al. 2003; Tee et al. 2003; Long et al. 2005). mTOR signaling has been implicated in tumor development, as well as drug resistance against chemotherapy and radiotherapy. There are two mTOR complexes; mTORC1 is involved in sensing nutrient signals, and mTORC2 mediates actin remodeling (Jiang et al. 2008). mTORC1 is comprised of TOR, Raptor, and LST8; which is strongly sensitive to inhibition by rapamycin (Beretta et al. 1996; Gingras et al. 1999; Gingras et al. 2001; Beugnet et al. 2003; Shaw et al. 2006; Huang et al. 2008). mTORC1 regulates mRNA translation and ribosome biogenesis through modulation of eukaryotic translation initiation factor 4E binding protein 1 (4EBP1) and p70/S6K, respectively (Jiang et al. 2008). The mTORC1 is intricately regulated by the tuberin/harmartin complex to inhibit unecessary protein synthesis, cell proliferation and cell cycle progression, and cell survival (**Figure 1.2**) (Huang et al. 2008; Jiang et al. 2008).

Tuberin may also be involved in regulating the Raf/MEK/ERK mitogen-activated protein kinase (MAPK) cascade in human cancer. Current research shows that ERK can phosphorylate tuberin on S540 and S664, which disrupts the association between tuberin and harmartin, allowing for activation of downstream mTOR signaling (Roux et al. 2004; Ma et al. 2005); (Ballif et al. 2005; Ma et al. 2005). But tuberin may also be involved in a negative feedback loop with Raf/ERK kinases. The carboxy-terminus of tuberin also shares sequence homology with a portion of the catalytic domain of the GAP for Rap1 (Wienecke et al. 1995). Rap1 bound to GTP can complex with both C-Raf and B-Raf serine/threonine kinases, thus regulating cellular proliferation and differentiation through the Raf/MEK/ERK/MAP kinase signaling cascades, which is hyperactivated in approximately 30% of all cancers (Cook et al. 1993; Hu et al. 1997). However, it is unclear if tuberin can exert its tumor suppressor activity upstream of the Raf/ERK/MAP kinase pathway. Our studies in the *Tsc-2*$^{EK/+}$ rat aim to elucidate the signal transduction pathways regulating the Raf/ERK/MAPK cascade in tuberin null renal tumors, and in transformed proximal tubule cells derived from the *Tsc-2*$^{EK/+}$ rat that are also null for tuberin.

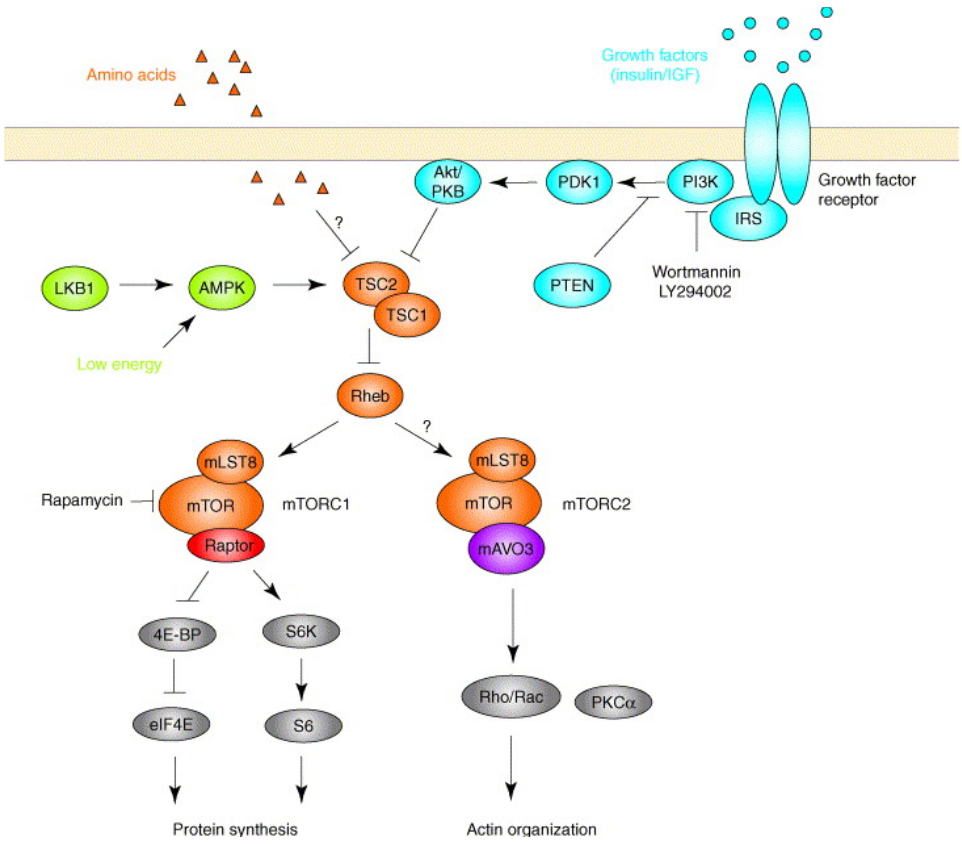

Figure 1.2. The Tuberous Sclerosis-2 signaling network.

The tuberin-harmartin protein complex integrates inputs of kinases, nutrients (amino acids), growth factors, and cellular energy status to control cell growth. Modulation of tuberin by Akt/PKB or amino acids results in breakdown of the tuberin-harmartin complex and downstream activation of Rheb. Whereas, AMPK phosphorylation of tuberin strengthens the protein complex and keeps Rheb in its GDP conjugated inactive state. Rheb-GTP directly activates the mTOR complex mTORC1, and may also be an upstream regulator of mTORC2. mTORC1 activation results in downstream phosphorylation of 4EBP1 that leads to eIF4E directed cap-dependent translation (Martin et al. 2005).

1.6. The Eker Rat and QTRRE Cell Models

Studies completed in our laboratory, as well as by others, have confirmed *Tsc-2* to be a tumor suppressor gene in renal tumor formation. The Eker rat (*Tsc-2*$^{EK/+}$), carrying an inactive allele of the *Tsc-2* gene, is a useful experimental animal model to enhance our knowledge of the pathology and signal transduction cascades involved in kidney tumorigenesis. The *Tsc-2*$^{EK/+}$ rat is a derivative of the Long Evans strain, bearing a 6.3 kb intracisternal-A partial insertion that contains multiple stop codons that disrupt transcription of the *Tsc-2* gene (Eker et al. 1981; Kobayashi et al. 1995). Nearly 100% of *Tsc-2*$^{EK/+}$ rats develop RCC by 12 months of age (Eker et al. 1981); compared to spontaneous tumor formation in wild-type rats, which occur in most strains with a frequency of <0.05% (Yeung et al. 1995). Homozygosity of the Eker mutation *Tsc-2*$^{EK/EK}$ is embryonic lethal and the rats die by 9.5-13.5 days of gestation, which illustrates the essential role of tuberin in development (Rennebeck et al. 1998). The *Tsc-2*$^{EK/+}$ rat is also predisposed to developing tumors in the spleen, pituitary gland, and uterus (Yeung et al. 1994; Kobayashi et al. 1995; Yeung et al. 1995).

Tsc-2$^{EK/+}$ rats are particularly useful because of the pathobiology of their renal tumors (i.e. cellular, molecular, and phenotypic components) are strikingly similar to human RCC (Everitt et al. 1992; Everitt et al. 1995; Yoon et al. 2002). The *Tsc-2*$^{EK/+}$ rat and human RCCs are derived from proximal tubule cells within the tubular epithelium of the nephron (Hard 1986), overexpress transforming growth factor alpha (TGF-α) (Walker et al. 1991), and lack Ras and p53 mutations (Recio et al. 1991; Kobayashi et al. 1999). Tuberin is also involved in cell cycle control (Soucek et al. 1997; Soucek et al. 1998; Ito et al. 1999), but the precise physiological or cellular role(s) of tuberin in renal

carcinogenesis still remain elusive. Tuberin also shares a similar downstream effector of the *VHL* tumor suppressor gene, to regulate the cyclin dependent kinase inhibitor $p27^{Kip1}$ (Rosner et al. 2007). Recent reports identify tuberin as a direct inducer of nuclear p27 localization, allowing p27 to mediate cell cycle arrest (Rosner et al. 2007). But the modulation of p27 following loss of tuberin in renal tumor formation is relatively unknown.

Using the $Tsc\text{-}2^{EK/+}$ rat we have shown that TGHQ, a reactive metabolite of HQ, is mutagenic and can transform primary renal epithelial cells isolated from the $Tsc\text{-}2^{EK/+}$ rat (Yoon et al. 2001). Immortalization of $Tsc\text{-}2^{EK/+}$ rat primary proximal tubule cells following transformation with TGHQ, established the quinol-thioether rat renal epithelial cells (QTRRE1, 2, and 3 cell lines) (Yoon et al. 2001). QTRRE cells exhibit cytogenetic alterations, LOH at the *Tsc-2* locus, and are null for tuberin protein expression. Additionally, subcutaneous injection of QTRRE cells to athymic nude mice results in tumors, comprised of neoplastic cells, resembling renal carcinoma cells with varying degrees of atypia, with the presence of apoptotic and mitotic figures (Patel et al. 2003). TGHQ administration to $Tsc\text{-}2^{EK/+}$ rats induces a sustained regenerative hyperplasia at sites that subsequently give rise to tumors (Lau et al. 2001; Yoon et al. 2001; Yoon et al. 2002). Preneoplastic lesions and tumors formed in TGHQ-$Tsc\text{-}2^{EK/+}$ rats displayed a LOH of the *Tsc-2* wild-type allele (Lau et al. 2001) and subsequent loss of tuberin expression (Yoon et al. 2002). Furthermore, the OSOM of TGHQ-$Tsc\text{-}2^{EK/+}$ rats at 4 months and TGHQ-induced tumors both displayed high ERK kinase activity, as well as high levels of cyclin D1 protein expression in tumors (Yoon et al. 2002). These data also demonstrated that stimulation of cell proliferation following toxicant insult is insufficient

for tumor formation, but loss of tuberin is associated with cell cycle deregulation (Yoon et al. 2002).

Mechanistic studies in QTRRE cells, which are null for tuberin, revealed that tuberin is also a tumor suppressor for the Raf/MEK/ERK MAPK cascade (Yoon et al. 2004). QTRRE cells express constitutively high levels of fully activated ERK, B-Raf and Raf-1 (Yoon et al. 2004). Transient transfection of *Tsc-2* cDNA in QTRRE cells resulted in a substantial decrease in both ERK and B-Raf kinase activity, with a less substantial decrease in Raf-1 activity (Yoon et al. 2004). Restoration of tuberin expression in QTRRE cells resulted in a decrease in cyclin D1 protein levels. Further dissection of the tuberin/MAPK signaling cascade is necessary to determine the link between MAPK signaling and cyclin D1 protein expression.

1.7. Mitogen-Activated Protein Kinase (MAPK) Cascades

The mitogen-activated protein kinase (MAPK) cascade regulates gene expression, metabolism, and the cellular cytoskeleton, thus directly modulating cellular proliferation, differentiation, senescence, and survival. MAPK enzymes catalyze the transfer of high energy gamma-phosphate from ATP to the subsequent kinase, resulting in activation within the kinase domain. Activation of enzymes within the Raf/MEK/ERK MAPK cascade is modulated by receptor tyrosine kinases and a number of Ras related small G proteins; such as Ras, Rheb, and Rap. The Ras/Raf/ERK cascade has been implicated in a number of different cancers. Recently, activated Rheb, the target of the GAP domain of tuberin, was found to inhibit B-Raf/Raf-1/ERK signaling in human embryonic kidney (HEK293) cells (Karbowniczek et al. 2006), suggesting that TSC patients may have

benign tumors because of the duality of Rheb-GTP function (**Figure 1.3**). Although the mTOR pathway is activated by Rheb-GTP, it is simultaneously inhibiting the MAPK cascade as well (Karbowniczek et al. 2006) (**Figure 1.3**). Less is known about how Rap regulates the MAPK cascade.

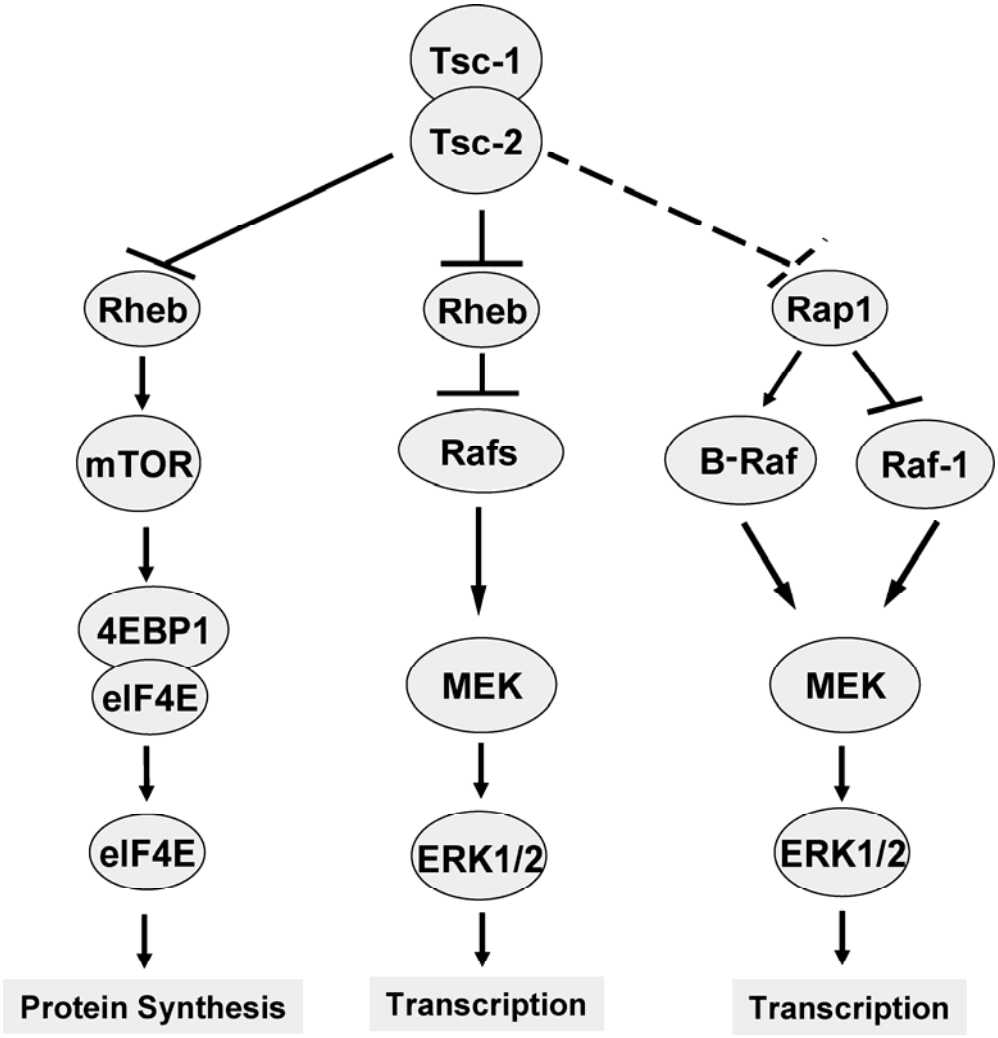

Figure 1.3. Tuberin modulation of small G-proteins.

Tuberin and harmartin form a heterodimeric protein complex that negatively regulates the intrinsic GTPase activity of Rheb. Activated Rheb-GTP binds and activates mTOR but inhibits Raf kinase activation. Tuberin may also negatively regulate Rap, which when bound to GTP will facilitate the activation of B-Raf but inhibit Raf-1 activation.

1.7.1. Rap1

Rap belongs to the Ras superfamily of small GTP-binding proteins (Peyssonnaux et al. 2001). The Rap subfamily consists of Rap1A, Rap1B, Rap2A and Rap2B (Reuther et al. 2000). The activity of Raps is dependent on cycling between an inactive GDP-bound state and an active GTP-bound state (Boguski et al. 1993). The molecular switch between GDP and GTP is modulated by guanine exchange factors (GEF) to activate Rap. The Ral GEF (RGF) is an effector of Rap, and binds directly to the Ras-binding domain (RBD) of RGF (Herrmann et al. 1996). Therefore, Ral directly binds Rap to facilitate the switch between GDP to GTP to activate Rap. Similarly, a GTPase-activating protein (GAP) inactivates Rap by catalyzing the hydrolysis of bound GTP to GDP (Boguski et al. 1993). Tuberin may serve as a GAP for Rap1, as the C terminus of tuberin shares 30% homology with the catalytic domain for Rap1GAP (Wienecke et al. 1995). However, in astrocytomas formed in TSC patients, there was no correlation between tuberin expression and Rap1 activity or expression (Lau et al. 2003). The functionality of tuberin as a GAP for Rap1 has yet to be validated *in vivo* in rodents or in human cancer.

Rap1 GEFs and GAPs are modulated by a number of upstream inducers or repressors. Rap1 is activated by similar extracellular signals as Ras, as well as by second messengers such as calcium (Ca^{2+}) and diacylglycerol in human neutrophils and/or platelets (Franke et al. 1997; M'Rabet et al. 1998). Intracellular Ca^{2+} is necessary for Rap1 activation. Neuronal Ca^{2+} increases cAMP/PKA mediated activation of Rap1 and subsequent downstream activation of B-Raf (Grewal et al. 2000). cAMP regulates Raf by modulating ras/Raf and Rap1/Raf complexes. Rap1 can bind B-Raf and Raf-1, but Rap1 binding results in activation of B-Raf and inhibition of Raf-1 (Peyssonnaux et al.

2001) (**Figure 1.3**). All cell types in which Rap1 has been shown to activate the ERK pathway also express B-Raf (Vossler et al. 1997; Garcia et al. 2001). Therefore, Rap activation of ERK is dependent on cellular levels of B-Raf. In cell lines where B-Raf is not expressed, Rap1 inhibits Raf-1/ERK activation (Okada et al. 1998; Dugan et al. 1999; Schmitt et al. 2001). Although cAMP modulates the balance between Ras/Raf-1 active and Rap1/Raf-1 inactive state, other small monomeric G proteins like Rheb may play a role in Raf/ERK activation/inhibition as well. Activated Rheb inhibits B-Raf/Raf-1/ERK signaling in human embryonic kidney (HEK293) cells (Karbowniczek et al. 2006). But, the existence of a cAMP/Rap/B-Raf activation pathway/cascade has yet to be confirmed in renal tissue.

1.7.2. Raf Kinases

The Raf-A (68 kDa), -B (75-100 kDa), and –C (72-74 kDa) proteins contain three conserved regions (CR); with the N-terminal CR1 and CR2 regions, and the C-terminal CR3 kinase domain (**Figure 1.4**) (Wellbrock et al. 2004). *B-Raf* mRNA gives rise to a range of proteins from 75 to 100 kDa due to alternative splicing within a number of different domains (Barnier et al. 1995). C-Raf is most commonly referred to as Raf-1. The expression patterns of the Rafs vary greatly; Raf-1 is ubiquitously expressed, but A-Raf and B-Raf have restricted expression (Wellbrock et al. 2004). Very limited data exist on the tissue specific expression levels of A-Raf and B-Raf protein and mRNA. *A-Raf* mRNA is expressed highly in urogenital organs and *B-Raf* mRNA is predominately expressed in neuronal tissues (Storm et al. 1990; Barnier et al. 1995). B-Raf protein is predominately expressed in neuronal tissues, with significantly lower levels detected in a wide range of other tissue (Wellbrock et al. 2004).

Raf proteins are crucial in embryonic development. Mice that are *A-Raf*$^{-/-}$ die 7-21 days after birth from neurological and gastrointestinal defects (Pritchard et al. 1996); whereas *B-Raf*$^{/-}$ or *Raf-1*$^{-/-}$ mouse embryos die *in utero* (Wellbrock et al. 2004). The cause of embryonic death is distinctly different for both; *Raf-1*$^{-/-}$ embryos die from severe liver apoptosis and *B-Raf*$^{/-}$ embryos die from vascular and neuronal defects, and growth retardation (Wellbrock et al. 2004). These results suggest that each Raf isoform carries out a distinctly different function in the cell. The effects of upstream modulators on Rafs also vary for each isoform. Adenylate cyclase/cAMP signaling can activate B-Raf/ERK kinases (Busca et al. 2000). cAMP may regulate B-Raf kinase activity through regulation of Rap1, as cAMP has been shown to regulate exchange factors for Rap1 (Peyssonnaux et al. 2001). cAMP modulation of Raf-1 kinase activity is highly controversial, as activation and inhibition of Raf-1 have both been described. In terms of downstream signaling, when B-Raf is expressed and activated it may have a higher affinity for MEK1/2 than Raf-1 (Peyssonnaux et al. 2001; Garnett et al. 2005). Activation of the Rafs is highly dependent on the protein being phosphorylated on a number of crucial sites within all three domains. Although B-Raf is highly modified by posttranslational modifications (PTM), it may require fewer PTM than Raf-1 to achieve maximal activity.

Hyperactivation of ERK has been identified in over 30% of cancers (Wellbrock et al. 2004; Rushworth et al. 2006). This increased activity may result from increased expression of mitogens, constitutive activation of Rafs by upstream kinases, or activating point mutations in B-Raf. Mutations in B-Raf have been identified in approximately 7% of human cancers, with around 70 different mutations known (Gray-Schopfer et al. 2007), but none have yet to be determined in RCC. Of eleven human RCC biopsies

studied, no B-Raf point mutations were identified (Davies et al. 2002). Alternatively, activating mutations may not be necessary to drive constituitive B-Raf kinase activity. Wild-type B-Raf may be involved in driving the progression of RCC.

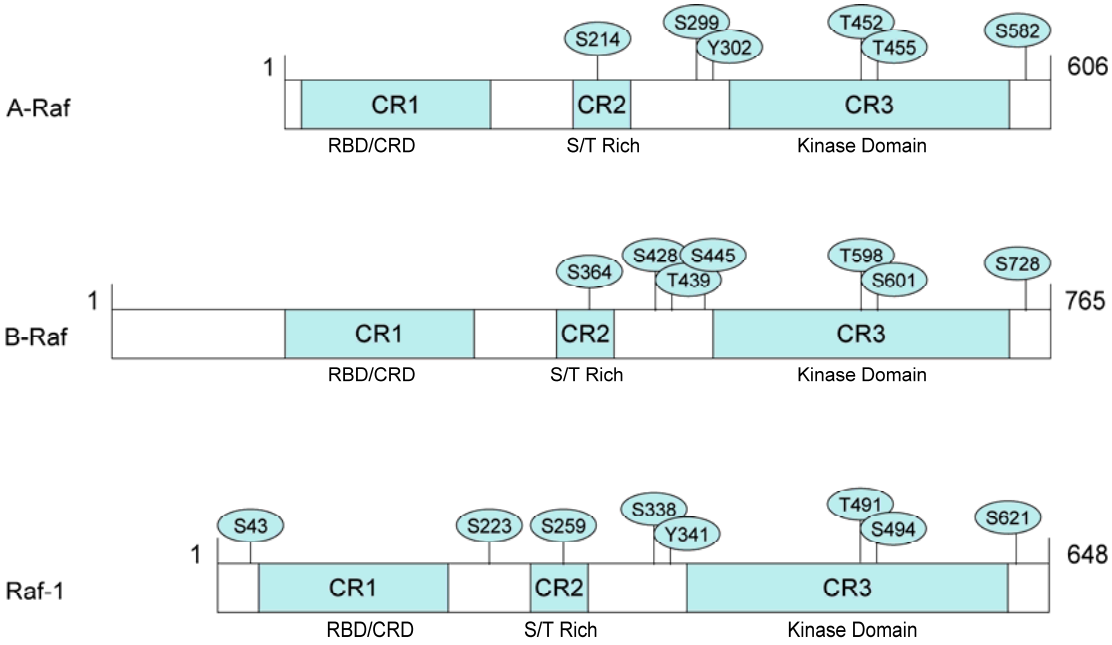

Figure 1.4. Structure of Raf protein kinases.

There are three Raf isoforms, A-Raf, B-Raf, and Raf-1. These isoforms share three conserved regions: CR1 (RAS Binding Domain (RBD)/Cysteine Rich Domain (CRD)), CR2 (Serine (S)/Threonine (T) Rich), and CR3 (Kinase Domain). The highlighted amino acids refer to known human isoform phosphorylation sites (Wellbrock et al. 2004).

1.7.3. B-Raf/Raf-1 heterodimers

A number of studies have identified B-Raf/Raf-1 heterodimers (Garnett et al. 2005; Karbowniczek et al. 2006; Rushworth et al. 2006). Constitutively activated B-Raf can bind and activate Raf-1 in the cytosol in a Ras-independent manner (Garnett et al. 2005). This dimerization requires that Raf-1 is phosphorylated in its activation domain to facilitate 14-3-3 binding and subsequent activation by B-Raf (Garnett et al. 2005; Rushworth et al. 2006). Compared to the formation of Raf homodimers or monomers, isolated B-Raf/Raf-1 heterodimers have amplified kinase activity (Rushworth et al. 2006). It is hypothesized that the cytosolic heterdimerization may allow for signaling to alternative effectors that it would not normaly encounter at the plasma membrane. A more specific role of the heterodimers has yet to be determined.

1.7.4. Extracellular-Signal-Regulated Kinase (ERK) MAPK

The extracellular regulated kinases (ERK1/2) are mitogen-activated protein kinases (MAPK). Including ERK1/2, there six different groups of MAPKs: Jun NH2 terminal kinases (JNK1/2/3), p38 (p38 a/b/g/d), ERK7/8, ERK3/4 and ERK5 (Krishna et al. 2008). Each member of the MAPK family has numerous common features. The MAPK is the final tier of a three-tiered signaling pathway, consisting of a MAPK kinase kinase (MAPKKK), a MAPK kinase (MAPKK), and a MAPK, which activates the subsequent kinase sequentially (Krishna et al. 2008). The MAPKKKs are Ser/Thr kinases that are activated by small G-proteins, such as Ras/Rap/Rheb/Rho, and/or by phosphorylation (Uhlik et al. 2004). MAPKKK activation leads to phosphorylation and activation of MAPKKs, which results in downstream phosphorylation of MAPKs on either threonine and/or tyrosine residues (Uhlik et al. 2004).

Substrates for MAPKs are diverse, and include transcription factors, other kinases, or cytoskeletal proteins. MAPKs target a number of downstream MAPK-activated protein kinases (MKs), such as downstream p90 ribosomal S6 kinases (RSK 1–4) (Sturgill et al. 1988; Zhao et al. 1996), mitogen and stress activated kinases (MSK1 and 2), the MAPK-interacting kinases (MNK1 and 2), MAPK-activated protein kinases -2 and -3 (MK2 and MK3 or MAPKAP-K2 and MAPKAP-K3) and MAPK-activated protein kinase 5 (MK-5 or MAPKAP-K5) (Krishna et al. 2008). MAPK is also involved in the activation of a number of transcription factors, such as Ekl-1, c-Myc, c-Jun, c-Fos, NF-IL6, p62TCF, and ATF-2 (Alvarez et al. 1991; Marais et al. 1993; Davis 1995). MAPKs target downstream effectors through a proline-directed recognition sequence of amino acids; Pro-X-(Ser/Thr)-Pro (Alvarez et al. 1991).

ERK1 and ERK 2 isoforms posses an 83% amino acid identity and are ubiquitously expressed in all tissue (Krishna et al. 2008). ERK1/2 signaling is activated by upstream growth factors, receptor tyrosine kinases (RTK), serum, phorbol esters, ligands of G-protein coupled receptors (GPCRs), cytokines, osmotic stress and microtubule disorganization (Lewis et al. 1998). Signaling from RTKs transduce through small G proteins to activate MAPKKKs (A-Raf, B-Raf or Raf-1) that phosphorylate/activate MEK1/2, which results in activation of ERK1/2. In the cytosol, activated ERK1/2 can phosphorylate PLA2, CD120a, Syk and calnexin; as well as the cytoskeletal proteins paxillin and neurofilaments (Yoon et al. 2006). Upon activation, ERK1/2 translocates to the nucleus to phosphorylate transcription factors, such as PLA2, CD120a, Syk and calnexin, as well as MKs (Yoon et al. 2006).

ERK activation appears to play a dual role in regulation of apoptosis, as it is capable of activating and inhibiting apoptotic cell death. The regulation of apoptosis by ERK occurs in a variety of cell types (Bhat et al. 1999; Pavlovic et al. 2000; Wang et al. 2000; Lesuisse et al. 2002). In renal cells treated with cisplatin, ERK activation of caspase-3 induced apoptosis (Nowak 2002). ERK may also stimulate apoptosis by inducing the up-regulation of TNFα (Jo et al. 2005) or by activation of caspase-8 (Cagnol et al. 2006). Other studies suggest that ERK may inhibit anti-apoptotic proteins, such as Bcl-2 and Bcl-xl, through the upregulation of Bax to induce apoptosis (Park et al. 2005; Wu et al. 2005). Alternatively, ERK activity has been implicated in cell survival and in the decline of apoptosis. In fibroblast cells overexpressing B-Raf, ERK activation was associated with the inhibition of cytosolic caspase activation following cytochrome c release from the mitrochondria (Erhardt et al. 1999).

As hyperactivation of ERK signaling has been identified in over 30% of cancers (Wellbrock et al. 2004; Rushworth et al. 2006), it becomes increasingly important to determine ERKs involvement in carcinogenesis. Although ERK is generally implicated in transcriptional regulation of proliferation, it may also be involved in disregulating protein synthesis. ERK activates transcription factors, such as c-myc and c-fos, which can increase transcription of elongation factor eIF4E, an activator of RNA polymerase I and cap-dependent translation. Furthermore, in an *in vitro* kinase assay, recombinant eukaryotic translation initiation factor 4E binding protein 1 (4EBP1) was a substrate for ERK/MAP kinase, suggesting that ERK may also play a role in the hierarchical phosphorylation of 4EBP1 (Haystead et al. 1994). Phosphorylation of 4EBP1 suppresses its ability to bind and inhibit eIF4E, allowing for the initiation of translation (Gingras et

al. 1999; Gingras et al. 2001; Beugnet et al. 2003; Huang et al. 2008). Thus, there are different mechanisms by which ERK could be involved in upregulating translation initiation and increased protein synthesis.

A known gate-keeper for translation initiation is the tumor suppressor tuberin, which modulates the tuberin/Rheb/mTOR/4EBP1 cascade. A recent study shows that activated ERK1/2 can directly phosphorylate tuberin on Ser 664 to disrupt the association between tuberin and harmartin, stimulating downstream mTOR signaling (Ballif et al. 2005; Ma et al. 2005). It has been well established that activation of mTOR results in the disassociation of 4EBP1 from eIF4E, thus allowing eIF4E to initiate cap-dependent translation of cyclin D1 (Gingras et al. 1999; Gingras et al. 2001; Jiang et al. 2008). Alternatively, in hamster fibroblast cells (CCL39), ERK1/2 signaling was a major regulator of cyclin D1 protein expression (Lavoie et al. 1996). Since transient transfection of a *Tsc-2* plasmid in tuberin null QTRRE cells resulted in decreased ERK1/2 kinase activity, as well as decreased cyclin D1 protein levels (Yoon et al. 2004); the necessary next step is to determine if ERK1/2 activity is partly responsible for regulating cyclin D1 mRNA and/or protein levels in our renal carcinogenesis models. In melanoma cell lines, B-Raf regulates the expression of the cyclin D1 and the cyclin dependent kinase inhibitor $p27^{Kip1}$ at the mRNA level (Bhatt et al. 2005). Inhibition of B-Raf with siRNA in melanoma cells resulted in a substantial decrease in cyclin D1 and an increase in p27 (Bhatt et al. 2005). Therefore, the ability of activated ERK to inhibit cell cycle arrest in cancer, through the downregulation of p27 and upregulation of cyclin D1, may be a crucial step in the progression of tumors. Thus, it is important to determine the role of ERK1/2 in cell cycle progression in renal tumors.

1.8. Cell Cycle Regulation

The major components involved in regulation of the cell cycle are cyclins (the A-, B-, D- and E-type cyclins), cyclin dependent kinases (CDK1, CDK2, CDK4 and CDK6), cyclin dependent kinase inhibitors (Cip/Kips and Ink4s), and two E3-ubiquitin-ligase complexes (Skp1, Cullin and F-box (SCF), and the Anaphase-Promoting Complex (APC/C)) (van Leuken et al. 2008; Malumbres et al. 2009). Throughout the cell cycle CDK levels remain constant, whereas the synthesis and degradation of cyclins are intricately regulated at specific stages of the cell cycle (Malumbres et al. 2009). The CDKs are ser/thr kinases that elicit organized progression of the cell cycle. Activation of CDKs is dependent on PTMs and via binding to a cyclin regulatory subunit (Morgan 1995). Distinct CDK-cyclin complexes modulate progression through the cell cycle, as well cell cycle arrest. Activation of cell cycle checkpoints (G1 and G2) results in inhibition of CDK kinases, which halts progression of the cell cycle and allows for proper detection of possible defects in the DNA (Bartek et al. 2004). If DNA damage is beyond repair, cells may undergo senescence or apoptosis to prevent genetic defects from being replicated (Malumbres et al. 2009). During the G1 checkpoint D-type cyclins (D1, D2 and D3) bind and activate CDK4 and CDK6 (Malumbres et al. 2009). The regulation of p27-cyclin D-CDK4/6 complex formation during the progression from a quiescent G_o to G_1 state is described in **Figure 1.5**. Expression and activation of cyclins (E1 and E2)-CDK2 complexes drives the G1/S transition into synthesis (Hochegger et al. 2008). In late S phase, cyclin A-CDK2 activated complexes drives cell cycle arrest in G2. In the final phase of the cell cycle, active cyclin B-CDK drives the cell through mitosis (Malumbres et al. 2009).

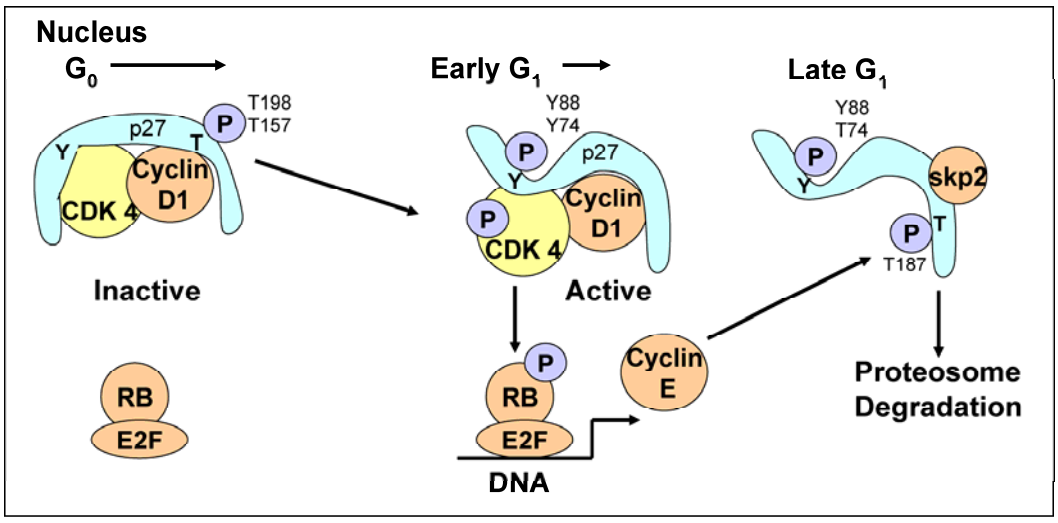

Figure 1.5. Role of p27 in the progression from a quiescent G_o to G_1 state.

In Go, phosphorylation on T157 activates nuclear localization of p27, and further modification of p27 on T198 also allows for p27-cyclin D-CDK complex formation. Phosphorylation of p27 on Y74 or Y88 results in a conformational shift that will push the C-terminal tail of p27 from the CDK4 active site. Activation of CDK4 results in phosphorylation of RB, which permits the transcription of cyclin E. Inhibition of p27 during the G_1 to S phase transition is modulated by its phosphorylation on T187 by cyclin E and A-CDK2.

1.8.1. Cyclin Dependent Kinase Inhibitor p27

Cyclin dependent kinase inhibitors (CKIs) are comprised of two families, the Cip/Kips (p27, p21, and p57) and the Ink4s (p15, p16, p18, and p19) (Blain 2008). Ink4s are rapidly induced in response to antiproliferative signals and specifically inhibit cyclin D-CDK4/6 complexes; whereas, Cip/Kips associate with all cyclin-CDK complexes (Blain 2008). $p27^{Kip1}$ is constitutively expressed throughout the cell cycle (Soos et al. 1996) and is never found unbound *in vivo* (Vervoorts et al. 2008). p27 is an extremely versatile CKI, in that in can regulate proliferation and cell cycle exit (Blain 2008; Vervoorts et al. 2008). In normal G_o quiescent cells p27 levels are typically high and CDK activity is low (Kaldis 2007). The end result of p27 modulation depends on its protein concentration, phosphorylation status, and subcellular localization (Vervoorts et al. 2008). Each of these factors depends on the dynamic regulation of p27 by multiple signaling cascades (Vervoorts et al. 2008).

The localization of p27 is complex and dependent on its phosphorylation status at a number of key residues (**Figure 1.6**) (Vervoorts et al. 2008). Nuclear p27 preferentially binds cyclin A/E-CDK1/2 complexes to inhibit catalytic activity, maintaining a G_o quiescent state (Coats et al. 1996; Rivard et al. 1996). In G_o phosphorylation on either S10 by MIRK or T198 by AKT or RSK1/2 stabilizes p27 in the nucleus (Deng et al. 2004; Kotake et al. 2005; Besson et al. 2006; Kossatz et al. 2006). In G_1 p27 is phosphorylated by KIS on S10 to inhibit its CKI function, stimulate assembly of p27-cyclin D-CDK complexes, and enhance export from the nucleas to the cytoplasm via CRM1-mediated export pathway (Rodier et al. 2001; Ishida et al. 2002; Connor et al. 2003). The consequence of AKT or ERK2 phosphorylation on p27 S10 has yet to be

determined (Vervoorts et al. 2008). ERK and/or AKT may aid in p27-cyclin D-CDK complex formation and stability. Further modification of p27 in G_1 by AKT or RSK1/2 on T198 also allows for p27-cyclin D-CDK complex formation in the cytosol (Fujita et al. 2002; Fujita et al. 2003; Kossatz et al. 2006). Additional phosphorylation by AKT on T157, within the p27 nuclear localization sequence, cooperates with T198 to enhance cytoplasmic localization of p27 (Liang et al. 2002; Shin et al. 2002; Motti et al. 2004). The T157 site has never been identified as a phosphorylation site in rodents (Vervoorts et al. 2008).

Dual phosphorylation on T157 and T198 allows for 14-3-3 to associate with p27, which inhibits Importin-α5 binding to p27, resulting in cytoplasmic localization (Sekimoto et al. 2004; Shin et al. 2005). p27 is also tyrosine phosphorylated at a number of sites to modulate its binding to specific CDKs. Phosphorylation on either Y74 by SRC or YES, or on Y88/89 by LYN or ABL kinases, results in a structural change within p27 that inhibits its function as a CKI (Kardinal et al. 2006; Chu et al. 2007; Grimmler et al. 2007). p27 interaction is within the catalytic cleft of CDK2 that prevents it from being bound to ATP (Chu et al. 2007). The p27 tyrosine sites are within its CDK2 binding domain, and when phosphorylated CDK2 is displaced, which allows for restoration of ATP-binding and CDK2 catalytic activity (Chu et al. 2007; Grimmler et al. 2007).

Inhibition of p27 during the G_1 to S phase transition is modulated by its phosphorylation on T187 by cyclin E and A-CDK2 (Sheaff et al. 1997; Vlach et al. 1997). Phosphorylation on T187 allows for recognition by E3-ubiquitin-ligase Skp-Cullin-F-box (SCF^{SKP2}) and CKS1 to target p27 for proteosome degradation (Carrano et al. 1999; Sutterluty et al. 1999). p27 degradation allows for increased CDK1 and CDK2

activity (Kaldis 2007). If p27 is bound to cyclin D-CDK4 complexes, it is protected from degradation by the SCF^{SKP2} E3-ubiquitin-ligase complex (Kamura et al. 2004). Due to the instability of the cyclin D1-CDK4 complex, p27 interaction is necessary for complex assembly and stabilization (Cheng et al. 1999; Sherr et al. 1999). In both in vitro and in vivo models, isolated p27-cyclin D-CDK4 complexes have intact kinase activity (Blain et al. 1997; James et al. 2008). Therefore, cytoplasmic p27-cyclin D-CDK4 active complexes may play a crucial role in tumor formation.

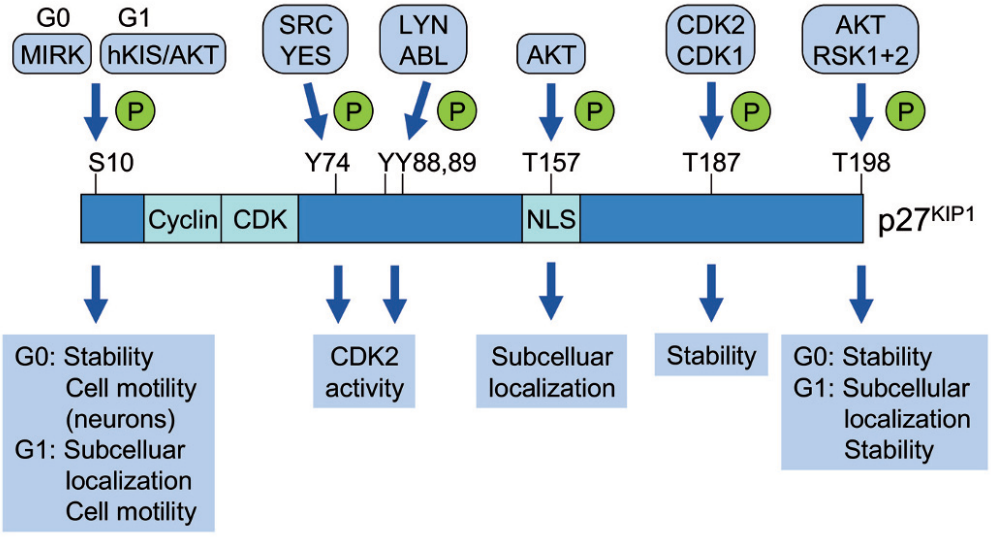

Figure 1.6. Known post translational modifications to p27.

p27 is a highly modified protein with many known kinases that modify specific sites. The functional significance of each site specific modification is described above. Modification to specific amino acid residues is associated with variable biological outcomes; as it is dependent on the kinase modifying it (Vervoorts et al. 2008).

1.8.2. Role of p27 in Cancer

The role of p27 in cancer progression is rather complex. p27 is classically considered to be an atypical tumor suppressor, in which mutation or homozygous loss of p27 in cancer is extremely rare (Sicinski et al. 2007; Blain 2008; Vervoorts et al. 2008). Recent developments have revealed the duality of p27 as an oncogene in certain cancers. Depending on the tissue specificity and pathology of the tumor, p27 expression in the tumor is either low in the total cell lysate, or elevated in the cytosol due to cytoplasmic relocalization (**Figure 1.7**) (Sicinski et al. 2007; Short et al. 2008).

Most recently, data suggests that the tumor suppressor tuberin can affect subcellular localization and protein accumulation of p27 (**Figure 1.7**) (Short et al. 2008). Analysis of *Tsc2* null uterine leiomyomas from the Eker rat revealed cytoplasmic mislocalization of p27 (Short et al. 2008). Furthermore, tuberin can interact with p27 to negatively regulate its degradation by the ubiquitin-proteosome (Rosner et al. 2004; Rosner et al. 2007; Rosner et al. 2008). Tuberin directly binds to p27 to inhibit targeted degradation by the E3 ubiquitin ligase skp2. Tuberin inhibits degradation by interacting with p27 in its 14-3-3 binding cleft, which decreases cytoplasmic retention, resulting in nuclear p27 localization (Rosner et al. 2007). Tuberin can complex with p27 to block its site specific degradation by the proteosome (Rosner et al. 2004; Rosner et al. 2008), inhibit 14-3-3 mediated cytoplasmic retention of p27 (Rosner et al. 2007), and to promote nuclear localization of p27 (Rosner et al. 2007). Dual phosphorylation of p27 on T157, its nuclear localization signal, and T198 allows for 14-3-3 to associate with p27, which inhibits Importin-α5 binding to p27 and results in cytoplasmic localization (Fujita et al. 2002; Fujita et al. 2003; Sekimoto et al. 2004; Shin et al. 2005). Upon examination of

Tsc2$^{-/-}$ MEFs, and microscopic kidney lesions in *Tsc2*$^{+/-}$/p27$^{+/+}$ mice and *Tsc2*$^{+/-}$/p27$^{+/-}$ mice, p27 was predominately expressed in the cytosolic fraction (Short et al. 2008). These data provide evidence that links tuberin expression to p27 compartmental localization, and therefore we seek to further explore the relationship between tuberin and p27 in tuberous sclerosis renal cell carcinoma.

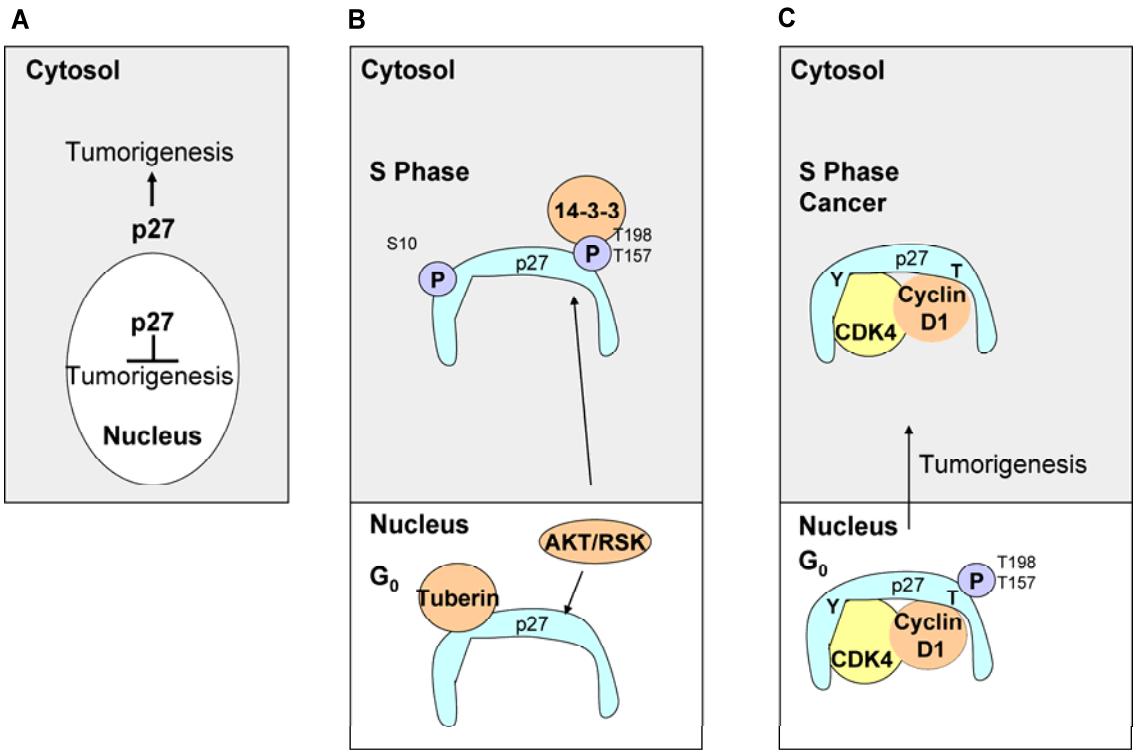

Figure 1.7. Subcellular compartmentalization of p27.

A) Nuclear p27 complexes with cyclin-CDK to inhibit its activity and inhibit cell growth. Cytoplasmic mislocalization of p27 is associated with tumorigenesis. B) Depicts the role of tuberin in p27 subcellular localization. In Go cells tuberin binds p27 and directs its nuclear retention. In the transition from Go to S phase p27 is phosphorylated by Akt, which downregulates tuberin-p27 complex stability and increases 14-3-3 binding to phosphorylated p27. 14-3-3 binding to p27 triggers cytoplasmic retention of p27. C) Cytoplasmic mislocalization of p27 determined in late stage tumors. Specific post translational modifications to p27 direct its cytosolic mislocalization.

1.9. Dissertation Aims

The *VHL* tumor suppressor gene is a primary target in human RCC that does not contribute to rodent renal carcinomas. In contrast, loss of heterozygosity at the *Tsc-2* locus occurs in human and rodent renal tumors. *VHL* and *TSC* congenital diseases result in similar histological clear cell RCCs, and have in common the disregulation of cell cycle proteins cylcin D1 and p27. However, the signaling pathways that regulate cyclin D1 and p27 during renal tumor development is not well understood. Cyclin D1 is a key protooncogene in numerous cell types, and p27 is a possible oncogene in metastatic RCC. In the Eker rat (*Tsc-2*$^{EK/+}$), the *Tsc-2* gene is the target of TGHQ-mediated nephrocarcinogenicity, and the *Tsc-2* gene product, tuberin, exerts its tumor suppressor activity upstream of the Rheb/mTOR/4EBP1 and Raf/ERK/MAP kinase cascades. Studies described in this dissertation, therefore, aim to determine (i) the relationship between the loss of tuberin and activation of the Rheb/mTOR/4EBP1 and Raf/ERK/MAPK cascades, and (ii) how these pathways modulate cyclin D1 and p27 transcription, translation, and/or (iii) protein compartmentalization druing RCC.

The gene products of *Tsc-1* (harmartin) and *Tsc-2* (tuberin) form a heterodimeric protein complex that negatively regulates the Rheb/mTORC1 (TOR, Raptor, and LST8)/4EBP1-eIF4E signaling cascade to directly modulate the cap-dependent translation of cylcin D1. However, whether or not the Raf MAPK signaling cascade can regulate the transcription of cyclin D1 in proximal tubule cells is not known. Therefore, in Chapter 2, extensive *in vitro* (cascade dissection) and *in vivo* (probing protein levels) investigations were performed to determine possible transcriptional regulation of cyclin D1 by Raf, MEK, and ERK kinases (Aim #1). Results from these studies identified

possible novel ERK crosstalk with 4EBP1, since only mTOR has been reported as capable of phosphorylating 4EBP1. We, therefore subsequently explored Raf directed ERK crosstalk with 4EBP1 (Aim #2, Chapter 3).

Results from studies described in Chapter 2 identified increased levels of cyclin D1 in the cytoplasm of necrotic proximal tubules. Cyclin D1 typically co-localizes with CDK4/6 and p27 in the nucleus to facilitate the G_1 to S phase progression of the cell cycle. Thus, in the third aim we investigated the subcellular compartmentalization of p27 and cyclin D1, and the mechanism(s) responsible for p27 localization and stabilization during renal tumor formation (Chapter 4).

In summary, the work presented in this dissertation identifies Raf kinases as pivotal signaling molecules involved in the progression of tuberous sclerosis renal cell carcinoma. These data provide evidence for novel interactions between Raf/MAPK and mTOR/4EBP1 signaling pathways as well. Furthermore, these pathways play a key role modulating cyclin D1 and p27 subcellular compartmentalization and stabilization in RCC. Elucidating the impact Raf and mTOR signaling on RCC may be useful in determining more efficacious drug combinations to treat the disease.

CHAPTER 2: RAF MAPK MODULATES EXPRESSION OF CYCLIN D1

2.1. Introduction

Cyclin D1 controls the G1 to S-phase progression of the cell cycle, and as opposed to other D-type cyclins, is commonly deregulated in cancer (Tashiro et al. 2007; Kim et al. 2009). Overexpression of cyclin D1 and hyperactivation of cyclin D1/CDK4/6 complexes are thought to contribute to neoplastic transformation and growth; as identified in breast, head and neck, esophageal, and non-small cell lung cancers, as well as in lymphoma (Barnes et al. 1998; Jin et al. 2001; Cario et al. 2007; Kim et al. 2009). Numerous mechanisms have been identified to account for the abundance of cyclin D1 in tumors; such as genomic alterations, posttranslational modifications, and protein stabilization (Kim et al. 2009). Receptor tyrosine kinases trigger activation of the Ras/Raf/MEK/ERK MAPK cascade, which results in increased transcription of cyclin D1 (Lavoie et al. 1996; Watanabe et al. 1996; Weber et al. 1997; Balmanno et al. 1999; Page et al. 1999; Talarmin et al. 1999; Villanueva et al. 2007). The transcriptional regulation of cyclin D1 by the Raf MAPK cascade has yet to be determined in kidney proximal tubule cells or renal tumorigenesis.

To study the role of Raf MAPK regulation of cyclin D1 in tuberous sclerosis renal tumor formation, we utilize the Eker rat (*Tsc-2*$^{EK/+}$) model. The Eker rat (*Tsc-2*$^{EK/+}$) is a derivative of the Long-Evans strain, bearing a mutation in one allele of the *Tsc-2* gene, which predisposes these animals to renal cancer (Eker et al. 1961; Everitt et al. 1992; Walker et al. 1992; Yeung et al. 1993; Kobayashi et al. 1995). A germline insertion of an endogenous retrovirus in the *Tsc-2* gene is responsible for the predisposing Eker mutation

(Yeung et al. 1994; Hino et al. 1995). Treatment of wild-type (*Tsc-2*$^{+/+}$) and mutant (*Tsc-2*$^{EK/+}$) Eker rats with 2,3,5-*tris*-(glutathion-*S*-yl)hydroquinone (TGHQ), a potent nephrotoxic (Peters et al. 1997) and nephrocarcinogenic (Lau et al. 2001) metabolite of HQ, induced preneoplastic lesions, including toxic tubular dysplasias, and increased the incidence of renal tumors only in animals carrying the mutant *Tsc-2*$^{EK/+}$ allele (Lau et al. 2001). Loss of heterozygosity (LOH) at the *Tsc-2* locus occurred in the tumors and the toxic tubular dysplasias, consistent with TGHQ-induced loss of tumor suppressor function of the *Tsc-2* gene (Lau et al. 2001). Tuberin null renal tumors, formed in 4-month TGHQ-treated-*Tsc-2*$^{EK/+}$ rats, displayed high ERK kinase activity, as well as high levels of cyclin D1 protein expression (Yoon et al. 2002).

Additionally, TGHQ is mutagenic and can transform primary renal epithelial cells isolated from Eker rats *in vitro,* giving rise to the quinol-thioether-transformed rat renal epithelial (QTRRE) cell lines (Yoon et al. 2001). These cells are tuberin null due to loss of heterozygosity (LOH) at the Tsc2 gene locus (Yoon et al. 2001), and give rise to tumors when subcutaneously injected into athymic nude mice (Patel et al. 2003). QTRRE cells exhibit elevated ERK, B-Raf and Raf-1 kinase activity (Yoon et al. 2002; Yoon et al. 2004), and increased expression of cyclin D1 compared to HK2 or LLCPK1 cells (**Chapter 4**). Restoration of tuberin expression in QTRRE cells decreases ERK, B-Raf, and Raf-1 activity, suggesting that tuberin modulates the Raf/MEK/ERK upstream of Raf (Yoon et al. 2002; Yoon et al. 2004). Furthermore, transient transfection of *Tsc-2* plasmid in QTRRE cells results in a decrease in cyclin D1 protein levels.

The LOH in the *Tsc-2* gene and subsequent loss of tuberin expression observed in TGHQ induced renal tumors (Lau et al. 2001; Yoon et al. 2002) and tumorigenic

QTRRE cells (Yoon et al. 2001), makes this a unique model to study the role of constitutive Raf/ERK MAP kinases in tuberin deficient renal carcinogenesis. In this study, we examine the relationship between the B-Raf/Raf-1/ERK MAP kinase cascade and cyclin D1 in renal tumorigenesis.

2.2. Materials and Methods

2.2.1. TGHQ renal tumor formation in Eker rats

Male Eker rats (wild-type, *Tsc-2*$^{+/+}$, and mutant, *Tsc-2*$^{EK/+}$), 8 weeks old, were obtained from the University of Texas MD Anderson Cancer Center, Smithville, TX. The animals were housed according to a 12:12-h light-dark cycle and allowed food and water *ad libitum*. TGHQ was synthesized as previously described and used at >98% purity, as determined by high performance liquid chromatography (Lau et al. 1988). The rats were divided into four subgroups: 1) *Tsc-2*$^{EK/+}$ control, 2) *Tsc-2*$^{EK/+}$ TGHQ-treated, 3) *Tsc-2*$^{+/+}$ control and 4) *Tsc-2*$^{+/+}$ TGHQ-treated. The rats were administered TGHQ [2.5 μmol/kg in 0.5 ml of 1x phosphate-buffered saline (PBS), i.p.] 5 days a week for 4 months; then increased to 3.5 μmol/kg for 4 months, according to previously established protocol (Lau et al. 2001). Control rats were administered PBS only. The TGHQ dosing solution was prepared fresh in 1xPBS daily. The animals were euthanized by CO_2 asphyxiation. For histological studies, a mid-sagital longitudinal section of the left kidneys was fixed in 10% phosphate-buffered formalin and paraffin embedded. For biochemical assays, the outer-strip of the outer medulla (OSOM), cortex, and renal tumors were excised, frozen immediately in liquid nitrogen, and stored at -80^{o}C.

2.2.2. Cell culture

The tuberin-negative cell line QTRRE was established from primary renal epithelial cells (Yoon et al. 2001). QTRRE cells were grown in DMEM/F12 (1:1) (Invitrogen, Carlsbad, California) with 10% FBS. Cells were grown at 37°C in a humidified atmosphere of 5% CO_2.

2.2.3. Immunohistochemistry

The formalin-fixed, paraffin-embedded kidney sections were sliced into 5 μm sections, de-paraffinized in xylene, and dehydrated by decreasing concentrations of ethanol. The sections were incubated in 0.5% hydrogen peroxide to quench endogenous peroxidase activity. Next, the slides were placed in 10 mM sodium citrate buffer (pH 6.0) and heated at 100°C to unmask antigens. The slides were then incubated with cyclin D1 (A-12) (Santa Cruz) 1:200 dilution for 1hr, followed by incubation with biotin-conjugated secondary antibody, AB enzyme reagents, and peroxide substrate solution provided in the ABC staining kit (Santa Cruz). Counterstaining was performed with hematoxylin. Color was fixed with acid alcohol and dehydration steps. Slides were mounted with Permount mounting media.

2.2.4. MTS Proliferation Assay

QTRRE cells were seeded at 3.1×10^3 cells/well in 96-well flat-bottomed plates in DMEM/F12 with 10% FBS. At 80-90% confluency cells were treated with 50 μM sorafenib or PD 98059 in DMEM/F12 with 2% FBS for 5, 25, 60, 90 min and 24 h. Following sorafenib or PD 98059 incubation, cells were washed twice with treatment media (DMEM (-) phenol red, (-) Na pyruvate, (+) 25 mM Hepes, (+) L-glutamine) (Invitrogen) and the proliferative activity of cells was determined by MTS assay (CellTiter 96 Non-Radioactive Cell Proliferation Assay; Promega, Madison, WI), according to the manufacturer's recommendations. In metabolically active cells, MTS was reduced by dehydrogenase enzymes into a formazan product that was soluble in tissue culture medium. The absorbance of the formazan at 490nm was measured in a

SpectraMax M2 (Molecular Devices, Sunnyvale, CA) 96-well plate reader. Values represent means ± SD (n=6).

2.2.5. Neutral Red Cell Viability Assay

QTRRE cells were seeded at a density of 5 x 10^4 cells/well in twenty-four-well plates. At 80-90% confluency cells were treated with 50 μM sorafenib or PD 98059 in DMEM/F12 with 2% FBS for 0.5, 1, 1.5, 2, and 24 h. Following dosing, cells were washed with HBSS, and then incubated with 50 μg/ml neutral red solution in DMEM (no phenol red) for 1 h at 37°C/5% CO_2. The neutral red solution was removed and cells were washed with fixation solution (1% formaldehyde/1% $CaCl_2$ mixture) for 2 min. This was followed by extraction using 1% glacial acetic acid/50% ethanol solution for 15 min at room temperature in the dark. Neutral red dye accumulation in lysosomes was assessed by measuring the absorbance at 540 nm. Values represent means ± SD (n=4).

2.2.6. Trypan Blue Cell Viability Assay

QTRRE cells were seeded at a density of 2.5 x 105 cells/well in twelve-well plates. At 80-90% confluency cells were treated with 50 μM sorafenib or PD 98059 in DMEM/F12 with 2% FBS for 0.5, 1, 2, and 24 h. Following treatment, cells were washed with PBS, incubated with 10% trypsin for 5 min at 37˚C/5% CO2, and trypsinization quenched with DMEM/F12 with 10% FBS. Detached cells were mixed with equal volume of trypan blue solution (Cellgrow) and counted on a haematocytometer. Values are means ± SD (n=3).

2.2.7. siRNA transfection

QTRRE or were seeded at a density of 3 x 10^5 cells/well in six-well plates. When cells were 50-60% confluent, each well was replaced with 1.7 ml fresh media. For transfection, 100 nM B-Raf or Raf-1 ON_TARGETplus SMARTpool siRNA, or siCONTROL Non-Targeting siRNA #5 (Dharmacon RNA Technologies, NY) was combined with 100 µl of serum-free DMEM/F12 media and incubated for 5 min at RT. In parallel, 5 µl of DharmaFECT #2 was incubated in 200 µl serum-free DMEM/F12 for 5 min at RT. siRNA solution (100 µl) was then combined with the 200 µl DharmaFECT #2 solution and incubated for 20 min at RT. The siRNA-DharmaFECT complex solution was added directly to each well, mixed gently and incubated for 24, 48, 72, or 96 h at 37°C in a CO_2 incubator.

2.2.8. Real-Time-PCR determination of B-Raf and Raf-1

Total RNA from B-Raf, Raf-1, or control siRNA transfected in QTRRE cells were isolated with TRIReagent (Sigma) utilizing the manufacturer's protocol, and 4.5 µg RNA, in a 20 µl total reaction volume, was reverse transcribed using the Fermentas First Strand cDNA Synthesis kit according to the manufacturer's protocol. Amplification of B-Raf, Raf-1, or GAPDH for Real-Time-PCR was performed in a volume of 20 µl, containing 2 µl of cDNA, 4 µl Roche Universal PCR Master Mix (Roche Applied Science, Indianapolis, IN), and 1 µl gene-specific TaqMan Gene Expression Assay primer/probe mix (Applied Biosystems). The probes are labeled with the 5' reporter dye, FAM, and a nonfluorescent quencher at the 3' end of the probe. The Light Cycler 2.0 (Roche Applied Science, Indianapolis, IN) was programmed to cycle at 95°C for 10 min,

followed by 40 cycles of 95°C for 15 sec alternating with 60°C for 1 min. Each tissue group was analyzed in triplicate for B-Raf and GAPDH, with RNA extracted from three rats per group. The statistical analysis of relative amounts of transcripts between samples was analyzed as follows: cycle threshold values (C_T) for B-Raf and Raf-1 were normalized to GAPDH C_T values, the average and standard deviation were calculated with the normalized C_T values in each group, and the 2-tailed student T-test with non-equal variance; p values less than 0.05 were considered to be statistically significant.

2.2.9. Western blot analysis

The OSOM of kidney tissue, renal tumors, and QTRRE cells were homogenized with Cell Lysis Buffer 10X (Cell Signaling Technology, Inc, Beverly, MA) containing 1 mM Pefabloc SC (Roche) and Complete protease inhibitor cocktail tablets (Roche). Protein concentration was determined with the DC Protein Assay (BioRad). Protein was subjected to 7, 10 or 12% SDS-PAGE and proteins were electrophoretically transferred to PVDF membranes. Primary antibodies used were cyclin D1 (A-12), B-Raf (H-145), and Raf-1 (C-20) purchased from Santa Cruz Biotechnologies; p42/44 and phospho-p42/44 (T202/Y204) (20G11) purchased from Cell Signaling Technologies, and GAPDH (Ambion, Austin, Texas). The secondary-immunoglobulin conjugated with horseradish peroxidase (Santa Cruz Biotechnology, CA) was used at a 1:3000 dilution. The blots were visualized with Amersham ECLTM Western Blotting Detection Reagents (GE Healthcare, UK).

2.2.10. Reverse Transcription (RT)-Polymerase Chain Reaction (PCR) of cyclin D1

Total RNA from sorafenib (50 μM) and PD 98059 (50 μM) treated QTRRE cells was isolated with TRIReagent (Sigma) utilizing manufacturer's protocol, and 4.5 μg RNA, in a 20 μl total reaction volume, was reverse transcribed using the Fermentas First Strand cDNA Synthesis kit according to the manufacturer's protocol. PCR products were generated using the Advantage cDNA PCR kit (Clontech, Mountain View, CA) according to manufacturer's protocol. Amplicon sizes and primers were as follows: 233 bp cyclin D1 (forward: 5'-GCG TAC CCT GAC ACC AAT CT-3', reverse: 5'-GGC TCC AGA GAC AAG AAA CG-3'), 228 bp actin-beta (forward: 5'-AGC CAT GTA CGT AGC CAT CC-3', reverse: 5'-CTC TCA GCT GTG GTG GTG AA-3'). The thermocycling conditions for cyclin D1 were 95°C for 5 minutes; then 28 cycles of 95°C for 30 seconds, 59°C for 40 seconds, and 72°C for 60 seconds, followed by a 10 minute 72°C final extension. The thermocycling conditions for actin-beta were 95°C for 2 minutes; then 26 cycles of 95°C for 15 seconds, 55°C for 30 seconds, and 72°C for 60 seconds, followed by a 10 minute 72°C final extension. PCR products were separated on 2% ethidium bromide stained agarose gel. Each PCR reaction was repeated twice to confirm reproducibility.

2.2.11. Statistics

Data are expressed as means ± standard deviation. Mean values were compared using a Students T-test, two tails, with equal variances.

2.3. Results

2.3.1. TGHQ-induced expression of cyclin D1

Cyclin D1 facilitates tumor growth by promoting the transition from G_0/G_1 to S phase, and by modulating a number of proteins involved in transcriptional activation (Coqueret 2002; Alao 2007). Loss of tuberin expression results in an increase in cyclin D1 protein expression, inducing quiescent cells to enter S phase and subsequently, an increase in proliferation (Soucek et al. 1997; Soucek et al. 1998; Yoon et al. 2002). In the present study, we investigated the expression of cyclin D1 protein in TGHQ-treated rats. Western immunoblotting demonstrated that cyclin D1 protein expression was not increased in the OSOM until 6-months of TGHQ treatment (**Figure 2.1B**), with the largest increase occurring in renal tumors formed in the 8-month-TGHQ-treated *Tsc-2*$^{EK/+}$ rats (**Figure 2.1C**). In both the 6- and 8-month treatment groups, cyclin D1 expression was more elevated in the OSOM of TGHQ-*Tsc-2*$^{EK/+}$ rats than TGHQ-*Tsc-2*$^{+/+}$ rats. Importantly, the vehicle treated animals did not exhibit a rise in cyclin D1 expression compared to naïve animals at any time-point, indicating that there was no injection/stress induced proliferation occurring (**Figure 2.1**). Immunohistochemical (IHC) staining revealed that cyclin D1 is increased in proximal tubules of *Tsc-2*$^{+/+}$ and *Tsc-2*$^{EK/+}$ rats treated with TGHQ for 4-months (**Figure 2.2**). Compared to saline treated animals, IHC staining for cyclin D1 was greater in *Tsc-2*$^{EK/+}$ rats relative to *Tsc-2*$^{+/+}$ (**Figure 2.2**). The differences in the observation of increases in cyclin D1 between the Western and IHC analyses is probably simply due to differences in the sensitivity of the two assays. These results are in keeping with previous findings that cell proliferation per se is necessary, but not sufficient for tumor development, and that additional genetic alterations (i.e. loss of

the wild-type *Tsc-2* allele) play an important role in TGHQ-induced nephrocarcinogenesis (Yoon et al. 2002).

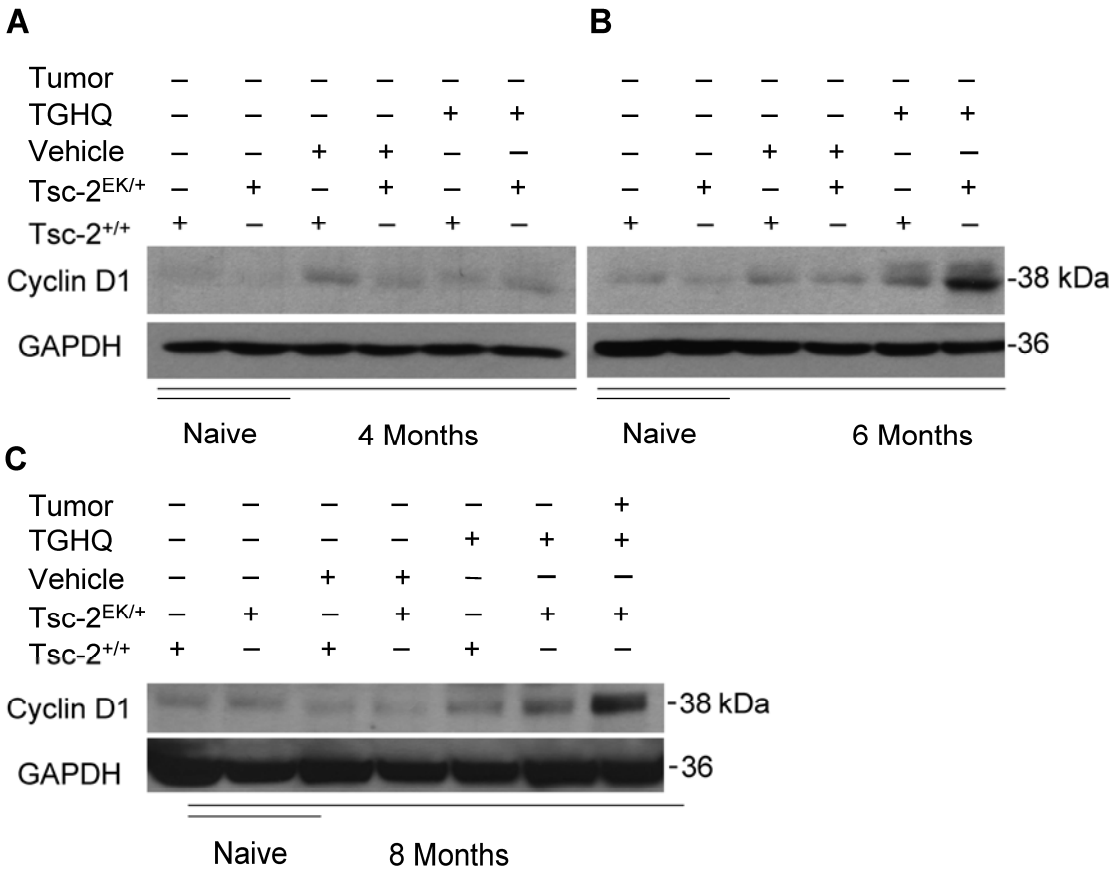

Figure 2.1. TGHQ induces cyclin D1 expression in OSOM and renal tumors from *Tsc-2*$^{EK/+}$ rats.

TGHQ induces cyclin D1 expression in OSOM and renal tumors from *Tsc-2*$^{EK/+}$ rats. Cyclin D1 was visualized by Western blot analysis of tissue obtained from *Tsc-2*$^{+/+}$ or *Tsc-2*$^{EK/+}$ rats treated with TGHQ or saline for (*A*) 4-months *(B)* 6-months or *(C)* 8-months (OSOM and renal tumor). GAPDH (bottom panels) *(A-C)* was used as a loading control. Similar results were obtained in multiple tissue samples.

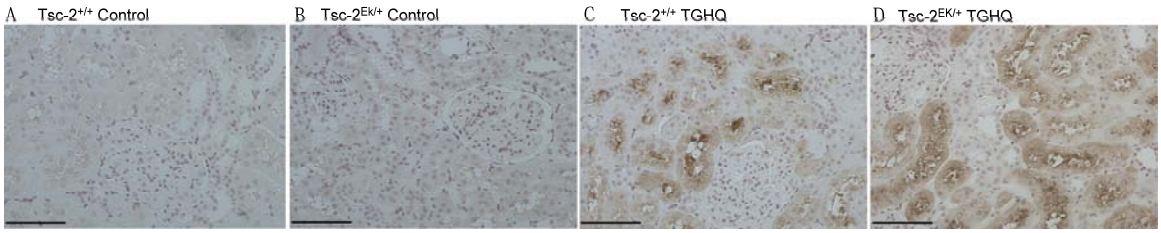

Figure 2.2. Immunohistochemical detection of cyclin D1 expression in renal tissue.

Kidney slices immunoblotted for cyclin D1, from *(A) Tsc-2*$^{+/+}$ rats treated with saline *(B) Tsc-2*$^{EK/+}$ rats treated with saline *(C) Tsc-2*$^{+/+}$ treated with 2.5 μmol/kg (ip) of TGHQ for 4 months and *(D) Tsc-2*$^{EK/+}$ rats treated with 2.5 μmol/kg (ip) of TGHQ for 4 months. Scale bars, 200 μm

2.3.2. Increases in B-Raf/Raf-1/p-ERK kinases during renal tumor formation.

The ser/thr kinase Raf-1 is ubiquitously expressed in all tissues and cell types, but B-Raf has restricted expression (Wellbrock et al. 2004). Each Raf isoform is differentially and dynamically activated, carrying out distinct functions in cells (Garnett et al. 2005). Western blot analysis of the OSOM of 4- or 6-month vehicle- or TGHQ-treated-*Tsc-2*$^{EK/+}$ and *Tsc-2*$^{+/+}$ rats revealed that B-Raf was not detected earlier than 8-months of TGHQ treatment (**Figure 2.3A and 2.3B**); but there was an induction of B-Raf protein in a spontaneous tumor formed in a 6-month vehicle-treated-*Tsc-2*$^{EK/+}$ rat (**Figure 2.3A**). Western blot analysis of the OSOM of 8-month-vehicle-control *Tsc-2*$^{EK/+}$ and *Tsc-2*$^{+/+}$ rats revealed that neither animal had detectable levels of B-Raf, but both expressed equivalent levels of Raf-1 (**Figure 2.3B**). Although Raf-1 induction was observed within 8-month-TGHQ-*Tsc-2*$^{EK/+}$ OSOM and renal tumors, there was a more substantial induction of B-Raf (**Figure 2.3B**). Non-specific binding of the B-Raf antibody in tissue prevented us from obtaining IHC data. A previous study demonstrated that renal tumors derived from TGHQ-treated *Tsc-2*$^{EK/+}$ rats had significantly elevated ERK activity compared to the OSOM tissue from all other treatment groups (Yoon et al. 2002). To confirm that the induction of Raf proteins in TGHQ-tumors corresponds with an increase in MAP kinase activity, we probed for pERK by Western blot analysis. Concomitant with the increase in B-/Raf-1 protein expression, there was a parallel increase in pERK1/2 expression in TGHQ-*Tsc-2*$^{EK/+}$ tumors; with little observed change in total ERK1/2 or GAPDH (**Figure 2.3C**).

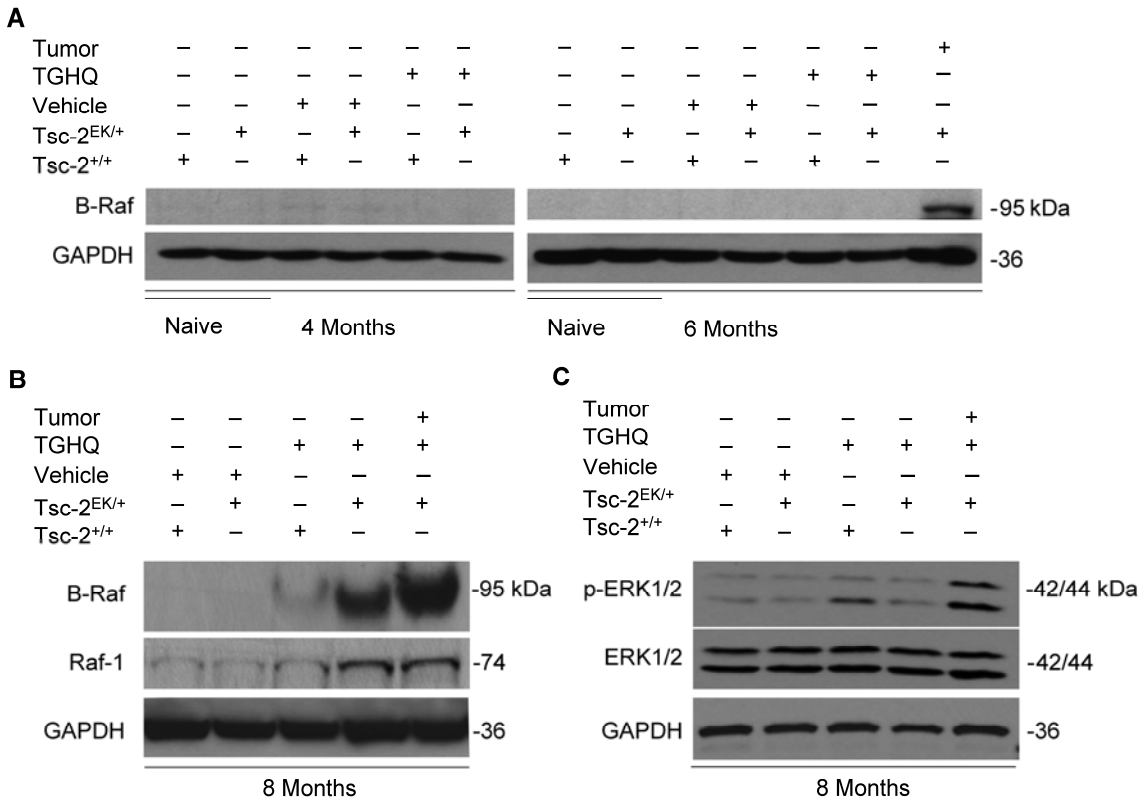

Figure 2.3. Raf-1, B-Raf, and p-ERK1/2 ptotein levels are elevated in TGHQ-induced renal tumors from *Tsc-2*$^{EK/+}$ rats.

Whole tissue lysates from the OSOM or from renal tumors of 4, 6, or 8-month-vehicle or TGHQ treated *Tsc-2*$^{+/+}$ and *Tsc-2*$^{EK/+}$ rats were immunoblotted for (*A*) B-Raf in 4 or 6-month tissues (*B*) B-Raf (top panel) and Raf-1 (middle panel) in 8-month tissues *(C)* p-ERK1/2 (T202/Y204) (top panel) and ERK1/2 (middle panel) in 8-month tissues. GAPDH *(A-C,* bottom panels*)* was used as a loading control. Similar results were obtained in multiple tissue samples.

2.3.3. Sorafenib treatment decreases mitochondrial dehydrogenase enzyme activity and lysosomal membrane integrity in QTRRE cells

Mitochondrial dehydrogenase enzyme activity was quantified using the MTS assay, which measures the reduction of MTS to formazan. Lysosomal membrane integrity was measured by neutral red dye uptake, and dye accumulation in lysosomes (**Figure 2.4A**). The small molecule inhibitor, sorafenib, is a new cancer therapeutic utilized in the treatment of advanced renal cell carcinoma (RCC). Sorafenib is a dual-action Raf kinase and vascular endothelial growth factor receptor inhibitor that targets tumor cell proliferation and tumor angiogenesis (Wilhelm et al. 2004). Treatment of QTRRE cells with sorafenib resulted in a sustained decrease in both cellular mitochondrial dehydrogenase enzyme activity and lysosomal membrane integrity over the 2 h time course, with a maximum decrease of greater than 80% by 24 h (**Figure 2.4A**). Although mitochondrial dehydrogenase enzyme activity and lysosomal membrane integrity were severely impaired, by 65% and 75% respectively, following 1.5 or 2 h of sorafenib treatment, only a 20% decrease in cellular membrane integrity was measured by the trypan blue assay (**Figure 2.4A**). By 24 h a 90% loss of cell viability was observed (**Figure 2.4A**). Thus, decreases in mitochondrial dehydrogenase enzyme activity and lysosomal membrane integrity precede overt cell death. Conversely, treatment of QTRRE cells with PD 98059, a MEK1/2 kinase inhibitor, resulted in a nominal but significant decrease in mitochondrial dehydrogenase enzyme activity after 5 and 25 min but complete metabolic recovery occurred by 90 min (**Figure 2.4B**). Furthermore, there was no significant decrease in lysosomal membrane integrity (neutral red assay) or cellular membrane integrity (trypan blue assay) over the 24 h time course following PD 98059 treatment (**Figure 2.4B**).

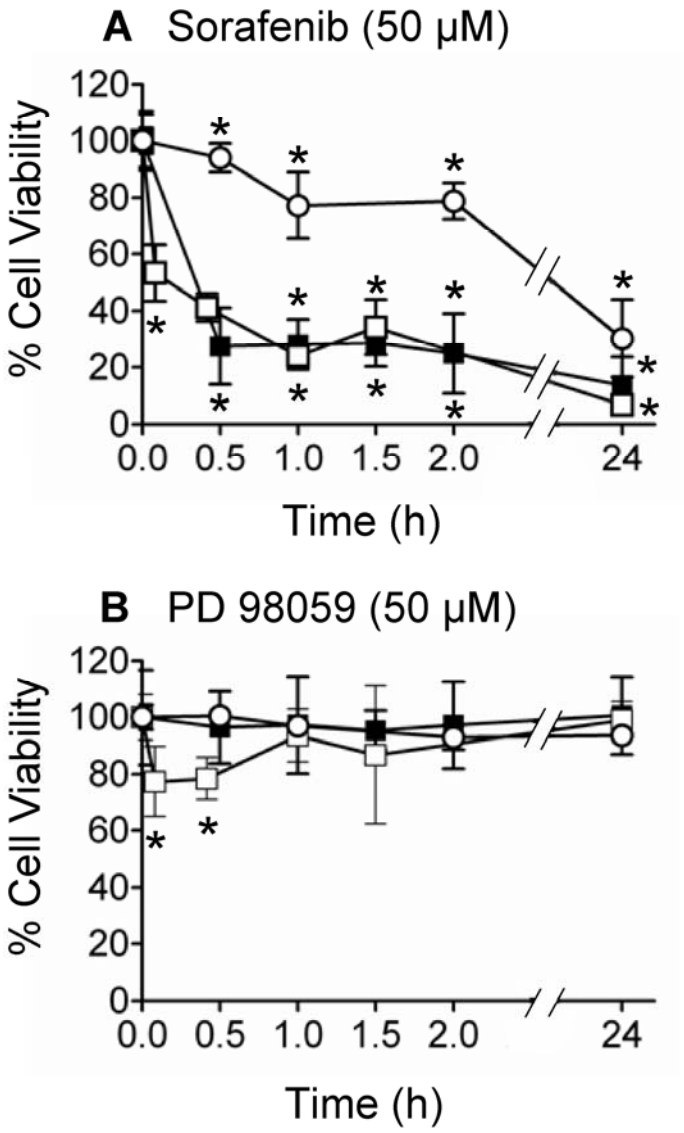

Figure 2.4. Effect of sorafenib or PD 98059 on mitochondrial dehydrogenase enzyme activity, lysosomal membrane integrity, and membrane integrity in QTRRE cells.

QTRRE cells were treated with 50 µM (A) sorafenib or (B) PD 98059 for various time points as indicated. Control cells were treated with an equal volume of DMSO. Mitochondrial dehydrogenase activity (□) of QTRRE cells affected by sorafenib or PD 98059 was quantitated using the CellTiter 96® Aqueous Non-Radioactive Cell Proliferation (MTS) Assay (Promega). Values represent the mean ± SD (n=6). Lysosomal membrane integrity (■) was determined by measuring neutral red (NR) accumulation in QTRRE cells at 540 nm. NR uptake is expressed in percentage terms relative to the DMSO control. Values represent the mean ± SD (n=4). Plasma membrane integrity (○) in QTRRE cells was measured by trypan blue exclusion. Values are means ± SD (n=3). A significant difference was seen between control (DMSO) and sorafenib or PD 98059 treated cells at * $P<0.01$.

2.3.4. Raf-1 regulates cyclin D1 protein levels

QTRRE cells, which are null for tuberin, express high levels of pERK1/2 and cyclin D1, as well as elevated ERK activity, all of which are reduced following restoration of tuberin expression (Yoon et al. 2004). To investigate whether Raf and MEK1/2 kinases contribute to high cyclin D1 protein levels in QTRRE cells, cyclin D1 was measured by Western blotting following treatment of cells with the Raf kinase inhibitor, sorafenib (50 μM), or the MEK1/2 kinase inhibitor PD 98059 (50 μM). There was a time-dependent disappearance in cyclin D1 protein subsequent to treatment with either of the inhibitors. Cells treated with sorafenib experienced a 50% reduction in cyclin D1 protein level by 45 min (**Figure 2.5A**). Continued reductions in cyclin D1 protein by sorafenib were observed at 90 min (**Figure 2.5A**). Similarly, treatment with PD 98059 resulted in a 50% reduction in cyclin D1 protein level by 25 min (**Figure 2.5B**) with maximal reduction at 60 min (**Figure 2.5B**). Sorafenib or PD 98059 treatment both resulted in an immediate (5 min) decrease in pERK1/2 (**Figure 2.5**). Treatment with sorafenib resulted in a sustained decrease in pERK1/2 over a 5 to 60 min period (**Figure 2.5A**); in contrast suppression of pERK1/2 by PD 98059 was reversed between 25 to 60 min (**Figure 2.5B**). The decrease in pERK following treatment with each inhibitor (**Figure 2.5**) correlated with the changes in metabolic activity measured in the MTS assay (**Figure 2.5**). There was little change in total ERK1/2 or GAPDH protein expression following treatment of cells with either inhibitor (**Figure 2.5**), indicative of selective drug action on metabolic function in the presence of sustained cell viability (**Figure 2.5**).

To identify which Raf isoform contributes to MAPK regulation of cyclin D1 protein levels, QTRRE cells were transfected with B-Raf or Raf-1 siRNA for 72 and 96

h. Real-time-PCR analysis of both Raf isoforms, following 48 h siRNA treatment, revealed an approximate 95% decrease in Raf mRNA levels (data not shown). Western blot analysis of Raf-1 siRNA knockdown resulted in a maximal 60% decrease in cyclin D1 protein levels by 96 h post-transfection (**Figure 2.6A**); whereas QTRRE cells treated with B-Raf siRNA experienced a maximal 20% reduction in cyclin D1 by 72 h (**Figure 2.6B**). Both Raf siRNA's were target specific, and neither Raf siRNA produced a significant change in GAPDH protein expression.

2.3.5. Cyclin D1 mRNA remains unchanged following MAPK inhibition

The expression of cyclin D1 mRNA was not affected by sorafenib (**Figure 2.7A**) or PD 98059 (**Figure 2.7B**) treatment, indicating that neither sorafenib nor PD 98059 transcriptionally regulated cyclin D1 expression.

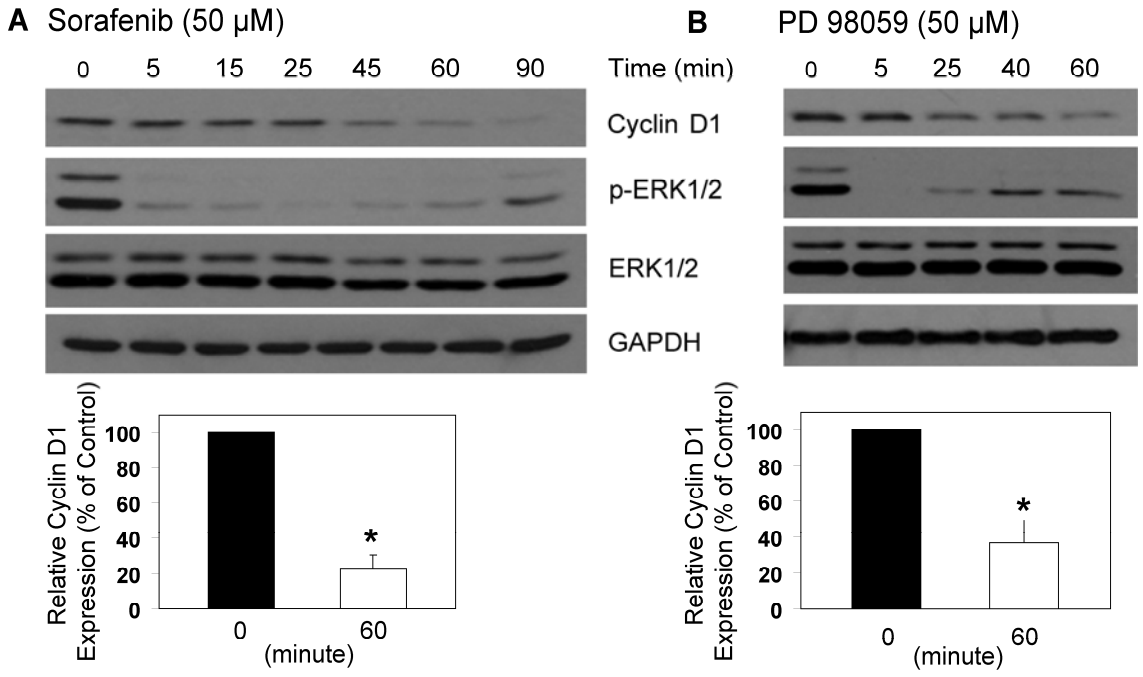

Figure 2.5. Inhibition of Raf and MEK kinases in QTRRE cells causes a decrease in cyclin D1 and p-ERK1/2 (T202/Y204) expression.

QTRRE cells were treated for 5, 15, 25, 45, 60, and 90 min with (A) sorafenib (50 μM), or for 5, 25, 40, and 60 min with (B) PD 98059 (50 μM). Equal amounts of extracted lysates were subjected to SDS-PAGE and immunoblotting with antibodies specific to cyclin D1, p-ERK1/2, ERK1/2, and GAPDH. Values represent the mean ± SD (n=3). A significant difference was seen between control (DMSO) and sorafenib or PD 98059 treated cells at * $P<0.01$.

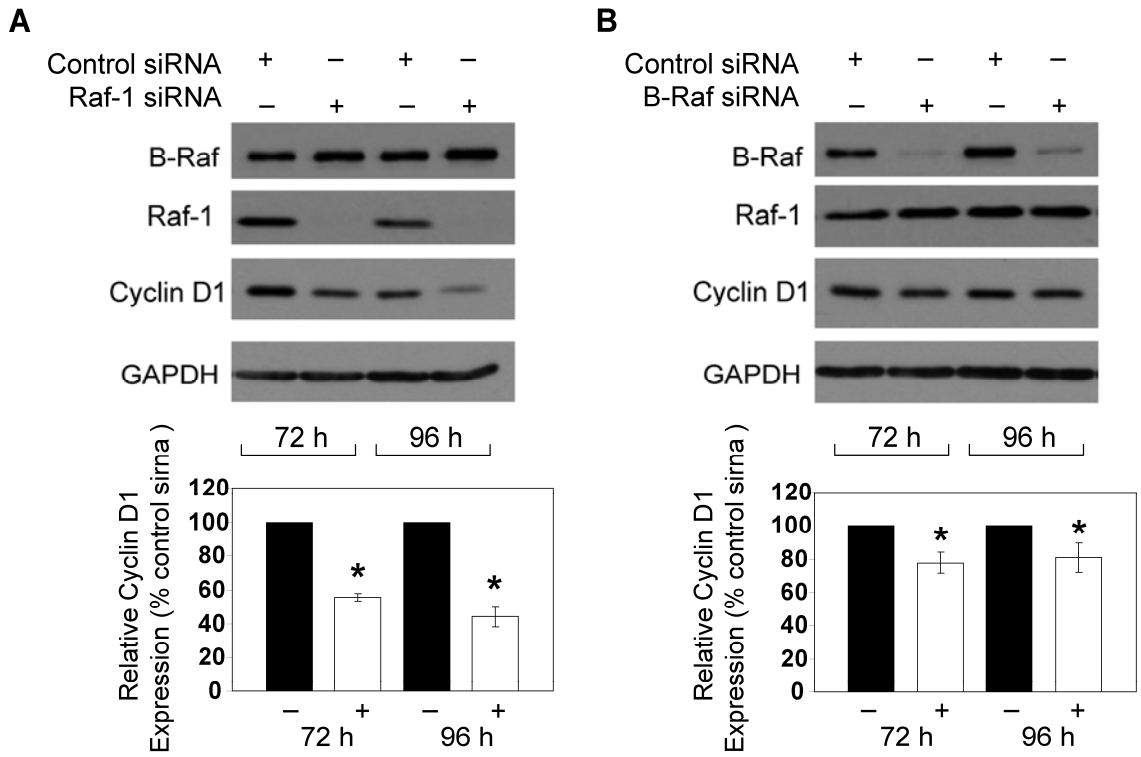

Figure 2.6. Raf-1 is the dominant regulator of cyclin D1 protein levels in QTRRE cells.

QTRRE cells were transfected with 100 nM (A) B-Raf or (B) Raf-1 ON_TARGETplus SMARTpool siRNA or siCONTROL Non-Targeting siRNA #5 (Dharmacon RNA Technologies, NY). The siRNA-DharmaFECT complex solution was incubated with cells for 72 or 96 h. Whole cell lysates were subjected to Western blotting with antibodies specific to B-Raf, Raf-1, cyclin D1, and GAPDH. Values represent the mean ± SD (n=3). A significant difference was seen between control siRNA and Raf-1 or B-Raf siRNA treated cells at * $P<0.05$.

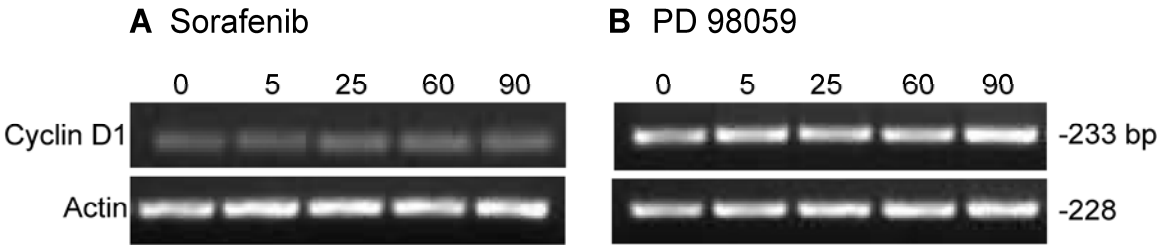

Figure 2.7. Inhibition of Raf and MEK kinases has no effect on cyclin D1 mRNA levels in QTRRE cells.

QTRRE cells were treated with (A) sorafenib (50 μM) or (B) PD 98059 (50 μM) for 5, 25, 60 and 90 min. PCR products were resolved by agarose gel electrophoresis. Similar results were obtained in three separate experiments.

2.4. Discussion

We describe a novel pathway by which the Raf/MEK/ERK MAP kinase cascade regulates cyclin D1 protein levels in tumorigenic proximal tubule cells (**Figure 2.5 and 2.6**). In our tuberin null kidney tumors and tumorigenic QTRRE cells we found that: (i) renal tumors expressed high protein levels of cyclin D1 (**Figure 2.1**), B-Raf , Raf-1, and p-ERK (**Figure 2.3**) (ii) treatment with sorafenib (Raf inhibitor) and PD 98059 (MEK inhibitor) in QTRRE cells resulted in a decrease in cyclin D1 protein levels (**Figure 2.5**), but no change in cyclin D1 mRNA levels (**Figure 2.7**) and (iv) Raf-1 and B-Raf siRNA knockdown in QTRRE cells elucidated Raf-1 as the dominant Raf responsible for regulating cyclin D1 protein levels (**Figure 2.6**).

Downstream signaling from ERK mediates gene expression, metabolism and cytoskeletal rearrangements, and dysregulation of the pathway alters normal cell growth, differentiation, senescence and survival (Wellbrock et al. 2004). Hyperactivation of the ERK pathway occurs in over 30% of cancer patients (Wellbrock et al. 2004). Consistent with the high occurrence of ERK activity in a number of cancers, renal tumors derived from *Tsc*-$2^{EK/+}$ rats treated for 8 months with TGHQ express elevated protein levels of B-Raf, Raf-1, and p-ERK (**Figure 2.3**) as well as increased kinase activity (Yoon et al. 2002). Furthermore, malignantly transformed QTRRE cells, null for tuberin, also display increased Raf-1, B-Raf, and ERK kinase activity (Yoon et al. 2004). Thus ERK hyperactivation in RCC is associated with loss of tuberin expression, suggesting that ERK regulation lies downstream of tuberin.

Previous studies, in a variety of cell types, have correlated sustained ERK activation with the induction of cyclin D1 mRNA (Lavoie et al. 1996; Watanabe et al.

1996; Weber et al. 1997; Balmanno et al. 1999; Page et al. 1999; Talarmin et al. 1999; Villanueva et al. 2007). A 6.5 fold increase in cyclin D1 gene expression occurs in kidney tumors derived from TGHQ-treated Tsc-$2^{EK/+}$ rats (Patel et al. 2003). QTRRE cells and renal tumors express constitutively high protein levels of cyclin D1 (**Figure 2.1**). Therefore, the Raf/ERK cascade may be modulating the transcription of cyclin D1 during renal tumor development. The inhibition of Raf and MEK kinases in QTRRE cells led to a decrease in cyclin D1 protein levels (**Figure 2.5**). Furthermore, treatment of cells with B-Raf and Raf-1 siRNA pinpoints Raf-1 as the dominant Raf regulating cyclin D1 protein levels (**Figure 2.6**). The Raf/MEK/ERK cascade is well established in the literature to directly alter the levels and activities of key transcription factors (Ekl-1, c-Myc, c-Jun, c-Fos, NF-IL6, p62TCF, and ATF-2) (Alvarez et al. 1991; Marais et al. 1993; Davis 1995), resulting in altered transcription of genes important for the cell cycle, such as cyclin D1 (Lavoie et al. 1996; Watanabe et al. 1996; Weber et al. 1997; Balmanno et al. 1999; Page et al. 1999; Talarmin et al. 1999; Villanueva et al. 2007). Unexpectedly, we found no change in cyclin D1 mRNA levels (**Figure 2.7**) following treatment with Raf and MEK inhibitors in QTRRE cells.

The lack of transcriptional regulation of cyclin D1 by ERK is intriguing and warrants further investigation. It is established that the tuberin/Rheb/mTOR/4EBP1 cascade regulates cyclin D1 translation. The hierarchical phosphorylation of 4EBP1 facilitates a complex and dynamic disassociation of 4EBP1 from eIF4E, thus resulting in eIF4E cap-dependent translation of cyclin D1 (Gingras et al. 1999; Gingras et al. 2001; Jiang et al. 2008). Although mTOR is the only kinase known to directly phosphorylate 4EBP1, data suggest that ERK may also play a role in the hierarchical phosphorylation of

4EBP1 (Haystead et al. 1994). Therefore, we will explore the potential crosstalk between ERK and 4EBP1 in **Chapter 3**.

CHAPTER 3: RAF-1 REGULATES ERK CROSSTALK WITH 4EBP1

3.1. Introduction

Hyperphosphorylation of the eukaryotic translation initiation factor 4E binding protein 1 (4EBP1) is associated with a variety of high grade tumors (Kremer et al. 2006; Rojo et al. 2007). When 4EBP1 is hypophosphorylated it is bound to eukaryotic translation initiation factor 4E (eIF4E), blocking eIF4E-complex cap-dependent initiation of translation (Gingras et al. 1999). The hierarchical phosphorylation of 4EBP1 on four proline-directed sites (ser/thr-Pro) suppresses 4EBP1's ability to bind and inhibit eIF4E, allowing for formation of the eIF4E complex and subsequent initiation of translation (Gingras et al. 1999; Gingras et al. 2001; Beugnet et al. 2003; Huang et al. 2008). Phosphorylation of 4EBP1 is abrogated by inhibition of the mammalian target of rapamycin complex 1 (mTORC1), comprised of TOR, Raptor, and LST8; which is highly sensitive to inhibition by rapamycin (Beretta et al. 1996; Gingras et al. 1999; Gingras et al. 2001; Beugnet et al. 2003; Shaw et al. 2006; Huang et al. 2008). Inhibition of mTORC1 is intricately regulated by the tuberous sclerosis complex (*TSC*) (Huang et al. 2008). Tuberous sclerosis is an autosomal dominant hereditary disease associated with the formation of hamartomas in multiple organs, and extensive renal disease (Okada et al. 1982; Stillwell et al. 1987; Osborne et al. 1991). Germ-line mutations in *Tsc-1* and *Tsc-2* genes results in cellular alterations in growth, survival, proliferation, angiogenesis, migration, and differentiation (Krymskaya 2003; Yeung 2003). Rats lacking one of the *Tsc-2* alleles (Eker rats) are predisposed to the development of renal tumors (Eker et al. 1961).

The gene products of *Tsc-1* (harmartin) and *Tsc-2* (tuberin) form a heterodimeric protein complex that negatively regulates the mTOR signaling pathways. Inhibition of mTOR by tuberin occurs through the GTPase-activating protein (GAP) activity of tuberin toward the small G protein Rheb, which acts upstream of mTOR (Inoki et al. 2003; Tee et al. 2003; Long et al. 2005). The carboxy-terminus of tuberin also shares sequence homology with a portion of the catalytic domain of the GAP for Rap1 (Wienecke et al. 1995). Rap1 bound to GTP can complex with both Raf-1 and B-Raf serine/threonine kinases, thus regulating cellular proliferation and differentiation through the Raf/MEK/ERK/MAP kinase signaling cascades, which is hyperactivated in approximately 30% of all cancers (Cook et al. 1993; Hu et al. 1997). Recent data indicate that activation of ERK signaling can negatively regulate tuberin by direct phosphorylation on Ser 664, thus disrupting the association between tuberin and harmartin, activating downstream mTOR signaling (Ballif et al. 2005; Ma et al. 2005). Additionally, in an *in vitro* kinase assay, recombinant 4EBP1 was a substrate for ERK/MAP kinase, suggesting that ERK may also play a role in the hierarchical phosphorylation of 4EBP1 (Haystead et al. 1994).

In this study, we examine the relationship between tuberin, the B-Raf/Raf-1/ERK MAP kinase cascade, and 4EBP1 hyperphosphorylation in our tuberin deficient renal tumor models: 2,3,5-*tris*-(glutathion-S-yl) hydroquinone (TGHQ) induced renal tumors in *Tsc-2*$^{EK/+}$ rats, TGHQ transformed *Tsc-2*$^{EK/+}$ cells (QTTRE), and QTRRE renal tumor xenografts in nude mice. These findings identify, for the first time, Raf-1 as an effective regulator of 4EBP1 phosphorylation and activator of cap-dependent translation in renal carcinogenesis.

3.2. Materials and Methods

3.2.1. Animal dosing and tissue preparation.

(A) TGHQ renal tumor formation in Eker rats. Male Eker rats (wild-type, *Tsc-2*$^{+/+}$, and mutant, *Tsc-2*$^{EK/+}$), 8 weeks old, were obtained from the University of Texas MD Anderson Cancer Center, Smithville, TX. The animals were housed according to a 12:12-h light-dark cycle and allowed food and water *ad libitum*. TGHQ was synthesized as previously described and used at >98% purity, as determined by high performance liquid chromatography (Lau et al. 1988). The rats were divided into four subgroups: 1) *Tsc-2*$^{EK/+}$ control, 2) *Tsc-2*$^{EK/+}$ TGHQ-treated, 3) *Tsc-2*$^{+/+}$ control and 4) *Tsc-2*$^{+/+}$ TGHQ-treated. The rats were administered TGHQ [2.5 μmol/kg in 0.5 ml of 1x phosphate-buffered saline (PBS), i.p.] 5 days a week for 4 months; then increased to 3.5 μmol/kg for 4 months, according to previously established protocol (Lau et al. 2001). Control rats were administered PBS only. The TGHQ dosing solution was prepared fresh in 1xPBS daily. The animals were euthanized by CO_2 asphyxiation. For histological studies, a mid-sagital longitudinal section of the left kidneys was fixed in 10% phosphate-buffered formalin and paraffin embedded. For biochemical assays, the outer-strip of the outer medulla (OSOM), cortex, and renal tumors were excised, frozen immediately in liquid nitrogen, and stored at -80^{o}C.

(B) Renal tumor xenograft nude mice. QTRRE-2 and -3 cell tumorigenicity in athymic NCI female nude mice was performed as described previously (Patel et al. 2003). Briefly mice 5-6 wk old were purchased from Taconic (Hudson, NY) and were maintained on a 12 h light/dark cycle and allowed food and water ad libitum. The animals were divided

into three groups (n = 2/group). Once QTRRE-2 or -3 cells reached log phase growth stage in culture, they were harvested and resuspended in matrigel (BD Biosciences, San Jose, California). The animals were injected subcutaneously at one site/animal with 5×10^6 cells/0.2 mL matrigel per site. When the size of a tumor reached 10-15 mm in diameter, the mice were euthanized, and sections of tumor were fixed in 10% phosphate-buffered formalin and embedded in paraffin, or snap frozen in liquid nitrogen and frozen in -80 ^{o}C.

3.2.2. Cell culture

The tuberin-negative cell line QTRRE was established from primary renal epithelial cells (Yoon et al. 2001) HK-2 (human kidney) cells were from American Type Culture Collection (Manassas, VA). HK2 and QTRRE cells were grown in DMEM/F12 (1:1) (Invitrogen, Carlsbad, California) with 10% FBS. Cells were grown at 37°C in a humidified atmosphere of 5% CO_2.

3.2.3. siRNA transfection

QTRRE or HK2 cells were seeded at a density of 3 x 10^5 cells/well in six-well plates. When cells were 50-60% confluent, each well was replaced with 1.7 ml fresh media. For QTRRE transfection, 100 nM B-Raf or Raf-1 ON_TARGETplus SMARTpool siRNA, or siCONTROL Non-Targeting siRNA #5 (Dharmacon RNA Technologies, NY) was combined with 100 µl of serum-free DMEM/F12 media and incubated for 5 min at RT. For HK2 transfection, 50 nM of Tsc2 ON_TARGETplus

SMARTpool siRNA or siCONTROL Non-Targeting siRNA pool (Dharmacon) was combined with 100 µl of serum-free DMEM/F12 media and incubated for 5 min at RT. In parallel, 5 µl of DharmaFECT #2 (QTRRE) or DharmaFECT #1 (HK2) was incubated in 200 µl serum-free DMEM/F12 for 5 min at RT. siRNA solution (100 µl) was then combined with the 200 µl DharmaFECT #2 (QTRRE) or #1 (HK2) solution and incubated for 20 min at RT. The siRNA-DharmaFECT complex solution was added directly to each well, mixed gently and incubated for 24, 48, 72, or 96 h at 37°C in a CO_2 incubator.

3.2.4. Western blot analysis

The OSOM of kidney tissue, renal tumors, HK-2 cells, and QT-RRE cells were homogenized with Cell Lysis Buffer 10X (Cell Signaling Technology, Inc, Beverly, MA) containing 1 mM Pefabloc SC (Roche) and Complete protease inhibitor cocktail tablets (Roche). Protein concentration was determined with the DC Protein Assay (BioRad). Protein was subjected to 7, 10 or 12% SDS-PAGE and proteins were electrophoretically transferred to PVDF membranes. Primary antibodies used were cyclin D1 (A-12), B-Raf (H-145), Raf-1 (C-20) and tuberin (C-20) purchased from Santa Cruz Biotechnologies; p42/44, phospho-p42/44 (T202/Y204) (20G11), 4EBP1, p-4EBP1 (Thr37/46), p-4EBP1 (Thr70), and p-4EBP1 (Ser65) purchased from Cell Signaling Technologies, and GAPDH (Ambion, Austin, Texas). The secondary-immunoglobulin conjugated with horseradish peroxidase (Santa Cruz Biotechnology, CA) was used at a 1:3000 dilution. The blots were visualized with Amersham ECLTM Western Blotting Detection Reagents (GE Healthcare, UK).

3.2.5. Statistics

Data are expressed as means ± standard deviation. Mean values were compared using a Students T-test, two tails, with equal variances.

3.3. Results

3.3.1. High p4EBP1 expression in renal tumors

The hierarchical phosphorylation of 4EBP1 plays a pivotal role in the dissociation of eIF4E from 4EBP1 and the initiation of eIF4E cap-dependent translation (Gingras et al. 1999). Recently, increased protein levels of 4EBP1 and p4EBP1 were correlated with high-grade prostate, breast and ovarian tumors (Castellvi et al. 2006; Kremer et al. 2006; Rojo et al. 2007). To determine whether 4EBP1 hyperphosphorylation occurs during TGHQ-induced nephrocarcinogenicity, p4EBP1 expression was determined by Western blot analysis in renal tumors derived from 8-month-TGHQ-treated Tsc-$2^{EK/+}$ rats and in the 8-month-OSOM. Interestingly, the OSOM of all treatment groups did not express detectable levels of 4EBP1, and p-4EBP1-Ser65, -Thr70, and -Thr37/46 (**Figure 3.1**). In contrast, renal tumors derived from TGHQ-treated *Tsc-2*$^{EK/+}$ rats expressed high levels of total 4EBP1 with three distinct species at 15, 18, and 20 kDa. Moreover, high levels of various post-translationally modified species of 4EBP1 and p-4EBP1-Ser65, -Thr70, and -Thr37/46 were observed (**Figure 3.1**). Similarly, kidneys of vehicle treated nude mice did not display detectable levels of 4EBP1 or p4EBP1s (**Figure 3.2B lane 2**), and neither did kidneys of nude mice with subcutaneous renal tumor xenografts (**Figure 3.2B lane 1**). While renal tumor xenografts derived from QTRRE cell lines express elevated levels of 4EBP1 and p-4EBP1-Ser65, -Thr70, and -Thr37/46 (**Figure 3.2B lanes 3-6**).

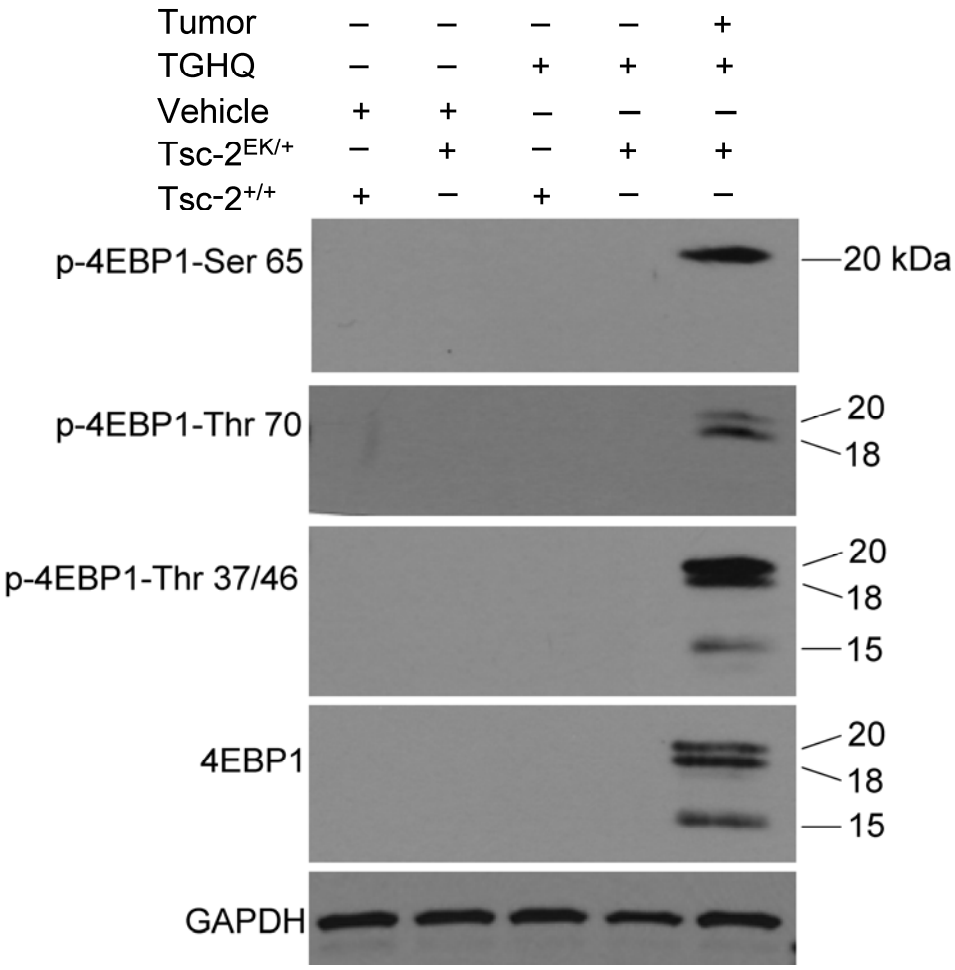

Figure 3.1. 4EBP1 and p-4EBP1 is upregulated in renal tumors from TGHQ-treated *Tsc*-2$^{EK/+}$ rats.

4EBP1 and p-4EBP1-Ser65, -Thr70, and -Thr37/46 were visualized by Western blot analysis of OSOM or renal tumor tissue obtained from *Tsc-2*$^{+/+}$ or *Tsc-2*$^{EK/+}$ rats treated with TGHQ or saline for 8-months. GAPDH was used as a loading control. Similar results were obtained in three separate experiments.

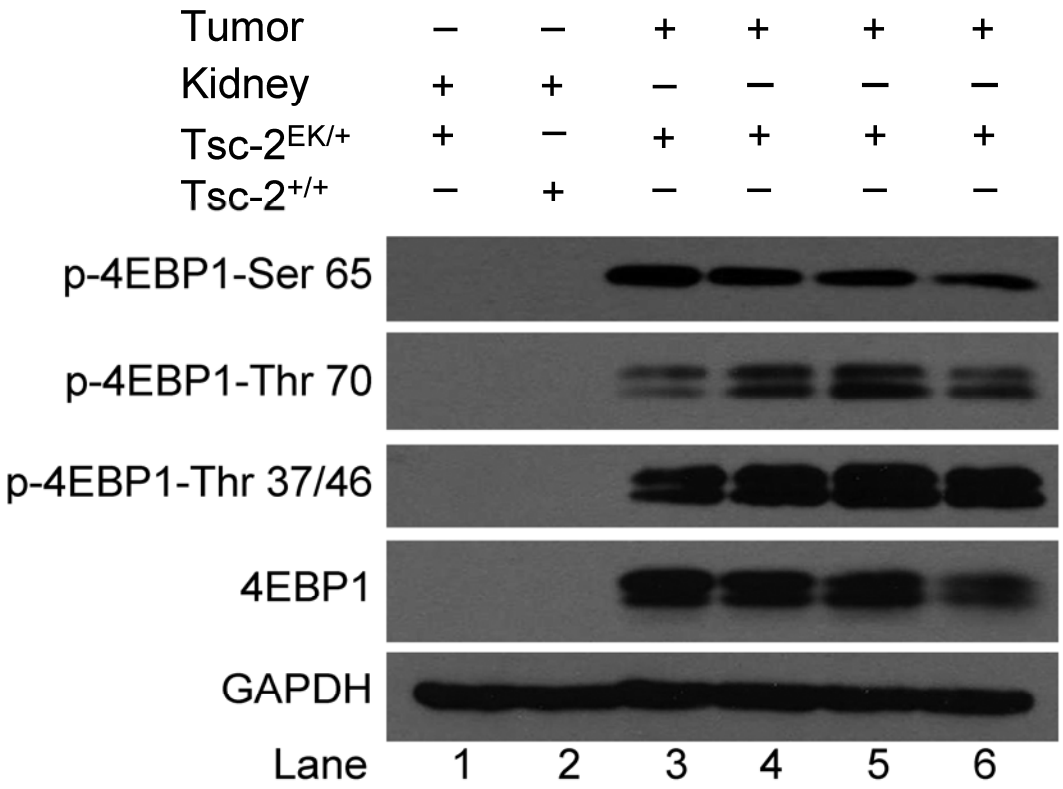

Figure 3.2. 4EBP1 and p-4EBP1 is increased in QTRRE tumor xenografts in nude mice.

Whole tissue lysates generated from kidneys of nude mice or renal tumor xenografts derived by subcutaneous injection of QTRRE (*Tsc-2*$^{EK/-}$) cells in nude mice were immunoblotted for 4EBP1, p-4EBP1-Ser65, -Thr70, and -Thr37/46.

3.3.2. Raf-1 regulates hyperphosphorylation of 4EBP1 protein levels

In parallel with the p4EBP1 Western analysis of renal tumors derived from TGHQ-treated *Tsc-2*$^{EK/+}$ rats, TGHQ transformed QTRRE cells express constitutively phosphorylated forms of 4EBP1 [**Figure 3.3A and B, Lane 1 (DMSO)**]; as well as two distinct species of 4EBP1. To examine whether Raf and MEK1/2 kinases contribute to phosphorylation of 4EBP1 in QTRRE cells, p-4EBP1-Ser65, -Thr70, and -Thr37/46 were determined by Western analysis following treatment with sorafenib (50 μM), or PD 98059 (50 μM). QTRRE cells constitutively express two species of 4EBP1. Subsequent to treatment with sorafenib there was a time-dependent disappearance of the higher molecular weight band in p-4EBP1-Ser65, -Thr70, and -Thr37/46; and a parallel shift in band intensity from the higher molecular weight 4EBP1 band to the lower molecular weight band in p-4EBP1-Thr 70 and -Thr 37/46 as early as 5 min (**Figure 3.3A**). Maximal changes in the pattern of p4EBP1 p-4EBP1-Ser65, -Thr70, and -Thr37/46 expression occurred 15 min after sorafenib treatment and was sustained for a further 45 min; by 90 min a return to the pre-treatment pattern of expression was observed (**Figure 3.3A**). Interestingly, sorafenib treatment resulted in a sustained increase in a "faster migrating" band when probed for total 4EBP1 protein (**Figure 3.3A**), and PD 98059 treatment resulted in the appearance of a third "faster migrating" species, although the appearance of this species was only transient in nature (**Figure 3.3B**). The maximal effect of PD 98059 on the pattern of p4EBP1 expression was observed at 25 min, with recovery occurring by 40 min (**Figure 3.3B**).

To identify which Raf isoform contributes to MAPK phosphorylation of 4EBP1, QTRRE cells were transfected with B-Raf and Raf-1 siRNA for 72 and 96 h. Western

blot analysis of Raf-1 siRNA knockdown revealed significant decreases in p-4EBP1-Ser65, -Thr70, and -Thr37/46 (**Figure 3.4A**), whereas B-Raf siRNA did not affect any p4EBP1 species (**Figure 3.4B**). Both Raf siRNA's were target specific, and neither Raf siRNA produced a significant change in GAPDH protein expression.

3.3.3. Tuberin negatively regulates p4EBP1 and cyclin D1 in human kidney cells

To determine whether loss of tuberin in human kidney (HK-2) cells causes similar changes in cell signaling similar to that observed in tumorigenic QTRRE cells, siRNA knockdown of *Tsc2* was carried out. *Tsc2* siRNA knockdown resulted in an increase in cyclin D1 and in the non-constitutive higher molecular species of p-4EBP1-Ser65, -Thr70, and -Thr37/46 protein levels (**Figure 3.5**). Tuberin siRNA did not produce a significant change in GAPDH protein expression.

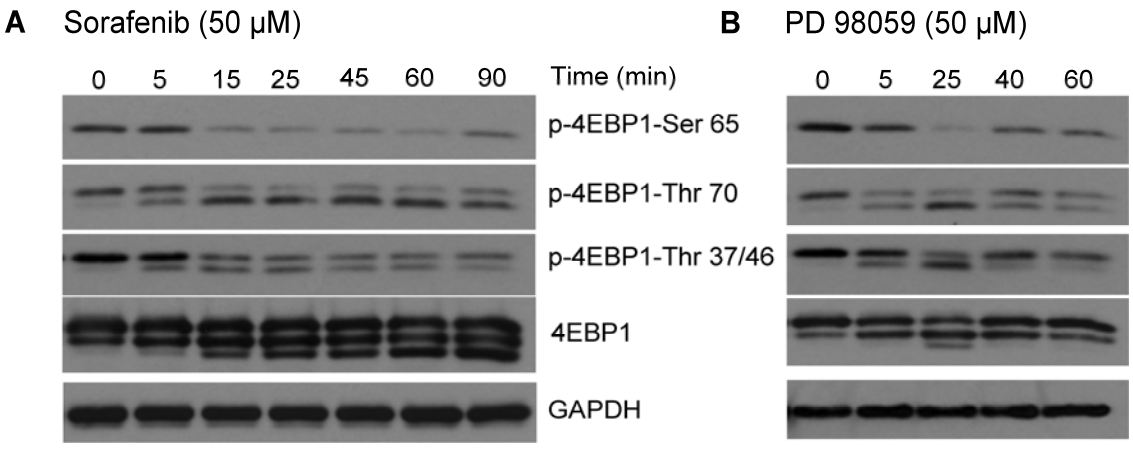

Figure 3.3. Inhibition of Raf and MEK kinases results in a decrease in 4EBP1 and p-4EBP1-Ser65, -Thr70, and -Thr37/46 in QTRRE cells.

(*A)* QTRRE cells were treated with sorafenib (50 μM) for 5, 15, 25, 45, 60, and 90 min. (*B*) QTRRE cells were treated with PD 98059 (50 μM) for 5, 25, 40, and 60 min. 4EBP1 and p-4EBP1-Ser65, -Thr70, and -Thr37/46 were visualized by Western blot analysis. GAPDH was used as a loading control.

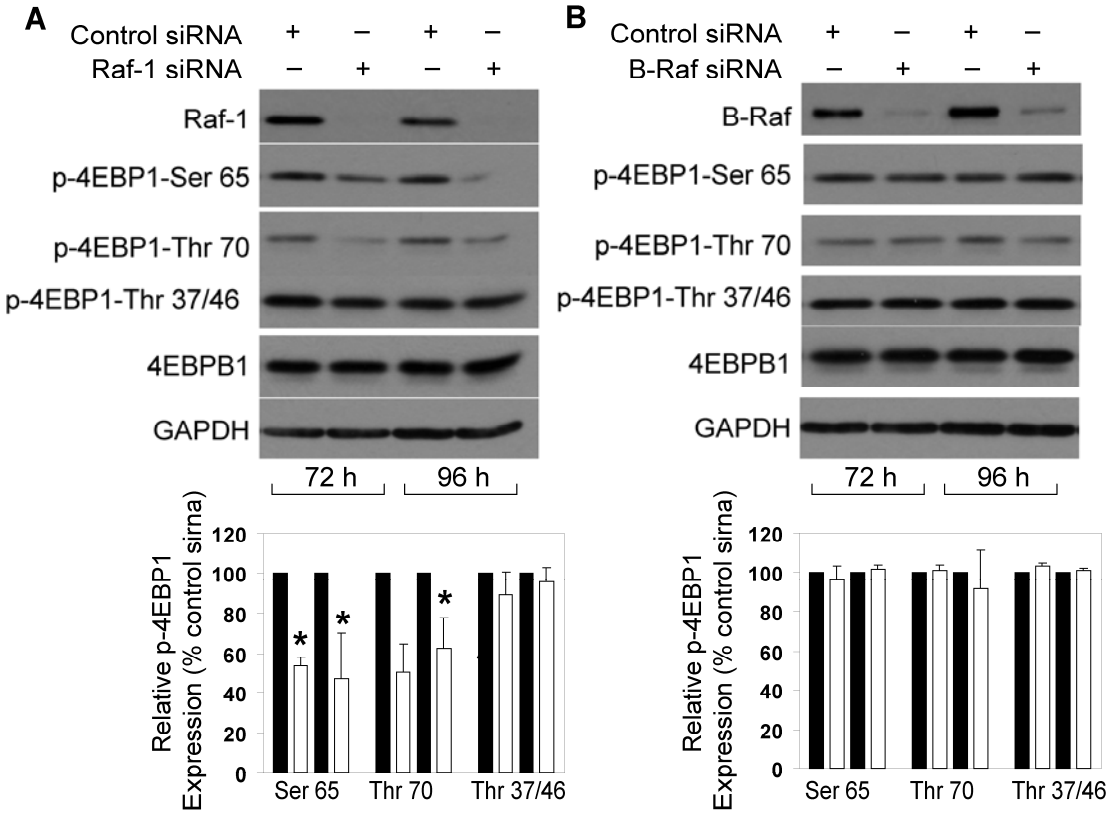

Figure 3.4. Raf-1 is the dominant regulator of p-4EBP1 protein levels in QTRRE cells.

QTRRE cells were transfected with either (A) Raf-1 (100 nM) or (B) B-Raf (100 nM) ON_TARGETplus SMARTpool siRNA or siCONTROL Non-Targeting siRNA #5 (Dharmacon RNA Technologies, NY). The siRNA-DharmaFECT complex solution was incubated with cells for 72 or 96h. 4EBP1 and p-4EBP1-Ser65, -Thr70, and -Thr37/46 were visualized by Western blot analysis. GAPDH was used as a loading control. Values are means ± SD (n=3). A significant difference was seen between control siRNA and Raf-1 or B-Raf siRNA treated cells at * $P<0.05$.

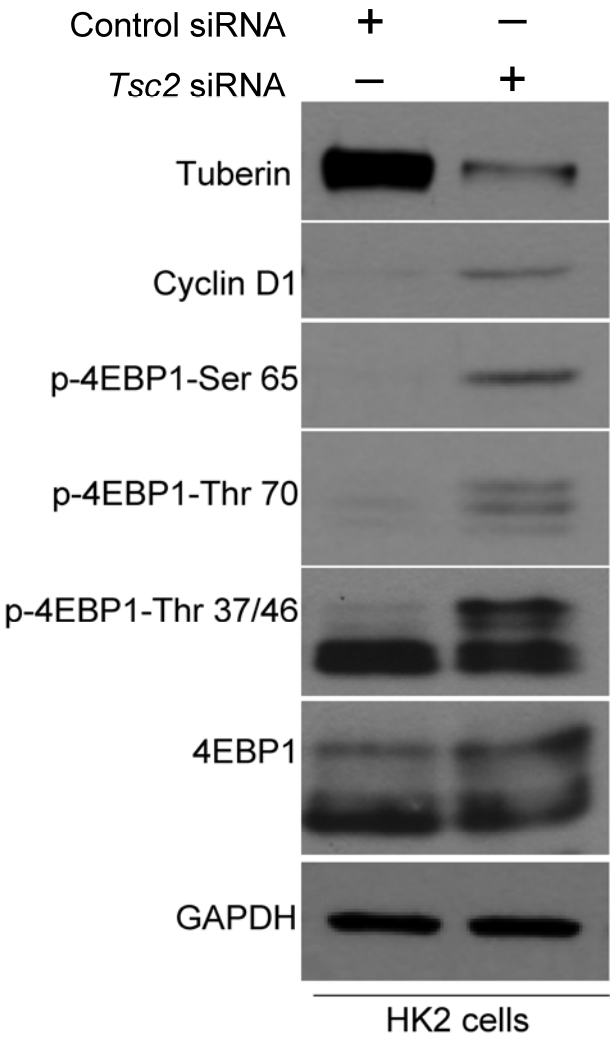

Figure 3.5. Tuberin negatively regulates p-4EBP1 and cyclin D1 in human kidney cells.

Human kidney-2 (HK2) cells were transfected with 50 nM Tsc2 ON_TARGETplus SMARTpool siRNA or siCONTROL Non-Targeting siRNA pool (Dharmacon RNA Technologies). The siRNA-DharmaFECT complex solution was incubated with cells for 72 h. Cyclin D1, 4EBP1, and p-4EBP1-Ser65, -Thr70, and -Thr37/46 were visualized by Western blot analysis. GAPDH was used as a loading control.

3.4. Discussion

We describe a novel pathway by which 4EBP1 phosphorylation is modulated by the Raf-1/MEK/ERK MAP kinase cascade (**Figure 3.3 and 3.4**). In our tuberin null kidney tumors and tumorigenic QTRRE cells we found that: (i) renal tumors express high protein levels of 4EBP1, p-4EBP1-Ser65, -Thr70, and -Thr37/46 (**Figure 3.1 and 3.2**), (ii) QTRRE cells express constitutively phosphorylated Raf-1, B-Raf, ERK1/2 (Yoon et al. 2004) and p4EBP1 (**Figure 3.3**); (iii) treatment with sorafenib (Raf inhibitor) and PD 98059 (MEK inhibitor) in QTRRE cells resulted in dephosphorylation of 4EBP1 at Thr 65, Thr 70 and Thr 37/46 (**Figure 3.3**) and (iv) Raf-1 and B-Raf siRNA knockdown in QTRRE cells elucidated Raf-1 as the dominant Raf responsible for downstream modulation of 4EBP1 phosphorylation (**Figure 3.4**).

In accordance with the established tuberin/Rheb/mTOR/4EBP1/cyclin D1 signaling cascade, renal tumors and QTRRE cells express constitutively high protein levels of p-4EBP1-Ser65, -Thr70, and -Thr37/46 (**Figure 3.1 and 3.3**), and cyclin D1 (**Chapter 2, Figure 2.1**). Increased expression of phosphorylated 4EBP1 was recently linked to high-grade prostate, breast, ovarian tumors (Castellvi et al. 2006; Kremer et al. 2006; Rojo et al. 2007); and the results of this study provide compelling evidence that p-4EBP1 is also be prevalent in RCC (**Figure 3.1 and 3.2**).

Inhibition of Raf and MEK with sorafenib or PD 98059, decreased ERK activity, and resulted in a decrease in 4EBP1 phosphorylation at sites that are necessary for displacing eIF4E-4EBP1 protein interactions (**Figure 3.3**). These data suggest that ERK1/2 can directly regulate the hierarchical phosphorylation of 4EBP1 downstream of the tumor suppressor tuberin. The order of 4EBP1 phosphorylation is hierarchical, with

phosphorylation of Thr37/46 occurring first, followed by Thr 70 phosphorylation, and Ser 65 last (Gingras et al. 2001). Although amino acids 51-67 on 4EBP1 encompass the eIF4E binding site, all four phosphorylation sites (Thr37/46, Thr70 and Ser65) are necessary for effectively releasing eIF4E from 4EBP1.

Treatment with either Raf or MEK kinase inhibitors appears to decrease phosphorylation on all four putative 4EBP1 phorsphorylation sites, as well as produce the rapid appearance of a lower molecular weight band (**Figure 3.3**). Interestingly, in combination with the appearance of a lower molecular weight species there was a substantial increase, most notably with sorafenib treatment, in all three variants in total 4EBP1 (**Figure 3.3**). Similar results on total 4EBP1 accumulation were observed in mouse hepatocytes following *in vivo* rapamycin treatment, where treatment resulted in an increase in abundance of the lowest molecular weight species (faster-migrating) but no decrease in the band intensity of the two higher molecular weight species (slower-migration) (Nelsen et al. 2003). This accumulation of total 4EBP1 is likely due to an increase in protein stability, because the resultant hypophosphorylation of 4EBP1 would facilitate its subsequent binding to eIF4E, thus decreasing translation initiation. The readily apparent shift in molecular weight between the three species of 4EBP1 is probably due to changes in numerous posttranslational modifications (PTM), beyond the 4 key sites with known functional significance. 4EBP1 is a highly modified protein, with 17 PTM already identified, most with unknown biological relevance (Gevaert et al. 2003; Matsuoka et al. 2007; Molina et al. 2007; Cantin et al. 2008; Dephoure et al. 2008; Imami et al. 2008).

The hyperphosphorylation of 4EBP1 results in an increased translation of cyclin D1 mRNA, due to the complex and dynamic disassociation of 4EBP1 from eIF4E, thus facilitating the ability of eIF4E to complex with its binding partners and initiate cap-dependent translation of cyclin D1 (Gingras et al. 1999; Gingras et al. 2001; Jiang et al. 2008). Subsequent to the inhibition of Raf and MEK kinases (**Figure 3.3**), the resulting decrease in phosphorylation of 4EBP1-Ser65, -Thr70, and -Thr37/46 led to a consequent decrease in cyclin D1 protein levels (**Chapter 2, Figure 2.5**). Treatment of cells with B-Raf and Raf-1 siRNA pinpoints Raf-1 as the dominant Raf regulating MAP kinase driven phosphorylation of 4EBP1 (**Figure 3.4**) and the consequent decrease in cyclin D1 (**Chapter 2, Figure 2.6**). Interestingly, in **Chapter 2**, treatment with sorafenib or PD 98059 did not result in a decrease in cyclin D1 mRNA (**Figure 2.7**). These results are consistent with previous findings demonstrating that inhibition of mTOR with rapamycin causes a decrease in p4EBP1 and a subsequent decrease in cyclin D1 protein levels, in the absence of changes in cyclin D1 mRNA (Beretta et al. 1996; Gingras et al. 1999; Hidalgo et al. 2000; Gingras et al. 2001; Beugnet et al. 2003; Nelsen et al. 2003). Therefore, we have elucidated a novel mechanism whereby ERK hyperactivation is responsible for increased translation of cyclin D1.

In summary, our data suggest that inhibition of either the MAPK or mTOR pathway alone is insufficient to abrogate 4EBP1 phosphorylation (**Figure 3.6**), since both mTOR and ERK are capable of phosphorylating 4EBP1 in renal proximal tubule cells. Accordingly, treatment with sorafenib in combination with an analog of rapamycin may be more efficacious than either single agent alone.

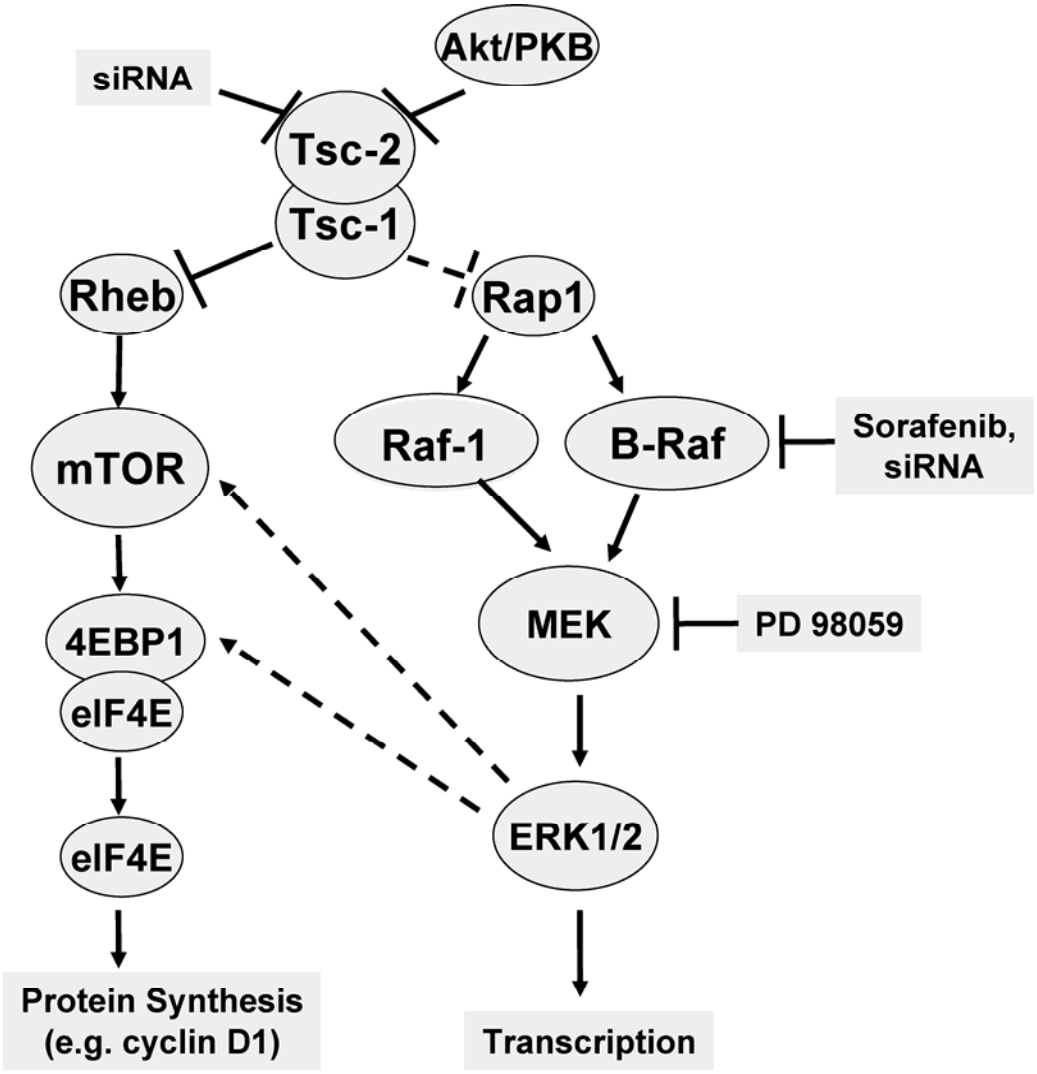

Figure 3.6. MAPK pathway crosstalk with 4EBP1.

Restoration of tuberin decreased B-Raf, Raf-1 and ERK1/2 activity in QTRRE cells (Yoon et al. 2004). Our data reveal that genetic and chemical knockdown of Raf kinases results in a reduction of pERK1/2 and downstream dysregulation of p4EBP1. Following a decrease in all forms of p4EBP1 there is an apparent reduction in cyclin D1 translation.

CHAPTER 4: cAMP-DEPENDENT PATHWAY DIRECTS THE RAP-GTP/B-RAF MAPK-MEDIATED CYTOSOLIC MISLOCALIZATION OF $P27^{KIP}$-CYCLIN D1 IN RENAL CANCER

4.1. Introduction

Tuberous sclerosis complex (TSC) is an autosomal dominant hereditary disease with a high rate of spontaneous mutations in *Tsc-1* and *Tsc-2* genes (Kida et al. 2005). Mutations in TSC genes have been demonstrated during human renal tumor formation (Bernstein et al. 1991; Bjornsson et al. 1996), and loss of heterozygosity (LOH) at the *Tsc-2* locus has been noted in renal tumors of TSC and sporadic RCC patients (Henske et al. 1995; Carbonara et al. 1996). The tumor suppressor tuberin, the protein product of *Tsc-2,* can affect subcellular localization and protein accumulation of the cyclin dependent kinase inhibitor p27 (kip) (Rosner et al. 2004; Short et al. 2008). Tuberin can complex with p27 to promote its nuclear localization (Rosner et al. 2007), and inhibit its ubiquitin mediated degradation by Skp1/cullin/F-box (SCF) proteosome (Rosner et al. 2004; Rosner et al. 2008).

Nuclear p27 typically associates with distinct cyclin dependent kinase (CDK)-cyclin complexes to initiate cell cycle arrest. Complex interactions between CDKs, cyclins, and p27 govern the G1-S phase transition of the cell cycle. During the G1 checkpoint D-type cyclins (D1, D2 and D3) bind and activate CDK4/6 (Malumbres et al. 2009). Due to the instability of the cyclin D1-CDK4 complex, p27 interaction is necessary for complex assembly and stabilization (Cheng et al. 1999; Sherr et al. 1999). Thus, p27 is an extremely versatile CDK inhibitor, in that in can regulate nuclear cell cycle exit and proliferation (Blain 2008; Vervoorts et al. 2008). Nuclear p27 is typically

characterized as a tumor suppressor, but recent developments have revealed the duality of p27 as an oncogene in certain cancers, subsequent to its cytoplasmic mislocalization.

In human kidney, breast, colon, ovarian, thyroid and esophageal cancers; cytoplasmic mislocalization of p27 is correlated with an aggressive tumor type and poor prognosis (Ciaparrone et al. 1998; Singh et al. 1998; Masciullo et al. 2000; Viglietto et al. 2002; Alkarain et al. 2004; Motti et al. 2005; Pantuck et al. 2007; Hennenlotter et al. 2008). Analysis of *Tsc2* null uterine leiomyomas from the Eker rat (*Tsc-2*$^{EK/+}$), *Tsc2*$^{-/-}$ mouse embryonic fibroblasts (MEF), and microscopic kidney lesions in *Tsc2*$^{+/-}$/p27$^{+/+}$ mice and *Tsc2*$^{+/-}$/p27$^{+/-}$ mice, all revealed cytoplasmic mislocalization of p27 (Short et al. 2008). The molecular mechanism allowing for p27 cytoplasmic retention, as well as evasion of targeted degradation, remains unclear. Degradation of p27 is necessary for the G_1 to S phase transition to occur, and is initiated by its phosphorylation on T187 by cyclin E- and A-CDK2, translocating it to the cytoplasm for SCF E3 ubiquitin ligation (Sheaff et al. 1997; Vlach et al. 1997; Carrano et al. 1999; Sutterluty et al. 1999). If p27 is bound to cyclin D-CDK4 complexes, it is protected from degradation by the SCF^{SKP} E3-ubiquitin-ligase complex (Kamura et al. 2004). As p27^{Kip1} has never been found unbound *in vivo* (Vervoorts et al. 2008), and cytoplasmic p27-cyclin D-CDK4 complexes have intact kinase activity (Blain et al. 1997; James et al. 2008), an oncogenic function of p27 may be its maintenance of constitutive p27-cyclin D-CDK4 activity. Cyclin D1 is overexpressed in a variety of cancers (Kim et al. 2009); and in tuberin null renal tumors and renal cells derived from *Tsc-2*$^{EK/+}$ rats, the loss of tuberin expression is associated with an increase in cyclin D1 protein levels (Soucek et al. 1997; Yoon et al. 2002), as well as an increase in cyclin D1 gene expression (Patel et al. 2003).

The signaling that drives p27 expression, localization, and stabilization in renal cell carcinoma is relatively unknown. In a variety of cells types the cAMP pathway is associated with increased levels of p27 (Paris et al. 2006; Bond et al. 2008; da Silva et al. 2008; Alderson et al. 2009). In retinal, schwannoma, and neuronal cells, the cAMP mediated increase in p27 is also linked to cell cyle exit and differentiation (Paris et al. 2006; da Silva et al. 2008; Alderson et al. 2009). Also, increases in cAMP mediate activation of Rap1 and subsequent downstream activation of B-Raf (Vossler et al. 1997; Grewal et al. 2000; Garcia et al. 2001). Rap activation of ERK is dependent on the expression levels of B-Raf in the cell; in cell lines where B-Raf is not expressed, Rap1 inhibits Raf-1/ERK activation (Okada et al. 1998; Dugan et al. 1999; Schmitt et al. 2001). These data suggest that cAMP signaling can regulate p27 expression, as well as Rap-GTP/B-Raf activation of the MAP kinase cascade.

In this study, we examined the relationship between cAMP, the B-Raf/ERK MAPK cascade, and p27 in our tuberin deficient renal tumor models: 2,3,5-*tris*-(glutathion-S-yl) hydroquinone (TGHQ) induced renal tumors in *Tsc-2*$^{EK/+}$ rats, TGHQ transformed *Tsc-2*$^{EK/+}$ cells (QTTRE), and QTRRE renal tumor xenografts in nude mice. Our data identifies cAMP as a modulator of Rap/B-Raf activity, B-Raf MAPK expression of p27, and p27-cyclin D1 cytosolic mislocalization in renal carcinogenesis.

4.2. Materials and Methods

4.2.1. Cell cultures

The tuberin-negative cell line quinol-thioether-transformed rat renal epithelial (QTRRE-3) cells was established from primary renal epithelial cells (Yoon et al. 2001). HK2 (human kidney cells) was from American Type Culture Collection (Manassas, VA). HK2 and QTRRE-3 cells were grown in DMEM/F12 (1:1) (Invitrogen, Carlsbad, California) with 10% FBS. Cells were grown at 37^{o}C in a humidified atmosphere of 5% CO_2.

4.2.2. Animal dosing and tissue preparation.

(A) Renal tumor xenograft nude mice. QTRRE-2 and -3 cell tumorigenicity in athymic NCI female nude mice was performed as described previously (Patel et al. 2003). Briefly mice 5-6 wk old were purchased from Taconic (Hudson, NY) and were maintained on a 12 h light/dark cycle and allowed food and water ad libitum. The animals were divided into three groups (n = 2/group). Once QTRRE-2 or -3 cells reached log phase growth stage in culture, they were harvested and resuspended in matrigel (BD Biosciences, San Jose, California). The animals were injected subcutaneously at one site/animal with 5×10^6 cells/0.2 mL matrigel per site. When the size of a tumor reached 10-15 mm in diameter, the mice were euthanized, and sections of tumor were fixed in 10% phosphate-buffered formalin and embedded in paraffin, or snap frozen in liquid nitrogen and frozen in -80 ^{o}C.

(B) TGHQ renal tumor formation in Eker rats. Male Eker rats (wild-type, *Tsc-2*$^{+/+}$, and mutant, *Tsc-2*$^{EK/+}$), 8 weeks old, were obtained from the University of Texas MD Anderson Cancer Center, Smithville, TX. The animals were housed according to a 12:12-h light-dark cycle and allowed food and water *ad libitum*. TGHQ was synthesized as previously described and used at >98% purity, as determined by high performance liquid chromatography (Lau et al. 1988). The rats were divided into four subgroups: 1) *Tsc-2*$^{EK/+}$ control, 2) *Tsc-2*$^{EK/+}$ TGHQ-treated, 3) *Tsc-2*$^{+/+}$ control and 4) *Tsc-2*$^{+/+}$ TGHQ-treated. The rats were administered TGHQ [2.5 μmol/kg in 0.5 ml of 1x phosphate-buffered saline (PBS), i.p.] 5 days a week for 4 months; then increased to 3.5 μmol/kg for 4 months, according to previously established protocol (Lau et al. 2001). Control rats were administered PBS only. The TGHQ dosing solution was prepared fresh in 1xPBS daily. The animals were euthanized by CO_2 asphyxiation. For histological studies, a mid-sagital longitudinal section of the left kidneys was fixed in 10% phosphate-buffered formalin and paraffin embedded. For biochemical assays, the outer-strip of the outer medulla (OSOM), cortex, and renal tumors were excised, frozen immediately in liquid nitrogen, and stored at -80^{o}C.

4.2.3. Nuclear and Cytoplasmic Extraction

The extraction of renal tumor xenografts derived from subcutaneous injection of QTRRE-2 or -3 cells in nude mice, kidney section from vehicle-treated nude mice, renal tumors from TGHQ-treated *Tsc-2*$^{EK/+}$ rats, or OSOM from vehicle-treated *Tsc-2*$^{EK/+}$ rats, was performed using NE-PER Nuclear and Cytoplasmic Extraction Reagents (Pierce

Biotechnology, Rockford, IL) according to the manufacturer's protocol. For the cellular extraction, QTRRE-3 or HK2 cells were seeded at a density of 3 x 10^5 cells/well in six-well plates. At 80-90% confluency cells were treated with 1 mg/ml pentoxifylline or 0.6 mg/ml theophylline for 24 h in DMEM/F12 with 10% FBS; or 50 μM sorafenib for 1.5 h in DMEM/F12 with 2% FBS. Following drug treatments, cells were harvested with trypsin and washed with PBS. The extraction was performed according to the manufacturer's protocol.

4.2.4. Western blot analysis

The OSOM of TGHQ or vehicle treated *Tsc-2*$^{EK/+}$ and *Tsc-2*$^{+/+}$ rats, TGHQ-*Tsc-2*$^{EK/+}$ rat renal tumors or QTRRE mouse xenograft tumors, and QTRRE-3 or HK2 cells were homogenized with Cell Lysis Buffer 10X (Cell Signaling Technology, Inc, Beverly, MA) containing 1 mM Pefabloc SC (Roche) and Complete Protease Inhibitor Cocktail tablets (Roche). Protein was subjected to 10 or 12% SDS-PAGE and proteins were electrophoretically transferred to polyvinylidene difluoride (PVDF; Bio-Rad Laboratories, Hercules, CA) membranes. Primary antibodies used were cyclin D1 (A-12), B-Raf (H-145), Raf-1 (C-20), p27 (F-8), p-p27 (Thr187) (Santa Cruz Biotechnologies); p42/44, phospho-p42/44 (T202/Y204) (20G11), skp1 (Cell Signaling Technologies); and GAPDH (Ambion, Austin, Texas). The secondary-immunoglobulin conjugated with horseradish peroxidase (Santa Cruz Biotechnology, CA) was used at a 1:3000 dilution. The blots were visualized with Amersham ECLTM Western Blotting Detection Reagents (GE Healthcare, UK).

4.2.5. Rap1 activation assay

Rap1 activation was determined as described (van Triest et al. 2004). The GST-Ral GDS-RBD fusion protein was isolated from *E. coli* strain BL21. A 10% suspension of glutathion-agarose beads was precoupled to 100 µl of cleared GST-Ral GDS-RBD lysate for 1 h on a tumbler at 4 ^{o}C. HK2 cells and QTRRE-3 cells were treated with 1mg/ml pentoxifylline (Sigma) for 24 h. Total cell lysates were isolated using Cell Lysis Buffer 10X (Cell Signaling Technology, Inc, Beverly, MA). For each sample, an equal number of micrograms of total cell lysate were incubated with the GST-Ral GDS-RBD protein and glutathione-agarose beads slurry for 1.5 h on a tumbler at 4 ^{o}C. After coupling, beads were washed 4 times with Cell Lysis Buffer and bound proteins were eluted in 15 µl of XT Sample Buffer (Bio-Rad). Precipitates were subjected to 12% SDS-PAGE followed by transfer onto PVDF membranes. PVDF membrane was incubated overnight with 1:1000 dilution of Rap1b (Santa Cruz Biotechnology), then washed and incubated with 1:3000 dilution of goat-immunoglobulin conjugated with horseradish peroxidase (Santa Cruz Biotechnology, CA). The blots were visualized with Amersham ECLTM Western Blotting Detection Reagents (GE Healthcare, UK).

4.2.6. B-Raf and Raf-1 kinase activity assay

At 80-90% confluency QTRRE cells were treated with 1 mg/ml pentoxifylline or 0.6 mg/ml theophylline for 24 h in DMEM/F12 with 10% FBS. Cells were lysed with using Cell Lysis Buffer 10X, as described above, and 500 µg of total cell lysate was immunoprecipitated using B-Raf and Raf-1 polyclonal antibodies (Santa Cruz Biotechnology, CA) bound to protein A/G-agarose beads (Pierce Biotechnology Inc, IL).

Kinase activity of the immunoprecipitates was determined using B-Raf or Raf-1 Kinase Cascade Assay Kits (Upstate Biotechnology) as previously reported (Yoon et al. 2004) and according to the manufacturer's protocol. The incorporated [γ-^{33}P]ATP was quantified by liquid scintillation spectroscopy.

4.2.7. Immunostaining

QTRRE cells grown on glass cover slips were treated with 1 mg/ml pentoxifylline or 0.6mg/ml theophylline for 24 h in DMEM/F12 with 10% FBS. Cells were fixed with 4% paraformaldehyde, permeabilized with acetone, and blocked with 10% goat serum in 1% BSA/PBS. Cells were incubated with anti-p27 (Santa Cruz Biotechnology, CA) overnight at 4^{o}C. Followed by incubation with secondary Alexa 546 goat anti-mouse IgG (Molecular Probes, Eugene, OR) and TO-PRO-3 (Invitrogen) for 1 h at room temperature; cells were mounted with vectashield (Vector Laboratories, Burlingame, CA). The slides were imaged using a 60x water immersion plan-apochromat objective on a LSM 510 multiphoton/confocal laser-scanning microscope (Carl Zeiss, Inc., Thornwood, New York).

4.2.8. siRNA transfection

QTRRE cells were transfected when 50-60% confluent. For QTRRE transfection, 100 nM B-Raf, Raf-1, or p27 ON_TARGETplus SMARTpool siRNA, or siCONTROL Non-Targeting siRNA #5 (Dharmacon RNA Technologies, NY) was combined with 100 µl of serum-free DMEM/F12 media and incubated for 5 min at RT. In parallel, 5 µl of DharmaFECT #2 was incubated in 200 µl serum-free DMEM/F12 for 5 min at RT.

siRNA solution 100 µl was then combined with the 200 µl DharmaFECT #2 solution and incubated for 20 min at RT. The siRNA-DharmaFECT complex solution was added directly to each well, mixed gently and incubated for 24, 48, 72, or 96 h at 37^{o}C in a CO_2 incubator.

4.2.9. Statistics

Data are expressed as means ± standard deviation. Mean values were compared using a Students T-test, two tails, with unequal variances.

4.3. Results

4.3.1. Increased p27 levels in TGHQ treated Tsc-2$^{+/+}$ and Tsc-2$^{EK/+}$ rats, and QTRRE tumor xenografts in nude mice

Tsc-2$^{EK/+}$ rats carry a single autosomal mutation on one allele of the tuberous sclerosis tumor suppressor gene that predisposes them to the development of spontaneous renal cell tumors at a very high incidence (Eker et al. 1981; Yeung et al. 1994; Kobayashi et al. 1995). The majority of renal cell tumors observed in the *Tsc-2*$^{EK/+}$ rat originate from the renal proximal tubules and are histologically similar to renal tumors in humans (Everitt et al. 1992; Walker 1998). Western blot analysis of the OSOM of 8-month vehicle-treated *Tsc-2*$^{EK/+}$ and *Tsc-2*$^{+/+}$ rats revealed that neither animal had detectable levels of p27, but both expressed equivalent levels of GAPDH (**Figure 4.1A lanes 1-4**). Interestingly, TGHQ treatment alone was sufficient to induce a substantial increase in p27 in the OSOM of 8-month *Tsc-2*$^{+/+}$ rats (**Figure 4.1A lanes 5-6**). The most substantial increase in p27 protein levels was observed within the OSOM 8-month-TGHQ-*Tsc-2*$^{EK/+}$ rats and renal tumors (**Figure 4.1A lanes 7-10**). Similarly, kidneys of vehicle treated nude mice did not display detectable levels of p27 (**Figure 4.1B lane 2**), but kidneys of nude mice with subcutaneous renal tumor xenografts showed a slight increase in p27 (**Figure 4.1B lane 1**). While renal tumor xenografts derived from QTRRE cell lines express elevated levels of p27 (**Figure 4.1B lanes 3-6**).

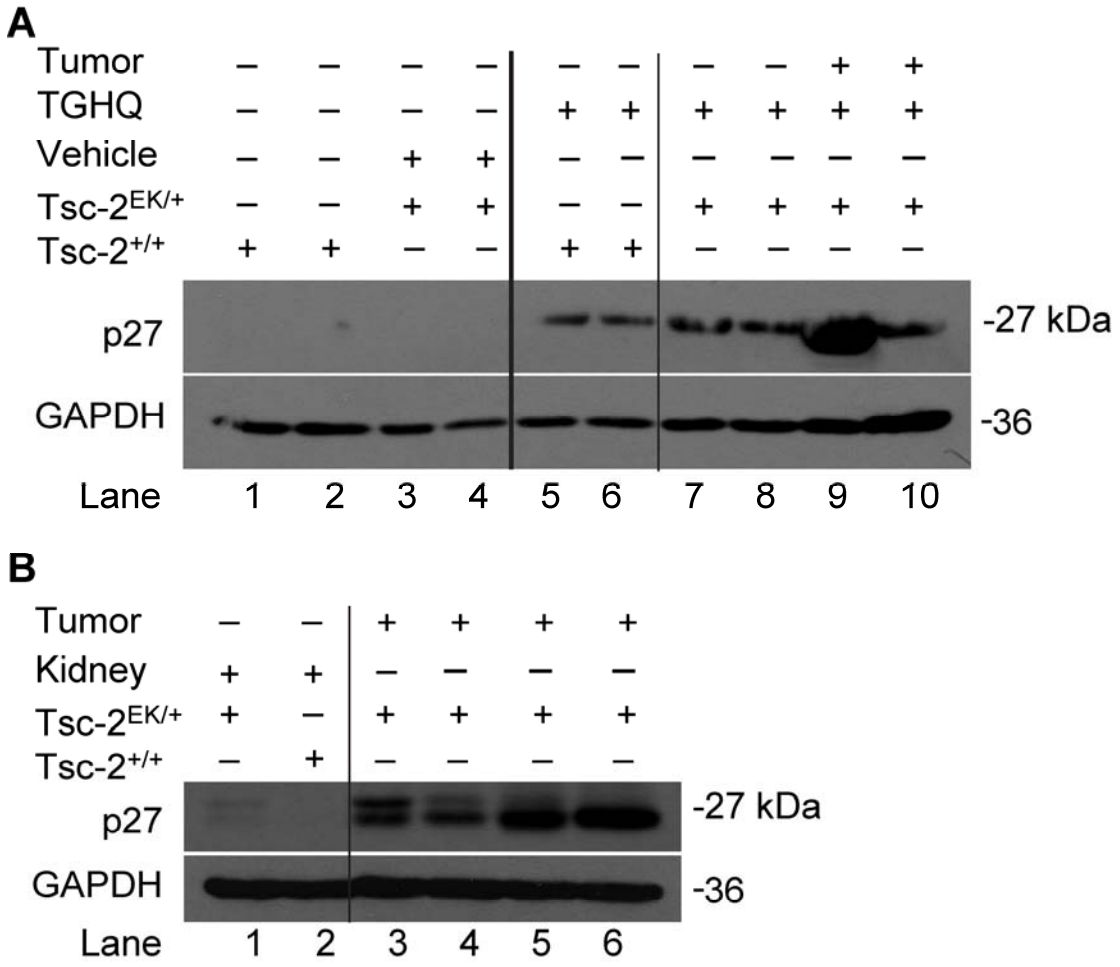

Figure 4.1. Increased p27 levels in TGHQ treated Tsc-2$^{+/+}$ and Tsc-2$^{EK/+}$ rats, and QTRRE tumor xenografts in nude mice.

(*A*) Whole tissue lysates from the OSOM or renal tumors of vehicle or TGHQ treated Tsc-2$^{+/+}$ and Tsc-2$^{EK/+}$ rats were immunoblotted for p27 and GAPDH. (*B*) whole tissue lysates generated from kidneys or renal tumor xenografts derived by subcutaneous injection of QTRRE cells in nude mice were immunoblotted for p27 and GAPDH.

4.3.2. Loss of Tsc2 correlates with cytoplasmic localization of p27 and cyclin D1 in Tsc2 null cells and renal tumors

QTRRE cells, which are null for tuberin, express high levels of pERK1/2 (Yoon et al. 2004); as well as high levels of cyclin D1 and p27 compared to *Tsc-2*$^{+/+}$ normal human kidney cells (HK2) and *Tsc-2*$^{+/+}$ porcine LLCPK1 proximal tubule cells (**Figure 4.2A**). We analyzed the localization pattern of p27 in HK2 and QTRRE cells. Nuclear-cytoplasmic extraction of HK2 cells displayed nuclear localization of p27 and non-detectable levels of cyclin D1 (**Figure 4.2B**), whereas in tumorigenic QTRRE cells, p27 and cyclin D1 were primarily detected in the cytosolic fraction (**Figure 4.2C**). We examined renal tumors from TGHQ-treated *Tsc-2*$^{EK/+}$ rats and renal tumor xenografts formed by subcutaneous injection of QTRRE cells in nude mice, compared with vehicle treated controls, for cytosolic localization of p27 and cyclin D1. Nuclear-cytoplasmic extraction of the OSOM of vehicle treated *Tsc-2*$^{EK/+}$ rats did not display detectable levels of p27 or cyclin D1 (**Figure 4.2D**) in either fraction. Whereas extraction of renal tumors derived from *Tsc-2*$^{EK/+}$ rats treated with TGHQ for 8-months revealed an increase in nuclear and cytoplasmic p27 (**Figure 4.2D**). Cytoplasmic localization of p27 correlated with increased levels of cyclin D1 in the cytosolic fraction (**Figure 4.2D**). A faint increase in p-p27 T187 was detected only in the cytosolic fraction of the renal tumors (**Figure 4.2D**). Similarly, renal tumor xenografts derived from QTRRE cells in nude mice expressed elevated levels of cytosolic and nuclear p27 (**Figure 4.2E**), as well as an increase in cyclin D1 in the cytoplasm (**Figure 4.2E**). Neither the tumor xenografts nor the vehicle treated controls displayed detectable levels of p-p27 T187 (**Figure 4.2E**). Differences between the nude mice tumor xenograft and TGHQ-*Tsc-2*$^{EK/+}$ rat tumor

models may account for the inability to detect the faint increase in p-p27 T187 in tumor xenografts. The kidneys of vehicle treated nude mice did not display detectable levels of p27 or cyclin D1 (**Figure 4.2E lane 2**) in either fraction.

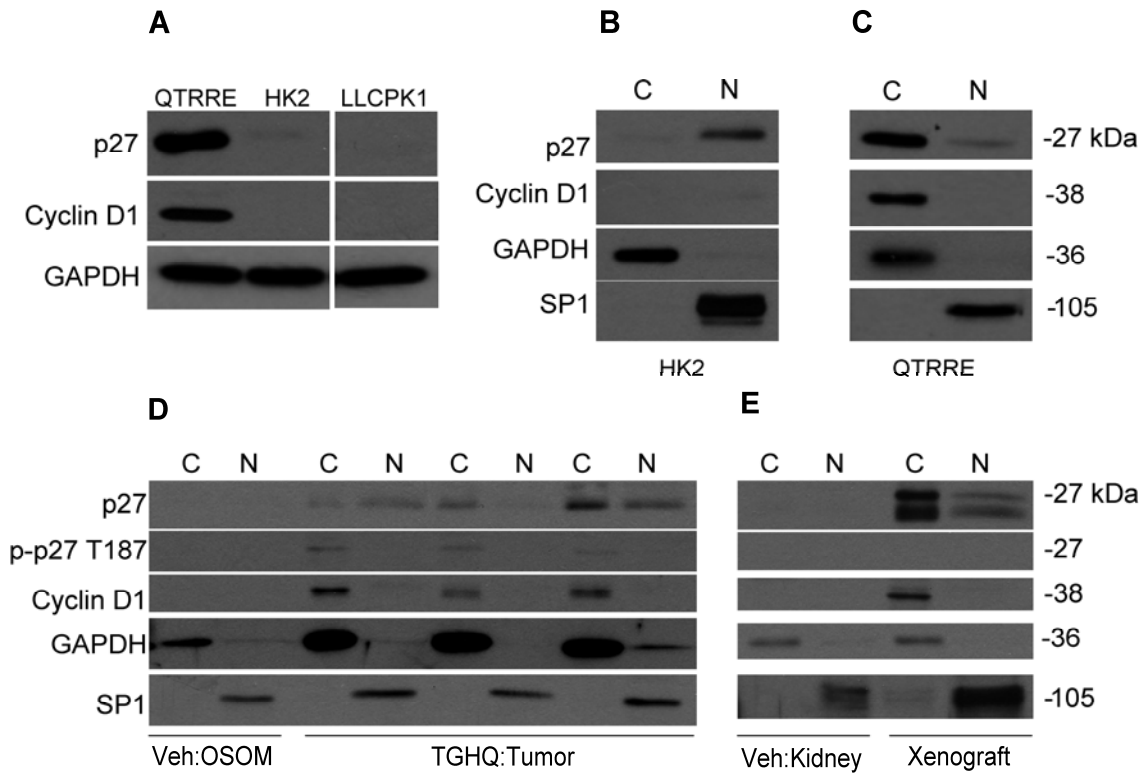

Figure 4.2. Cytoplasmic localization of p27 in tuberin-null renal tumors.

(*A*) Whole cell lysates from QTRRE, HK2, and LLCPK1 cells were immunoblotted for p27, cyclin D1, and GAPDH. Cytosolic [C] and nuclear [N] lysates were generated from (*B*) HK2 cells, (*C*) QTRRE cells, (*D*) kidney OSOM of 8-months-vehicle treated *Tsc-2*$^{EK/+}$ rats or tumors from 8-months-TGHQ treated *Tsc-2*$^{EK/+}$ rats, and (*E*) vehicle treated kidneys of nude mice or renal tumor xenografts derived by subcutaneous injection of QTRRE cells in nude mice. Samples were immunoblotted for p27, p-p27 T187, cyclin D1, GAPDH (cytosolic fractionation control), and SP1 (nuclear fractionation control).

4.3.3. cAMP mediated Rap1 and B-Raf activation

Increases in cAMP have been implicated in the activation of Rap1 and subsequent downstream activation of B-Raf in rat neuronal cells and human acute megakaryoblastic leukemia cells (Vossler et al. 1997; Grewal et al. 2000; Garcia et al. 2001). To measure the effects of cAMP on Rap1 activation in QTRRE and HK2 cells, we treated each with the phosphodiesterase inhibitor pentoxifylline, and isolated Rap1-GTP on GSH-agarose beads precoupled to GST-Ral GDS-RBD. Similar to data obtained in other cell models, Rap1b-GTP was elevated in both QTRRE and HK2 cells following an increase in cAMP (**Figure 4.3**).

Rap1 can bind both B-Raf and Raf-1, but Rap1 binding results in activation of B-Raf and inhibition of Raf-1 (Vossler et al. 1997; Okada et al. 1998; Dugan et al. 1999; Garcia et al. 2001; Peyssonnaux et al. 2001). B-Raf (**Figure 4.4A**) and Raf-1 (**Figure 4.4B**) activation by cAMP was determined by kinase specific activity assays following phosphodiesterase inhibition with pentoxifylline or theophylline in QTRRE cells. Treatment with pentoxifylline increased B-Raf kinase activity by approximately 40% (**Figure 4.4A**), but did not result in a statistically significant change in Raf-1 kinase activity (**Figure 4.4B**). Similarly, cAMP stabilization with theophylline resulted in a 50% increase in B-Raf kinase activity (**Figure 4.4A**), and a nominal 9% increase in Raf-1 kinase activity (**Figure 4.4B**).

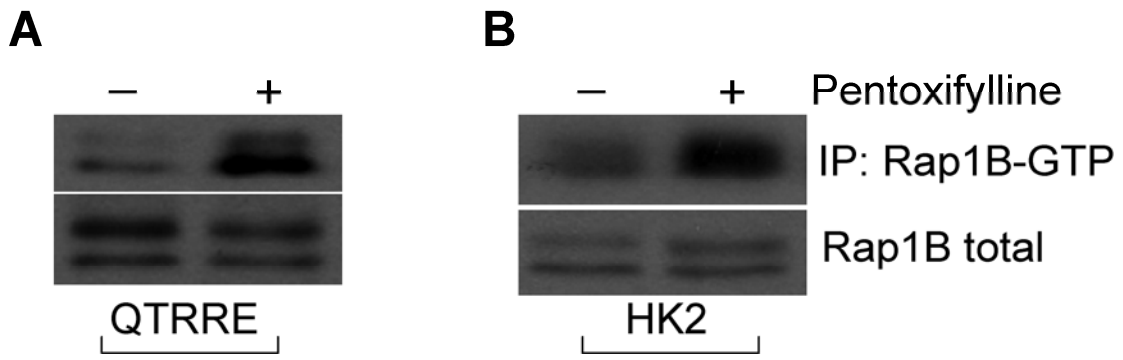

Figure 4.3. Phosphodiesterase inhibition activates Rap1 in QTRRE and HK2 cells.

(*A*) QTRRE or (*B*) HK2 cells were treated with pentoxifylline (1mg/ml) for 24 h. Rap1B-GTP was precipitated with GST-Ral GDS-RBD bound to glutathion-sepharose beads from 500 µg of QTRRE or HK2 total cell lysate, and after removal of the beads, identified with a Rap1B antibody following SDS-PAGE and Western blotting. Rap1B immunoblots of the same total cell lysates were performed to confirm equal expression of total Rap1B between DMSO and pentoxifylline treated lysates.

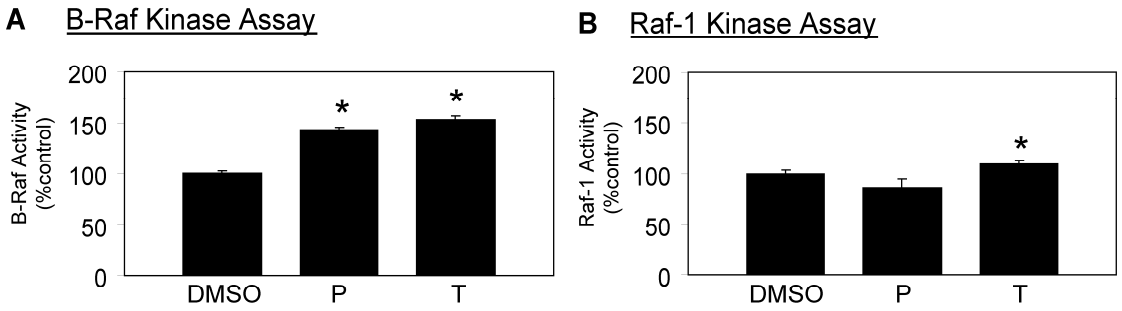

Figure 4.4. Phosphodiesterase inhibition activates B-Raf in QTRRE cells.

(*A*) and (*B*), QTRRE cells were treated with pentoxifylline (P, 1mg/ml), theophylline (T, 0.6 mg/ml), or DMSO for 24 h. Equal amounts of lysates were subjected to (A) B-Raf kinase activity assay or (B) Raf-1 kinase activity assay kits. B-Raf and Raf-1 activity were determined as described in EXPERIMENTAL PROCEDURES. Values represent the mean ± SD (n=3). A significant difference was seen between DMSO and pentoxifylline or theophylline treatments in QTRRE cells at * $P<0.05$.

4.3.4. B-Raf regulates p27 protein levels

To investigate whether Raf kinases contribute to high p27 protein levels in QTRRE cells, p27 was measured by Western blotting following treatment with the Raf kinase inhibitor sorafenib (50 μM). Cells treated with sorafenib experienced a time dependent decrease in p27, with a 40% reduction in p27 protein level by 90 min, and a sustained decrease in pERK1/2 between 30 to 60 min (**Figure 4.5A**).

To identify which Raf isoform is responsible for MAPK regulation of p27 protein levels, QTRRE cells were transfected with B-Raf and Raf-1 siRNA. Real-time-PCR analysis of both Raf isoforms, following 48 h siRNA treatment, revealed an approximate 95% decrease in Raf mRNA levels (data not shown). Western blot analysis of B-Raf siRNA knockdown of 75% resulted in a 40% decrease in p27 protein levels by 72 h post-transfection (**Figure 4.5B**), whereas Raf-1 siRNA knockdown to a non-detectable level did not result in a significant decrease in p27 (**Figure 4.5C**). Both Raf siRNA's were target specific, and neither Raf siRNA produced a significant change in GAPDH protein expression. These data, combined with the increase in Rap/B-Raf activation following cAMP stimulation in QTRRE cells (**Figure 4.3 and 4.4**), led us to investigate the connection between cAMP signaling and p27 expression.

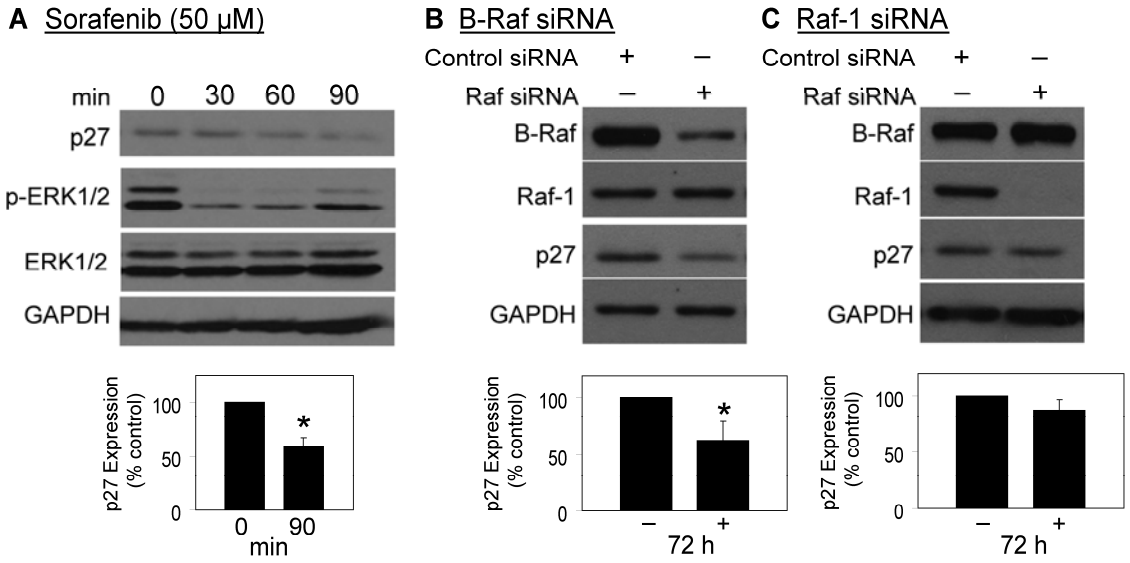

Figure 4.5. Effect of sorafenib and Raf siRNA on p27 expression in QTRRE cells.

(*A*) QTRRE cells were treated with sorafenib (50 μM) for 30, 60, and 90 min. QTRRE cells were transfected with (*B*) 100 nM B-Raf or (*C*) Raf-1 ON_TARGETplus SMARTpool siRNA or siCONTROL Non-Targeting siRNA #5 (Dharmacon RNA Technologies, NY) for 72 h. Whole cell lysates were subjected to Western blotting with antibodies specific to p27, pERK1/2, ERK1/2, and GAPDH. Values represent the mean ± SD (n=3). A significant difference in p27 protein levels was seen between control (DMSO) and sorafenib or B-Raf siRNA treated cells at * $P<0.01$.

4.3.5. cAMP signaling regulates expression, degradation, and cytoplasmic localization of p27

Recently, cAMP was found to regulate p27 protein levels in a variety of cell types (Paris et al. 2006; Bond et al. 2008; da Silva et al. 2008; Alderson et al. 2009; Kowalczyk et al. 2009). To examine whether cAMP modulation could alter p27 protein levels in QTRRE cells, we probed for p27 and p-ERK1/2 following treatment with phosphodiesterase inhibitors. Following 24 h incubation with pentoxifylline (**Figure 4.6A**) or theophylline (**Figure 4.6B**) there was a 2.8- and 2.2-fold increase in p27 protein levels, respectively, and an increase in the upper band of p-ERK1/2. The increase in p27 following pentoxifylline treatment was also confirmed by confocal microscopy (**Figure 4.7**). To investigate whether cAMP treatment can directly increase p27 protein levels, QTRRE cells were treated with dibutyryl cAMP for 19 h, which produced a 2.9-fold increase in p27 protein levels and a slight increase in the upper band of p-ERK (**Figure 4.6C**). Incubation with dibutyryl cAMP also resulted in a 1.4-fold increase in cyclin D1 (**Figure 4.6C**).

To determine if the phosphodiesterase inhibitors altered the degradation of p27, we probed for p-p27 T187 and the E3 ubiquitin ligase skp1. Phosphorylation on T187 allows for recognition by E3-ubiquitin-ligase Skp-Cullin-F-box (SCF^{SKP2}) and CKS1 to target p27 for proteosome degradation (Carrano et al. 1999; Sutterluty et al. 1999). Skp1 is a central component of the SCF ubiquitin complex. Treatment with pentoxifylline or theophylline caused a parallel decrease in p-p27 T187 and skp1 protein levels (**Figure 4.6A and B**). Inhibition of the proteosome with 1 mM MG132 for 4 h produced a 1.5-

and 1.7-fold increase in p27 and cyclin D1 protein levels, respectively; as well as a substantial increase in both bands of p-ERK (**Figure 4.8**).

To evaluate the effect of cAMP on the subcellular compartmental localization of p27, nuclear-cytoplasmic extraction of wild-type HK2 cells and tumorigenic QTRRE cells was performed following treatment with phosphodiesterase inhibitors. Treatment of HK2 cells with theophylline resulted in an increase in nuclear and cytosolic p27, as well as a slight increase in nuclear cyclin D1 (**Figure 4.9A**). Interestingly, theophylline produced a mark increase only in cytosolic p-p27 T187 in HK2 cells, a PTM that targets p27 for degradation by the proteosome (**Figure 4.9A**). Treatment of QTRRE cells with pentoxifylline or theophylline resulted in an increase in p27 in the cytosolic fraction (**Figure 4.9B**). Furthermore, treatment produced a corresponding increase of cyclin D1 in the cytoplasm (**Figure 4.9B**). Incubation with sorafenib resulted in undetectable nuclear p27, and a 25% decrease in cytosolic p27 levels (**Figure 4.9C**). The decrease in cytoplasmic p27 corresponded to a decrease in cytosolic cyclin D1 (**Figure 4.9C**).

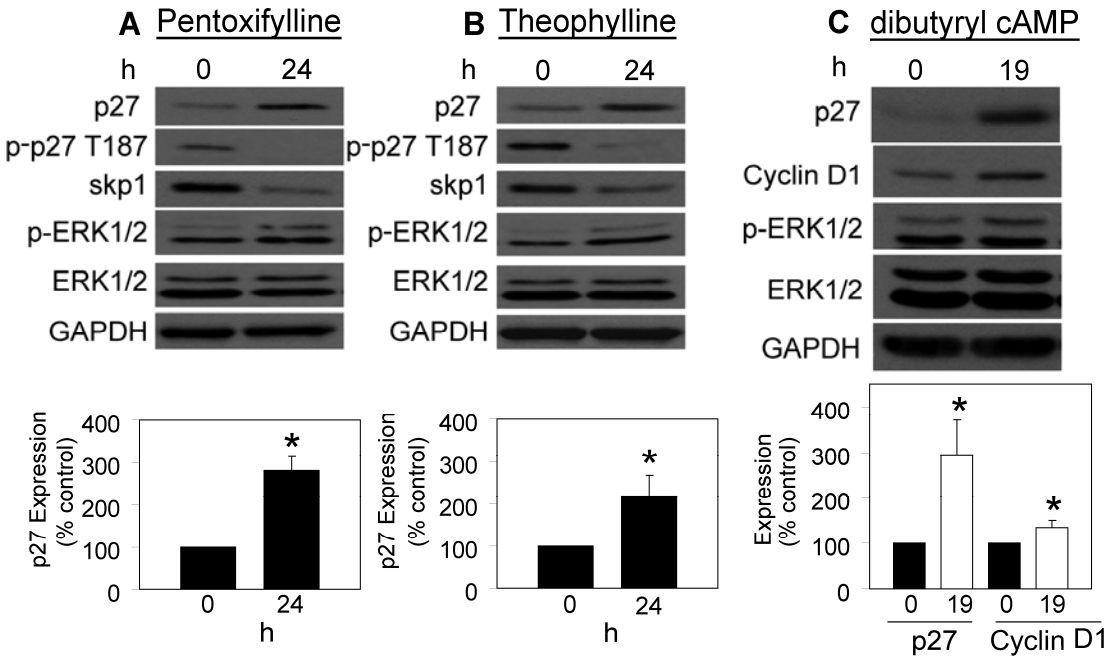

Figure 4.6. Phosphodiesterase inhibition and dibutyryl cAMP regulates p27 expression and protein stability in QTRRE cells

QTRRE cells were treated with (*A*) pentoxifylline (1mg/ml), (*B*) theophylline (0.6 mg/ml), (*C*) dibutyryl cAMP (1 mM), or DMSO. Equivalent whole cell lysates were subjected to Western blotting with antibodies specific to p27, p-p27 T187, skp1, cyclin D1, pERK1/2, ERK1/2, or GAPDH. Values represent the mean ± SD (n=3) for pentoxifylline and theophylline treatments, and the mean ± SD (n=4) for dibutyryl cAMP. A significant difference in p27 and/or cyclin D1 protein levels was seen between DMSO and pentoxifylline, theophylline, or dibutyryl cAMP treatments in QTRRE cells at * $P<0.05$.

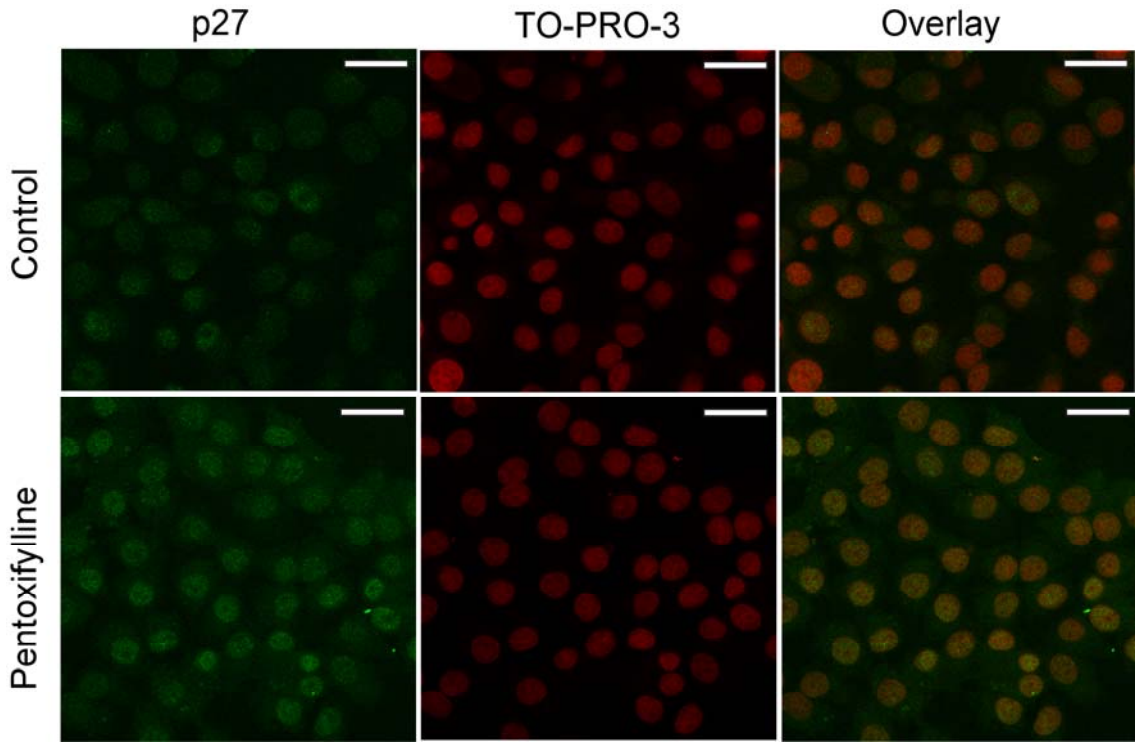

Figure 4.7. Effect of pentoxifylline on p27 protein levels in QTRRE cells.

QTRRE cells treated with pentoxifylline for 24 h were examined by immunocytochemistry with an anti-p27 antibody, TO-PRO-3 to detect nuclei, and an overlay of the two stains. Immunofluorescence was detected by confocal microscopy with a 60x water immersion plan-apochromat objective; white scale bars are 20 microns.

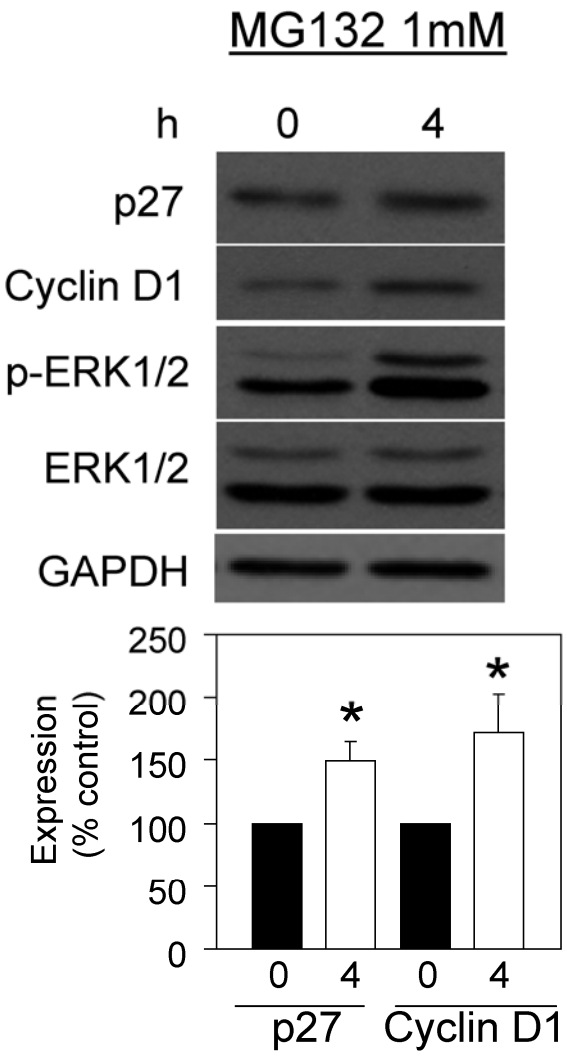

Figure 4.8. Elevated p27 and cyclin D1 protein levels following proteosome inhibition.

QTRRE cells treated with MG132 (1mM) for 24 h. Whole cell lysates were subjected to Western blotting with antibodies specific to p27, cyclin D1, pERK1/2, ERK1/2, and GAPDH. Values represent the mean ± SD (n=3). A significant difference in p27 and cyclin D1 protein levels was seen between control (DMSO) and MG132 treated cells at * $P<0.05$.

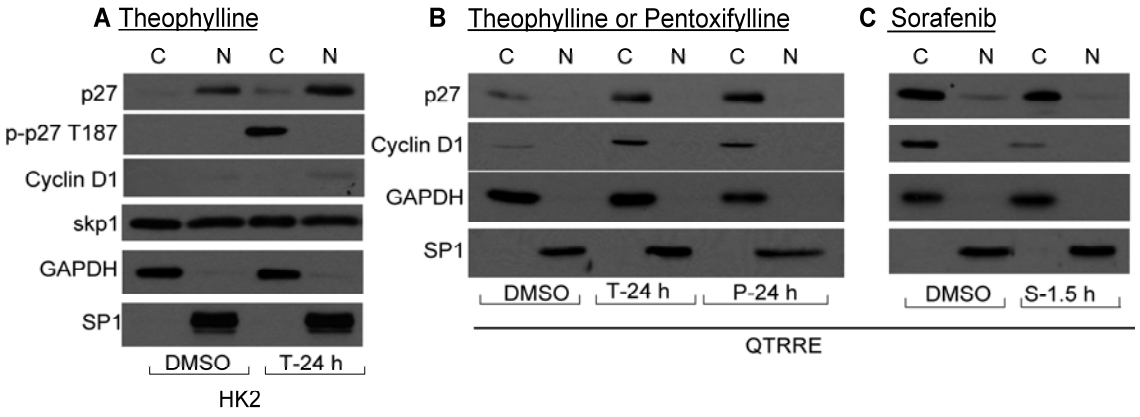

Figure 4.9. Cytoplasmic mislocalization of p27 and cyclin D1 modulated by cAMP-MAPK signaling.

(*A*) Cytosolic [C] and nuclear [N] lysates were generated from HK2 cells treated with theophylline (0.6 mg/ml) or DMSO for 24 h. (*B*), and (*C*), cytosolic [C] and nuclear [N] lysates were generated from QTRRE cells treated with (*B*) theophylline (0.6 mg/ml), pentoxifylline (1mg/ml) or DMSO for 24 h, or (*C*) sorafenib (50 μM) or DMSO for 1.5 h,. Equal amounts of extracted lysates were subjected to SDS-PAGE and immunoblotting with antibodies specific to p27, p-p27 T187, cyclin D1, skp1, GAPDH (cytosolic fractionation control), or SP1 (nuclear fractionation control).

4.3.6. Cytoplasmic stabilization of cylcin D1 is co-dependent on p27 cytosolic relocalization

In MEFs, lack of p27 expression is associated with decreased cyclin D1 protein levels (Cheng et al. 1999). Furthermore, p27 deficiency results in cyclin D1-CDK4 complex instability (Cheng et al. 1999; Sherr et al. 1999). To investigate whether cyclin D1 is a necessary component of p27 cytosolic relocalization and stabilization, we knocked down p27 with siRNA in QTRRE cells to determine its effect on expression of cyclin D1. Following a 48 h treatment of p27 siRNA in QTRRE cells there was an equivalent 88% decrease in both p27 and cyclin D1 protein levels (**Figure 4.10**).

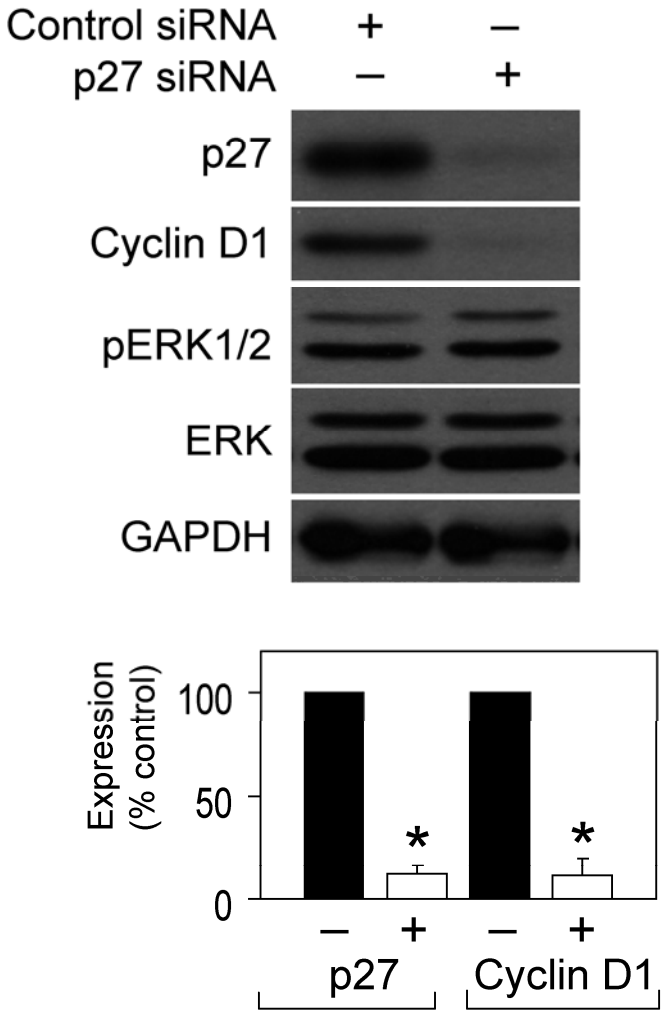

Figure 4.10. p27 stabilizes cyclin D1 in the cytoplasm of QTRRE cells.

QTRRE cells were transfected with 100 nM p27 ON_TARGETplus SMARTpool siRNA or siCONTROL Non-Targeting siRNA #5 (Dharmacon RNA Technologies, NY) for 48 h. Whole cell lysates were subjected to Western blotting with antibodies specific to p27, cyclin D1, pERK1/2, ERK1/2, and GAPDH. Values are means ± SD (n=3). A significant difference was seen between control siRNA and B-Raf siRNA treated cells at * $P<0.01$.

4.4. Discussion

We established that modulation of B-Raf kinase activity and mRNA levels directly alter p27 protein levels and cytoplasmic relocalization in tuberous sclerosis renal cell carcinoma. Cytoplasmic mislocalization and increased expression of both p27 and cyclin D1 were observed in tuberin null renal tumors from TGHQ-treated *Tsc-2*$^{EK/+}$ rats, renal tumor xenografts derived by subcutaneous injection of QTRRE (null of tuberin) cells in nude mice (**Figure 4.1 and 4.2**), and tumorigenic QTRRE cells (compared to HK2 and LLCPK1 cells) (**Figure 4.2**). Additionally, 8-months of TGHQ treatment was sufficient to induce increased p27 expression in the OSOM of *Tsc-2*$^{+/+}$ rats (**Figure 4.1**). Manipulation of cAMP and MAPK cascades revealed that cAMP activation of Rap-GTP/B-Raf (**Figure 4.3 and 4.4**) mediates increased protein expression (**Figure 4.5, 4.6, and 4.7**) and cytoplasmic mislocalization (**Figure 4.9**) of p27 protein levels in tuberin null QTRRE cells, as well as in human HK2 cells (**Figure 4.9**). We also found that phosphodiesterase inhibitors can inhibit the degradation of p27 by decreasing its phosphorylation on T187 and decreasing skp1 protein levels, thus resulting in an increase in p27 protein levels (**Figure 4.6**). Lastly, we identified that p27 stabilizes cyclin D1 in the cytosolic fraction of QTRRE cells; siRNA targeted degradation of p27 in QTRRE cells resulted in an equivalent decrease in cyclin D1 (**Figure 4.10**). Similarly, manipulation of p27 protein levels in QTRRE cells by phosphodiesterase inhibitors (**Figure 4.6A-B and 4.9B**), dBcAMP (**Figure 4.6C**), and the proteosome inhibitor MG132 (**Figure 4.8**) resulted in a parallel increase in both p27 and cyclin D1. Furthermore, sorafenib treatment caused a parallel decrease in both p27 and cyclin D1 (**Figure 4.5A and 4.9C**).

Our finding that tuberin null renal tumors derived from Eker rats (*Tsc-2*$^{EK/+}$) (Yoon et al. 2002), renal tumor xenografts derived by subcutaneous injection of tuberin null QTRRE cells in nude mice, and QTRRE cells that exhibit a loss of heterozygosity on the *Tsc-2* gene locus (tuberin null cells) (Yoon et al. 2001) all display cytoplasmic mislocalization of p27, confirms a previous report that *Tsc2* null uterine leiomyomas and *Tsc2*$^{-/-}$ MEFs displayed cytoplasmic localization of p27 (Short et al. 2008). Tuberin has a dual function in the regulation of p27, regulating both its nuclear localization and stability. Tuberin complex formation with p27 inhibits 14-3-3-mediated cytoplasmic retention of p27 and promotes nuclear localization of p27 (Rosner et al. 2007); complex formation also stabilizes p27 protein levels by inhibiting degradation of p27 by the SCF-type E3 ubiquitin proteosome (Rosner et al. 2004). Post translational modifications to p27, such as phosphorylation on T187, allows for recognition by skp-E3-ubiquitin-ligase to target p27 for proteosome degradation (Carrano et al. 1999; Sutterluty et al. 1999). Therefore, loss of tuberin expression should result in increased phosphorylation on T187 and eventual degradation of p27. Interestingly, the loss of tuberin in renal tumors from 8-month TGHQ-treated *Tsc-2*$^{EK/+}$ rats and QTRRE cells produced the expected increase in p-p27 T187, but also resulted in an unanticipated increase in total p27 protein levels. The constitutive phosphorylation of p27 on T187 does not correlate with its high levels in QTRRE cells. Therefore, we suggest that p27-cyclin D1 complex formation in the cytoplasm protects it from targeted degradation from the SCF proteosome.

Treatment of our tuberin null QTRRE cells with pentoxifylline or theophylline both caused a parallel decrease in both p-p27 T187 and E3 ubiquitin ligase skp1 protein levels, as well as concomitant increase in p27 protein levels (**Figure 4.6**). Moreover,

treatment with phosphodiesterase inhibitors and dibutyryl cAMP resulted in a parallel increase in p27 and cyclin D1 protein levels; which suggests that cAMP signaling is a key regulator of p27 expression and stabilization. cAMP is an effective inducer of p27 expression in a variety of cell types; including schwannoma, vascular smooth muscle, neural, and skin cells (Paris et al. 2006; Bond et al. 2008; da Silva et al. 2008; Alderson et al. 2009; Kowalczyk et al. 2009). cAMP also regulates p27 transcription in neuronal cells (Shin et al. 2009). Since phosphodiesterase inhibitors were able to increase p27 levels in both tuberin negative and positive cells, tuberin status may be an independent factor in cAMP regulation of p27 expression. Furthermore, in neuronal progenitor, retinal, schwannoma, and skin cells, a cAMP mediated increase in p27 promoted differentiation and/or cell cyle exit (Paris et al. 2006; da Silva et al. 2008; Alderson et al. 2009; Kowalczyk et al. 2009). In vascular smooth muscle cells, elevation of cAMP resulted in increased p27 levels and reduced skp2, which is part of the SCF^{SKP} E3-ubiquitin-ligase complex that targets p27 for degradation (Bond et al. 2008). Therefore, cAMP may regulate cell cycle exit by increasing p27 and decreasing skp protein levels. Our data also substantiates that modulation of cAMP levels results in similar p27 and skp1 expression changes.

In contrast, similar cAMP mediated increases in p27 and decreases in skp1 protein levels may not result in differentiation and/or cell cycle exit in cells with cytoplasmic mislocalization of p27. In our tuberin deficient QTRRE cells, modulation of cAMP or MAPK cascades resulted in a co-increase in p27 and cyclin D1 protein levels in the cytoplasm. Moreover, inhibition of the proteosome with MG132, and p27 siRNA knockdown in QTRRE cells, both resulted in a concomitant increase or decrease in cyclin

D1, respectively. In *in vitro* and *in vivo* models, isolated p27-cyclin D-CDK4 complexes have intact kinase activity (Blain et al. 1997; James et al. 2008). Therefore, cytoplasmic p27-cyclin D-CDK4 active complexes may play a crucial role in tumor formation.

We also show here that phosphodiesterase inhibitors activate Rap-GTP and B-Raf kinase activity, but have a negligible effect on Raf-1 kinase activity (**Figure 4.11**). This data supports previous reports by other groups that Rap activation of ERK is dependent on the expression levels of B-Raf, as characterized in B-Raf expressing CHO/IR, primary mouse neuronal, and HEK cells (Okada et al. 1998; Dugan et al. 1999; Schmitt et al. 2001). In B-Raf-negative NIH 3T3 cells, cAMP inhibition of the Raf-1/ERK MAPK cascade is mediated through Rap1 (Okada et al. 1998; Dugan et al. 1999; Schmitt et al. 2001). Therefore, we propose that cAMP is modulating the transcriptional activation of p27 through the Rap/B-Raf MAPK cascade (**Figure 4.11**). In tumorigenic QTRRE cells, Raf-1 regulates cyclin D1 protein translation through ERK crosstalk with 4EBP1 (**Chapter 2 and 3**). Whereas, inhibition of B-Raf did not have as a profound effect on decreasing cyclin D1 protein levels as Raf-1, and did not result in a statistically significant change on any p-4EBP1 site. Moreover, Raf inhibition with sorafenib did not result in a decrease in cyclin D1 mRNA levels (**Chapter 2**). Therefore, we suspect that B-Raf is regulating the transcription of p27, and the increased p27 is complexing with cyclin D1 to stabilize it in the cytosol. These data pinpoint cAMP as an effective regulator of B-Raf MAPK induction of p27 protein levels in a tuberous sclerosis renal tumor model (**Figure 4.11**).

Similar to *Tsc-2*, the von Hoppel-Lindau (*VHL*) tumor suppressor gene regulates cell cycle arrest through stabilization of $p27^{Kip1}$ (Pause et al. 1998). The *VHL* tumor

suppressor gene is a primary target for mutations in human RCC (Gnarra et al. 1994; Shuin et al. 1994) but has not been found to contribute to rodent renal tumorigenesis (Kikuchi et al. 1995; Walker et al. 1996); whereas LOH at the *Tsc-2* locus has been demonstrated in renal tumors in humans (Yu et al. 1986; Wagner et al. 1996) and in both rats and mice (Yeung et al. 1994; Kobayashi et al. 1995; Kobayashi et al. 1999; Onda et al. 1999). Although *Tsc-2* is the primary target for RCC in our Eker rat model, both *Tsc-2* and *VHL* result in predominately clear cell RCC pathology and have numerous converging signaling proteins, with p27 modulated by both. Over 370 human renal cell carcinoma (RCC) tissues were immunostained with p27 to determine its compartmentalization; the staining identified nuclear p27 in 78% of the tumors and cytoplasmic localization in 46% of the tumors (Pantuck et al. 2007). Furthermore, cytoplasmic p27 staining was higher in metastatic RCC, and identified as a predictor of disease specific survival time, with cytoplasmic mislocalization predicting a poor prognosis (Pantuck et al. 2007). Therefore, the induction of p27 expression may have a variable outcome depending on the tumor grade.

Cytoplasmic mislocalization of p27 has been observed in a variety of human cancers that correlate with a high tumor grade and poor survival rate (Ciaparrone et al. 1998; Singh et al. 1998; Masciullo et al. 2000; Viglietto et al. 2002; Alkarain et al. 2004; Motti et al. 2005; Pantuck et al. 2007; Hennenlotter et al. 2008). Depending on the tissue specificity and pathology of the tumor, p27 expression in the tumor is either low in the total cell lysate or elevated in the cytosol due to cytoplasmic localization (Sicinski et al. 2007; Short et al. 2008). Recently, transformed keratinocytes treated with phosphodiesterase inhibitors increased their sensitivity to growth inhibition by

glucocorticoids (Kowalczyk et al. 2009). The use of phosphodiesterase inhibitors as a method to induce p27 expression, and ultimately cell cycle exit, may be a useful tool to treat low-grade tumors but may exacerbate high grade tumor formation. Therefore, further characterization of the relationship between cAMP pathway activation and p27 cytoplasmic localization will shed light on the role of p27 in renal tumor formation.

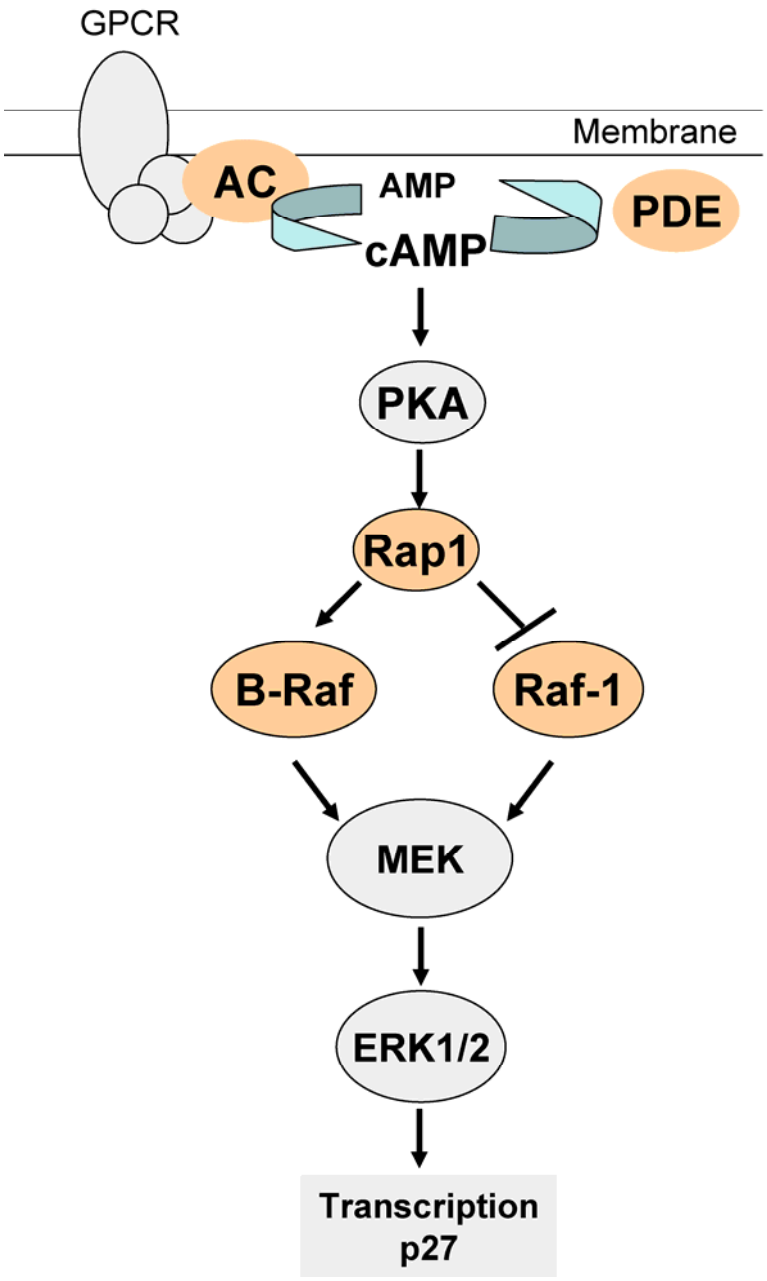

Figure 4.11. Rap1-GTP/B-Raf MAPK regulation of p27 in QTRRE cells.

Adenylate cyclase (AC) converts adenosine monophosphate (AMP) to cyclic adenosine monophosphate (cAMP), and phosphodiesterases (PDE) revert cAMP to AMP. cAMP mediates protein kinase A (PKA) activation of Rap1. Rap1-GTP activates B-Raf kinase activity and inhibits Raf-1. B-Raf phosphorylates and activates the MEK/ERK MAPK cascade. ERK1/2 regulates transcription of p27.

CHAPTER 5: CONCLUDING REMARKS

5.1. Introduction

HQ is a potential human nephrocarcinogen, and is both nephrotoxic and nephrocarcinogenic in rodent models. HQ is clastogenic (Tsutsui et al. 1997), causes DNA single-strand breaks in hepatocytes (Walles 1992), induces *in vitro* formation of 8-oxo-deoxyguanosine (Lau et al. 1996; Habib et al. 2003), and results in renal tubular hyperplasia and adenomas in Fisher 344 rats (Shibata et al. 1991; Kari et al. 1992). TGHQ is the most nephrotoxic metabolite of HQ, causing severe renal necrosis which is localized to proximal tubules within the S3 segment of the OSOM of Sprague Dawley rats (Lau et al. 1988). Furthermore, administration of TGHQ to *Tsc-2*$^{EK/+}$ rats induces a sustained regenerative hyperplasia at sites that subsequently give rise to tumors (Lau et al. 2001; Yoon et al. 2001; Yoon et al. 2002).

Preneoplastic lesions and tumors formed in TGHQ-*Tsc-2*$^{EK/+}$ rats display LOH at the *Tsc-2* wild-type allele (Lau et al. 2001) and subsequent loss of tuberin expression (Yoon et al. 2002). Furthermore, TGHQ transformation and immortalization of *Tsc-2*$^{EK/+}$ rat primary proximal tubule cells also resulted in LOH at the *Tsc-2* locus, and the cells are null for tuberin protein expression (Yoon et al. 2001). Thus, tuberin is a crucial target that facilitates the progression of renal tumors. In rats *Tsc-2* is a major target for spontaneous and chemically induced RCC (Yeung et al. 1994; Kobayashi et al. 1995; Urakami et al. 1997; Kobayashi et al. 1999; Onda et al. 1999).

In an effort to determine the pathways that the tumor suppressor tuberin regulates during renal tumor formation, tuberin null QTRRE cells were probed for activation of the

Raf/MEK/ERK MAPK cascade. Results showed that QTRRE cells express constitutively high levels of activated ERK, B-Raf and Raf-1 (Yoon et al. 2004). Transient transfection of *Tsc-2* cDNA in QTRRE cells resulted in a substantial decrease in both ERK and B-Raf kinase activity, with a lesser change in Raf-1 activity; and a decrease in cyclin D1 protein levels (Yoon et al. 2004). These data suggest that tuberin is a negative regulator of the Raf/ERK MAP kinase cascade.

5.2. Raf-1 modulates downstream 4EBP1 phosphorylation

A breakdown of the harmartin-tuberin complex, due to post translational modifications to tuberin or mutations in tuberin, results in Rheb-GTP activation of mTOR. Activated mTOR mediates the hierarchical phosphorylation of 4EBP1 that displaces eIF4E-4EBP1 protein interactions and allows for eIF4E-complex cap-dependent initiation of translation. In the literature, the only known kinase to directly phosphorylate 4EBP1 is mTOR. Our studies pinpointed the Raf-1/MEK/ERK kinase cascade as an effective regulator of 4EBP1 phosphorylation in tuberin null QTRRE cells.

Tuberin null renal tumors derived from 8-month-TGHQ-treated Tsc-$2^{EK/+}$ rats express high protein levels of B-Raf , Raf-1, p-ERK (**Figure 2.3**), 4EBP1, and p-4EBP1-Ser65, -Thr70, and -Thr37/46 (**Figure 3.1**). Also, tuberin null QTRRE cells express constitutively phosphorylated Raf-1, B-Raf, ERK1/2 (Yoon et al. 2004) and p4EBP1 (**Figure 3.3**). Furthermore, renal tumor xenografts derived from subcutaneous injection of QTRRE cells also express high levels of total and p4EBP1s, which were not detectable in the total tissue lysate of vehicle treated kidneys (**Figure 3.2**). These data suggest that loss of tuberin in renal tumors is associated with increased Raf and 4EBP1 signaling, and

that Raf and 4EBP1 signaling are critical signaling proteins during renal tumor development.

Inhibition of Raf kinases with sorafenib, or MEK1/2 with PD 98059 results in dephosphorylation of 4EBP1 at Thr 65, Thr 70 and Thr 37/46 (**Figure 3.3**), in the appearance and accumulation of a lower molecular weight species of 4EBP1. The three species of 4EBP1 most likely represent additional post-translational modifications of p-4EBP1. There are over 17 known post translational modifications to 4EBP1, the majority of which are of unknown biological relevance (Gevaert et al. 2003; Matsuoka et al. 2007; Molina et al. 2007; Cantin et al. 2008; Dephoure et al. 2008; Imami et al. 2008). Moreover, treatment with sorafenib or PD 98059 causes a significant shift in the relative abundance of the post-translationally modified form of 4EBP1, most likely due to re-association of 4EBP1 with eIF4E. Such changes likely account for an increase in the protein stability of 4EBP1.

Treatment of QTRRE cells with Raf-1 or B-Raf siRNA identified Raf-1 as the predominant Raf responsible for downstream modulation of 4EBP1 phosphorylation (**Figure 3.4**). Although Raf-1 has been pinpointed as the predominant Raf mediating ERK phosphorylation of 4EBP1, it is still unclear if ERK is directly phosphorylating 4EBP1, or an intermediate kinase, that subsequently phosphorylates 4EBP1.

5.3. Raf-1 regulates translation of cyclin D1 through ERK crosstalk with 4EBP1

A known translational target of the eIF4E-complex is cyclin D1. Transient transfection of QTRRE cells with a *Tsc-2* plasmid resulted in a decrease in cyclin D1 protein levels (Yoon et al. 2004). Although this verified that tuberin is involved in modulating cyclin D1 protein levels, it did not determine whether the resulting decrease was due to transcriptional or translational modulation. Furthermore, since it is known that tuberin mediates cyclin D1 translation through mTOR, it is unclear whether the Raf/MEK/ERK MAPK cascade is involved in any aspect of cyclin D1 expression. Inhibition of Raf kinases with sorafenib, or MEK1/2 with PD 98059, results in a decrease in cyclin D1 protein levels (**Figure 2.5**), verifying the Raf MAP kinase cascade as a regulator of cyclin D1 protein levels. Raf-1 and B-Raf siRNA knockdown in QTRRE cells identified Raf-1 as the predominant Raf responsible for downstream modulation of cyclin D1 (**Figure 2.6**). Since both chemical and genetic inhibition of Raf-1 kinase resulted in decreased phosphorylation of 4EBP1 and decreased cyclin D1 protein levels, it remains difficult to determine whether this is solely due to modulation of transcription or translation, or a combination of both. Consequently, neither treatment with sorafenib nor PD 98059 resulted in a change in cyclin D1 mRNA levels (**Figure 2.7**). Therefore, Raf-1 is responsible for modulating cyclin D1 protein translation through ERK crosstalk with 4EBP1.

Tuberin null renal tumors derived from 8-month-TGHQ-treated Tsc-$2^{EK/+}$ rats express high protein levels of cyclin D1 (**Figure 2.1**). Although we were not able to detect increased protein levels of cyclin D1 in the OSOM until 6-months of TGHQ

treatment by Western blot, IHC staining revealed that cyclin D1 is increased in proximal tubules of *Tsc-2*$^{+/+}$ and *Tsc-2*$^{EK/+}$ rats treated with TGHQ as early as 4-months (**Figure 2.2**). Interestingly, the more sensitive IHC analysis detected cyclin D1 staining in the cytoplasm of proximal tubules. These data led us to further explore the mislocalization and stabilization of cyclin D1 in the cytoplasm.

5.4. Cytosolic relocalization and stabilization of p27 and cyclin D1

TGHQ treatment for 8-months was sufficient to induce increased p27 expression in the OSOM of *Tsc-2*$^{+/+}$ rats (**Figure 4.1**), perhaps due to the loss of the tumor suppressor activity of tuberin. Tuberin directly binds to p27 to inhibit the 14-3-3-mediated cytoplasmic retention of p27, and to promote its nuclear localization (Rosner et al. 2007). TGHQ may effect the complex formation of tuberin with p27, decreasing its nuclear import.

Cytoplasmic relocalization and increased expression of both p27 and cyclin D1 were observed in (i) tuberin null renal tumors from TGHQ-treated *Tsc-2*$^{EK/+}$ rats, (ii) renal tumor xenografts derived by subcutaneous injection of tuberin null QTRRE cells in nude mice, and (iii) tumorigenic QTRRE cells (compared to HK2 and LLCPK1 cells) (**Figure 4.2**). The data is compelling, as both p27 and cyclin D1 are nuclear proteins that regulate the cell cycle. To facilitate the Go to G_1 transition, nuclear p27 complexes with CDK4/6-cyclin D1. The active p27-cyclin D-CDK4 complex directly phosphorylates RB to permit the transcription of cyclin E. Active CDK-cyclin E complexes target p27 for degradation by phosphorylation on T187, which is necessary for SCF E3 ligase binding to p27 (Sheaff et al. 1997; Carrano et al. 1999). Proteosome degradation of p27 is

necessary for CDK-cyclin E to initiate the G_1 to S phase transition. Therefore, if p27 is not degraded by the proteosome, it would inhibit the G_1 to S phase transition. Thus, constitutive expression of cyclin D1 and p27 in the cytoplasm, compared to normal HK2 and LLCPK1 cells, must have an alternative biological function, as it is not inhibiting the G_1 to S phase transition in QTRRE cells. Similar results were observed in uterine leiomyomas derived from *Tsc-2*$^{EK/+}$ rats and in *Tsc2*$^{-/-}$ MEFs, which displayed cytoplasmic relocalization of p27 (Short et al. 2008).

5.5. cAMP-PKA mediated Rap-GTP/B-Raf MAPK Regulation of p27

The loss of tuberin is associated with altered p27 localization. To determine the signaling mechanisms associated with p27 cytoplasmic relocalizaiton, we focused on the cAMP and Raf/ERK MAP kinase signaling pathways. Regulation of p27 protein levels by the B-Raf/ERK MAPK cascade has not been documented. Recent studies have identified cAMP as an effective inducer of p27 expression in a variety of cell types (Paris et al. 2006; Bond et al. 2008; da Silva et al. 2008; Alderson et al. 2009; Kowalczyk et al. 2009). cAMP regulates p27 transcription in neuronal cells (Shin et al. 2009). Manipulation of cAMP and MAPK cascades revealed that cAMP activation of Rap-GTP/B-Raf (**Figure 4.3** and **4.4**) mediates protein expression (**Figure 4.5**, **4.6, and 4.7**) and cytoplasmic mislocalization (**Figure 4.9**) of p27 protein levels in tuberin null QTRRE cells, as well as in *Tsc-2*$^{+/+}$ human HK2 cells (**Figure 4.9**). Since phosphodiesterase inhibitors increase p27 levels in both QTRRE (tuberin null) and HK2 (tuberin expressing) cells, tuberin status may be an independent factor in cAMP regulation of p27 expression. In neuronal progenitor, retinal, schwannoma, and skin

cells, a cAMP mediated increase in nuclear p27 promoted differentiation and/or cell cyle exit (Paris et al. 2006; da Silva et al. 2008; Alderson et al. 2009; Kowalczyk et al. 2009). Since cAMP mediated increases in cytoplasmic p27, it is incapable of mediating cell cycle exit. The biological effect of cytoplasmic p27 is still unknown, and the mechanism of cytosolic transport and stabilization of p27 is not well understood in any model.

Phosphodiesterase inhibitors can negatively modulate degradation of p27 by decreasing phosphorylation on T187 and decreasing skp1 protein levels, thus resulting in an increase in p27 (**Figure 4.6**). Similarly, in vascular smooth muscle cells, elevation in cAMP resulted in increased p27 levels and reduced skp2, which is part of the SCF^{SKP} E3-ubiquitin-ligase complex that targets p27 for degradation (Bond et al. 2008). cAMP may regulate cell cycle exit by increasing p27 and decreasing skp protein levels. Our data also confirm that modulation of cAMP levels results in similar p27 and skp1 expression changes.

Finally, we identified that p27 stabilizes cyclin D1 in the cytosolic fraction of QTRRE cells, as confirmed by (i) increasing cAMP levels with phosphodiesterase inhibitors and dibutyryl cAMP (**Figure 4.6**), (ii) inhibiting the proteosome with MG132 (**Figure 4.7**), and (iii) by siRNA targeted degradation of p27 (**Figure 4.10**) in QTRRE cells. In *in vitro* and *in vivo* models, isolated p27-cyclin D-CDK4 complexes have intact kinase activity (Blain et al. 1997; James et al. 2008). Therefore, cytoplasmic p27-cyclin D-CDK4 active complexes may play a crucial role in renal tumor formation. The function of cyclin D1 and p27 in the cytoplasm in TGHQ induced renal tumors and tumorigenic QTRRE cells warrants further exploration.

5.6. Role of p27 as an oncogene and possible biomarker in human RCC

Cytoplasmic p27 occurs in a number of human cancers, and is classified as an oncogene when mislocalized to the cytoplasm. In human kidney, breast, colon, ovarian, thyroid and esophageal cancers; cytoplasmic mislocalization of p27 is correlated with an aggressive tumor type and poor prognosis (Ciaparrone et al. 1998; Singh et al. 1998; Masciullo et al. 2000; Viglietto et al. 2002; Alkarain et al. 2004; Motti et al. 2005; Pantuck et al. 2007; Hennenlotter et al. 2008). Over 370 renal cell carcinoma (RCC) tissues were immunostained with p27 to determine its compartmentalization. Staining identified nuclear p27 in 78% of the tumors, and cytoplasmic localization in 46% of the tumors (Pantuck et al. 2007). Cytoplasmic p27 staining was higher in metastatic RCC, and was identified as a predictor of disease specific survival time, with cytoplasmic mislocalization predicting a poor prognosis (Pantuck et al. 2007). Therefore, the induction of p27 protein expression may have a variable outcome depending on the tumor grade.

There are a number of different possible oncogenic functions of p27. One theory proposes that cytoplasmic oncogenic activity of p27 may be mediated through its ability to interact with RhoGTPase to regulate actin cytoskeleton rearrangements and cell migration/motility (McAllister et al. 2003; Besson et al. 2004; Sicinski et al. 2007). p27 interacts with RhoGTPase in hepatocytes, which may enhance actin depolymerization and decrease stress fiber stability. (McAllister et al. 2003; Besson et al. 2004; Ridley 2006). Yet, the role of p27 as a cytoskeletal regulator in tumorgenesis still needs further exploration.

Recent data suggest that cytoplasmic relocalization of p27 results in a gain of function that leads to inhibition of apoptosis and advancement of tumorigenicity (Short et al. 2008). Phosphorylation of p27 on T170 by AMPK, in *Tsc2*$^{-/-}$ mouse embryonic fibroblasts (MEFs), mediates its accumulation in the cytoplasm, and may stimulate its antiapoptotic function (Short et al. 2008). In human RCC cells (786-0 and Caki-1), cytoplasmic sequestration of p27 confers resistance to apoptosis (Kim et al. 2009). In 786-0 cells, siRNA knockdown of p27 resulted in caspase cleavage and in an increased number of apoptotic nuclei (Kim et al. 2009), suggesting that p27 plays a direct role in the resistance to apoptosis in human RCC. Furthermore, treatment of 786-0 and Caki-1 cells with LY294002 (PI3K inhibitor) or wortmannin resulted in caspase cleavage and relocalization of p27 to the nucleus, whereas treatment with rapamycin had no effect (Kim et al. 2009). The resultant relocalization of p27 to the nucleus, following inhibition of AKT, was independent of *VHL* status, as Caki-1 cells are *VHL* positive. These data suggest that *VHL* status and the mTOR cascade do not play a direct role in p27 cytoplasmic relocalization or resistance to apoptosis. Therefore, we suspect that the B-Raf/MAPK cascade is the pathway that regulates p27 protein expression and cytoplasmic stabilization, and may also play a role in conferring resistance to apoptosis.

We also suspect that *Tsc-2* status in RCC may be an independent factor in cytoplasmic relocalization of p27, as phosphodiesterase inhibition in HK2 cells also resulted in an increase in p27 in the cytoplasm (**Chapter 4**). Therefore, our data, that B-Raf directly regulates p27 expression and cytoplasmic compartmentalization in tuberous sclerosis RCC may be applicable to human RCC as well. Human *VHL* RCC and rodent *Tsc-2* RCC not only share clear cell pathology, but also a number of common

downstream targets. Data in **Chapter 4** confirm that *Tsc-2* and *VHL* renal tumor development both involve relocalization of p27 to the cytoplasm, and that both wild-type *Tsc-2* and *VHL* directly bind p27 to stabilize it within the nucleus (Soucek et al. 1997; Rosner et al. 2007). *VHL* and *Tsc-2* RCC also both result in increased protein levels of VEGF (Brugarolas et al. 2003; Rebuzzi et al. 2007), and accumulation of HIFα (Brugarolas et al. 2003; Liu et al. 2003). These striking similarities between human *VHL* RCC and our rodent *Tsc-2* RCC model allow for plausible extrapolation between the two models. Therefore, B-Raf directed transcription of p27 and cytoplasmic relocalization of p27-cyclin D-CDK4 may aid in RCC cancer progression. Our studies may also aid in determining the significance of p27 as a biomarker in human RCC.

There are a number of potential biomarkers for RCC that are in the process of being validated; including proliferating cell nuclear antigen (Ki-67), *VHL* status, carbonic anhydrase, PTEN, and silver staining of nucleolar organizing regions (Kim et al. 2009). However, the correlation between cytoplasmic relocalization of p27 and an aggressive tumor type in human RCC highlights the potential use of p27 as a predictive biomarker (Pantuck et al. 2007; Hennenlotter et al. 2008; Kim et al. 2009). Identification of cytoplasmic p27 in metastatic RCC may also help delineate treatment regimens to be used in the clinic, since a more aggressive tumor type will require a more aggressive battery of chemotherapeutics and small molecule inhibitors.

CHAPTER 6: FUTURE DIRECTIONS

6.1. Overview

Signal transduction pathways regulating tumor growth are quite complex. Signaling cascades are modulated by intricate networks integrating cascades and effectors. The MAPK cascade is involved in crosstalk with the mTOR cascade (**Chapter 3**), and can regulate phosphorylation of 4EBP1. Therefore, inhibiting the MAPK cascade with sorafenib, or the mTOR cascade with a rapamycin analog, as a single therapy treatment, would not be sufficient to abrogate renal tumor growth. Rather, combination treatments with receptor tyrosine kinase inhibitors tarceva and MP470 produce synergistic effects on 4EBP1 phosphorylation. Therefore, the efficacy of combination therapies with sorafenib, rapamycin, tarceva, and MP470 needs to be determined in renal tumor xenografts in nude mice.

Moreover, cytoplasmic mislocalization of p27 and cyclin D1 is an important aspect of tuberous sclerosis renal cell carcinoma, and the cytosolic stability of cyclin D1 is dependent on p27 expression (**Chapter 4**). However, the functional significance of p27-cyclin D1 in the cytosol is unknown. Stable transfection of QTRRE cells with p27 shRNA should assist in determining the role of cytoplasmic p27 in QTRRE xenograft tumor formation in nude mice.

6.2. Validation of synergistic drug treatments in renal tumor xenografts in athymic nude mice.

6.2.1. Introduction

Our data suggest that there is cross talk between the mTOR and ERK cascades to regulate phosphorylation of 4EBP1. This occurs through a novel mechanism by which 4EBP1 phosphorylation is modulated by the Raf-1/MEK/ERK MAP kinase cascade following loss of tuberin expression in QTRRE cells. mTOR can regulate the phosphorylation of 4EBP1, resulting in increased translation, but our model is unique in that the ERK cascade can also regulate the phosphorylation of 4EBP1. Modulation of Raf/MEK/ERK signaling with the Raf kinase inhibitor sorafenib, or the MEK1/2 inhibitor PD 98059, in QTRRE cells (tuberin null), established that the Raf/MEK/ERK pathway regulates the hierarchical phosphorylation of 4EBP1 on Thr37/46, Thr70, and Ser65 (**Chapter 3**). Furthermore, utilizing B-Raf or Raf-1 siRNA, I determined that Raf-1 is responsible for downstream ERK, and 4EBP1 protein activation. These findings identify Raf-1 as an effective regulator of 4EBP1 phosphorylation and activator of cap-dependent translation.

Sorafenib is a dual-action Raf kinase and vascular endothelial growth factor receptor (VEGF) inhibitor that targets tumor cell proliferation and tumor angiogenesis. Another agent recently approved for the treatment of advanced RCC is temsirolimus, an analog of rapamycin that inhibits mTOR mediated signaling. Currently, patients are being treated with either sorafenib or temsirolimus as a single therapy, but not in combination. Our data suggest that inhibition of one pathway is not sufficient to abrogate 4EBP1 phosphorylation, since both mTOR and ERK are capable of activating 4EBP1;

therefore, treatment with sorafenib in combination with rapamycin may be more efficacious than either single agent alone.

We are interested in validating the significance of cross talk between mTOR and ERK pathways in regulating 4EBP1 phosphorylation, which results in increased protein translation and tumor formation. Studies combining sorafenib and rapamycin treatment in athymic mice to treat renal tumors have not been done. Additionally the xenographs could be used for global MALDI-tissue imaging on protein profiling and determination of drug (sorafenib, rapamycin, tarceva, and MP470) deposition in tumors.

6.2.2. QTRRE tumor xenografts as a model to study renal tumor burden.

Primary epithelial cells from the Tsc-$2^{EK/+}$ rat are sensitive to the transforming activity of TGHQ, and cell lines have been established from transformed foci induced by TGHQ. Tumorigenicity of QTRRE cell lines was assessed by injecting 5×10^6 cells into the backs of athymic nude mice at two sites per animal (Patel et al. 2003). All cell lines formed tumors in the nude mice, indicating malignant transformation. Histological examination of sections prepared from QTRRE derived tumors revealed that they were composed of large neoplastic cells, with eosinophilic cytoplasm and large nuclei, thereby resembling clear cell renal carcinoma cells. Tumors that developed from QTRRE cells were shown to be aggressive and exhibited a greater degree of vascularization.

Therefore, the QTRRE subcutaneous tumor formation model in athymic nude mice is optimal to test signal transduction changes following treatment with cancer therapeutics. Using this model we will be able to obtain *in vivo* derived renal tumors following drug treatments, for analysis of key signaling pathways involve in RCC and the

manner in which the cancer cells respond to drug treatment. Subcutaneous tumor growth will be determined with or without treatment with the anticancer agents (sorafenib, rapamycin, MP470 and tarceva) alone and in combination. Co-treatment with these anticancer agents will reveal whether there is a synergistic decrease in tumor growth due to interference with the crosstalk between the mTOR and ERK pathways discussed in this dissertation (**Chapter 3**). Tumor treatment with these drugs will also allow us to validate proteins necessary for malignant transformation. Traditional chemotherapy, hormonal therapy, and cytokine therapy have been relatively ineffective in treating renal cell carcinoma, with only 10-15% of the patients responding. A number of new agents designed to block tumor proliferation and angiogenesis have shown great promise in the treatment of RCC. Therefore, results from these studies will reveal whether combination therapies are more efficacious than individual agents alone, and will provide a comprehensive understanding of the signaling mechanisms governing renal tumor formation. Finally, these studies will provide increased confidence in applying the results of animal studies to humans.

6.2.3. Methods

A. In Vivo Bioassay (Establishment of Tumors): Female athymic nude mice (5-6 weeks old) will be injected via the subcutaneous injection route at two sites/animal with 5x10^6 cells/0.2 ml PBS per site. Mice will be divided into nine groups: 1) QT-RRE-2, 2) QT-RRE-2 + dose 1 of sorafenib, 3) QT-RRE-2 + dose 2 of sorafenib, 4) QT-RRE-2 + dose 1 of rapamycin, 5) QT-RRE-2 + dose 2 of rapamycin, 6) QT-RRE-2 + dose 1 of sorafenib and rapamycin, 7) QT-RRE-2 + dose 2 of sorafenib and rapamycin, 8) control rats administered PBS, 9) no SQ injection. Sorafenib will be given p.o. gavage 40 or 80 mg/kg daily, and rapamycin will be given p.o. gavage 6 or 12 mg/kg daily; as well as in combination with each dose. The experiment will be performed with 10 mice/group. Mice will be weighed once weekly, tumors measured 2 times per week, and observed. We will observe tumor progression, tumor necrosis, unusual behavior, activity, and respiration, and survival. Mice will be euthanized by overdose of pentobarbital (150-200 mg/kg), and/or tissues of interest will be harvested and analyzed.

B. Immunohistochemical ki-67 staining for tumor cell proliferation: Paraffin-embedded tissue sections of all tumors will be prepared and first labeled with Ki-specific monoclonal rat antibody (DAKO A/S), followed by staining with a biotinylated antirat immunoglobulin antibody (DAKO A/S). The biotinylated antibody will be detected histochemically using the DAKO StrepABComplex staining kit. The color reaction will be visualized with diaminobenzidine, and tissues will be counterstained with hematoxylin. The Proliferation Index will be determined by Ki-67 immunostaining and

calculating the number of 3,3'- diaminobenzidine-positive cells per total number of cells in 5 randomly selected fields.

C. Detection and degree of angiogenesis: The paraffin-embedded tissue sections, sectioned (8-10 micron thick), will be stained with CD31 and CD31-VEGFR-2. The CD31 antibody will be incubated for 18 h at 4^{o}C, followed by incubation with a goat anti-rat horseradish peroxidase secondary for 1 h at room temperature. Positive staining will be visualized by incubating the slides in 3,3'-diaminobenzidine chromogen and counterstained with hematoxylin. The CD31-VEGFR-2 double staining will be done with CD31 conjugated to secondary Alexa Fluor 594 and VEGFR-2 antibody conjugated to Alexa Fluor 448.

D. Detection and quantitation of apoptosis: The terminal deoxynucleotidyl transferase-mediated dUTP nick end labeling (TUNEL) method was based on the specific binding of terminal deoxynucleotidyl transferase to the 3'-OH ends of DNA, ensuring synthesis of a polydeoxynucleotide polymer. Therefore, the ApopTag Plus *In Situ* Apoptosis Detection kit-Peroxidase (Oncor) will be used on paraffin-embedded tissue sections. The Apoptosis Index of stained sections of tumors from each group will be determined by counting at least 1,000 cells in 5 randomly selected high-power fields.

E. MALDI-tissue imaging to determine drug deposition in tumors, and for global protein profiling in tumors compared to normal tissue. A matrix assisted laser desorption ionization (MALDI) tissue image is a three dimensional array of data with the plane of the tissue section representing the XY dimensions while thousands of MALDI spectra acquired across the surface of the tissue represent the Z dimension. Volumes, or m/z values, are extracted from the data set to create images of user defined m/z ranges. Our goal is to utilize this technique to determine drug deposition, and to profile global protein changes in the tumors of all the treatment groups, in order to identify protein biomarkers in renal cell carcinoma.

6.2.4. Anticipated Results and Alternative Approaches

Since histological examination of QTRRE xenograft tumors in nude mice revealed that they closely resemble human clear cell pathology (RCC), this model of tumor formation is optimal to validate signal transduction changes in TGHQ-Tsc-$2^{EK/+}$-rat renal tumors and QTRRE cell models. Specifically, we will validate Raf/MEK/ERK MAPK, AKT/PI3K/mTOR/4EBP1, RTKs, cAMP, and PKA protein expression and activation in the renal tumor xenografts formed in nude mice. We have already initiated the first phase of xenograft tumor formation in nude mice and measured tumor burden over a 7-month interval to determine staging of drug treatment. It is expected that the histological staining techniques and Western blot analysis will provide accurate information with regard to cell proliferation, tumor burden, angiogenesis, and apoptosis. In addition we anticipate appropriate modulation of 4EBP1 and its phosphorylated isoforms. MALDI imaging is also available as a technique to be combined with molecular biological techniques in unraveling complex signaling cascades. Moreover we have the ability to

determine active drug concentrations in treated xenografts. Determining the extent to which such treatments modulate the activity of key signaling proteins by MS-based imaging will provide a unique measurement of drug efficacy during the treatment of RCC.

Traditional chemotherapy, hormonal therapy, and cytokine therapy have been relatively ineffective in treating renal cell carcinoma, with only 10-15% of the patients responding. A number of new agents designed to block tumor proliferation and angiogenesis have shown great progress in the treatment of RCC. Therefore, results from these studies will determine if combination therapy is more efficacious than any single agent alone, and to provide a comprehensive understanding of the signaling mechanisms governing renal tumor formation. Also, these studies will provide increased confidence in applying the results of animal studies to humans.

6.3. p27 as a target in Renal Cell Carcinoma

p27 is necessary for the cytoplasmic stability of cyclin D1, as siRNA knockdown of p27 results in an equivalent decrease in cyclin D1 protein levels. Futhermore, manipulation of p27 protein levels in QTRRE cells by phosphodiesterase inhibitors, dibutyryl cAMP, and the proteosome inhibitor MG132 resulted in a parallel increase in both p27 and cyclin D1. Moreover, sorafenib treatment caused a decrease in p27 and cyclin D1. However, the biological significance of p27-cyclin D1 cytoplasmic mislocalization has yet to be determined and its role as a potential oncogenic switch in renal tumor formation needs to be further explored. Therefore, it will be important to manipulate p27 protein levels during renal tumor formation. In order to determine the

role of p27 as an oncogene in renal tumor formation, QTRRE cells will be stably transfected with shRNA and those cells will be subcutaneously injected into nude mice in comparison to scrambled shRNA, and non-transfected QTRRE cells. The difference in tumor burden will be measured, and changes to the genome and proteome will be discovered as well.

APPENDIX A: MODULATION OF B-RAF

A.1. INTRODUCTION

The expression patterns of the Rafs in tissue vary greatly. Raf-1 is ubiquitously expressed, but A-Raf and B-Raf have restricted expression (Wellbrock et al. 2004). B-Raf protein expression in neuronal tissues has been well characterized (Wellbrock et al. 2004), but its expression patterns in other tissues are not as well established. The expression of B-Raf may alter which Raf isoform predominately activates ERK. When B-Raf is expressed and activated it has a higher affinity for MEK1/2 than Raf-1 (Peyssonnaux et al. 2001; Garnett et al. 2005). Therefore, it will be important to determine the expression pattern of B-Raf during renal tumor development.

An increase in B-Raf protein expression may lead to increased activation of B-Raf signaling through the ERK MAPK cascade. Another aspect of constitutive B-Raf activation is possible mutations within its kinase domain. Mutations in B-Raf have been identified in approximately 7% of human cancers, with around 70 different known mutations (Gray-Schopfer et al. 2007). In one study, eleven human RCC biopsies were sequenced for point mutations in the kinase domain of B-Raf, but none were identified (Davies et al. 2002). Although this one study did not reveal any B-Raf mutations, TGHQ transformation of kidney cells may lead to point mutations in the kinase domain of B-Raf. Therefore, further analysis of the kinase domain of B-Raf in QTRRE cells and tumors derived from TGHQ-treated *Tsc-2*$^{EK/+}$ rats is necessary.

The activation of the Rafs is highly dependent on their being phosphorylated on a number of crucial sites within all three domains (**Figure 1.3**). But it is difficult to determine which sites are phosphorylated within B-Raf, as there is a lack of antibodies

available to sites outside of the kinase domain. Therefore, it will be important to utilize other methods than Western blot to determine post translational modification involved in the activation of B-Raf in our rat renal tumor models.

Phosphorylation of Raf-1 within its activation domain has been shown to facilitate 14-3-3 binding and subsequent activation by B-Raf (Garnett et al. 2005; Rushworth et al. 2006). B-Raf activation is modulated through the formation of B-Raf/Raf-1 heterodimers (Garnett et al. 2005; Karbowniczek et al. 2006; Rushworth et al. 2006). Compared to the formation of Raf homodimers or monomers, isolated B-Raf/Raf-1 heterodimers have amplified kinase activity (Rushworth et al. 2006). Although Raf-1/B-Raf heterodimers has been identified in a number of models, dimerization with A-Raf has yet to be explored in any model.

.

A.2. MATERIALS AND METHODS

A.2.1. Cell culture

The tuberin-negative cell line QTRRE was established from primary renal epithelial cells (Yoon et al. 2001). QTRRE and HK2 cells were grown in DMEM/F12 (1:1) (Invitrogen, Carlsbad, California) with 10% FBS. Cells were grown at 37°C in a humidified atmosphere of 5% CO_2.

A.2.2. Mass Spectrometry

Protein samples were electrophoresed on 7.5 % Criterion™ XT Bis-Tris Gels. The gel was silver-stained and the appropriate bands were excised. Samples were trypsin-digested and the peptides will then be subjected to LC-MS/MS. Peptides were run through a homemade C18 column at 300 nL/min. The mass spectrometer used was an LCQ-DECA XP PLUS quadrupole ion trap mass spectrometer equipped with a nanoESI source and a nanofl ow HPLC system. Raw data was analyzed using X!Tandem. The modified peptides were manually validated by the program iongen, which generates theorectical b and y ions from a user specified peptide and adjusts the masses for specified adductions.

A.2.3. PCR amplification of B-Raf kinase domain

Total RNA from QTRRE cells, 8-month TGHQ- or vehicle-treated *Tsc-2*$^{EK/+}$ and *Tsc-2*$^{EK/+}$ rats, or tumors excised from 8-month TGHQ- *Tsc-2*$^{EK/+}$ rats were isolated with TRIReagent (Sigma) utilizing the manufacturer's protocol, and 4.5 µg RNA, in a 20 µl total reaction volume, was reverse transcribed using the Fermentas First Strand cDNA

Synthesis kit according to the manufacturer's protocol. PCR products were generated using the Advantage cDNA PCR kit (Clontech, Mountain View, CA) according to manufacturer's protocol. Amplicon sizes and primers were as follows: bp B-Raf (forward: 5'-GGC TGA AAG CTT CAG CAC CCA CAC CTC AGC-3', reverse: 5'-AT CTG GAT CCT GTT GTT GAT GTT TGA ATA AGG-3'. The thermocycling conditions for B-Raf were 95°C for 5 minutes; then 28 cycles of 95°C for 30 seconds, 59°C for 40 seconds, and 72°C for 60 seconds, followed by a 10 minute 72°C final extension. PCR products were separated on 2% ethidium bromide stained agarose gel. Bands were excised and DNA was isolated and sent for sequencing.

A.2.4. Immunoprecipitation

2-4 μg of each phospho-immune complex (B-Raf, Raf-1, A-Raf, and 14-3-3 isoforms) were added to microcentrifuge tubes containing 5 mg of QTRRE tissue lysates and protein-A/G sepharose beads, and incubated with rotation for 18 h at 4°C. Microcentrifuge tubes were centrifuged at 7500 *g* for 2 min, supernatant removed, and beads washed three times with cell lysis buffer. Proteins were separated from protein-antibody bead complex with 4x XT sample loading buffer with β-mercaptoethanol. Samples were run on 7% SDS-PAGE gel, transferred to PVDF membrane, and the blots were visualized with Amersham ECLTM Western Blotting Detection Reagents (GE Healthcare, UK).

A.3. RESULTS

A.3.1. B-Raf is constitutively phosphorylated at serine residues S345 and S483 in QTRRE cells

Human B-Raf is phosphorylated on a number of sites: S364, S428, and T439 (inhibitory); S445, T598, S601, and S728 (activating) (**Figure 1.3**). In QTRRE cells B-Raf was found to have elevated kinase activity (Yoon et al. 2004). The kinase activity of B-Raf is known to be associated with phosphorylation of T598 and S601 within the kinase domain (CR3). In order to identify other constitutively phosphoryalted sites on B-Raf in QTRRE cells we isolated B-Raf by immunoprecipitation (IP), excised two bands at 100- and 95-kDa from a silver stained gel, and performed LC-MS/MS analysis on the samples (**Figure A.1**). Peptides SSSAPNVHINTIEPVNIDDLIR (345-386) and RDSSDDWEIPDGQITVGQR (481-499) were identified by LC-MS/MS as having an 80 kDa mass addition at S345 and S483 in both 100- and 95-kDa forms of B-Raf (**Figure A.1**). These sites correlate with human S364 and S445.

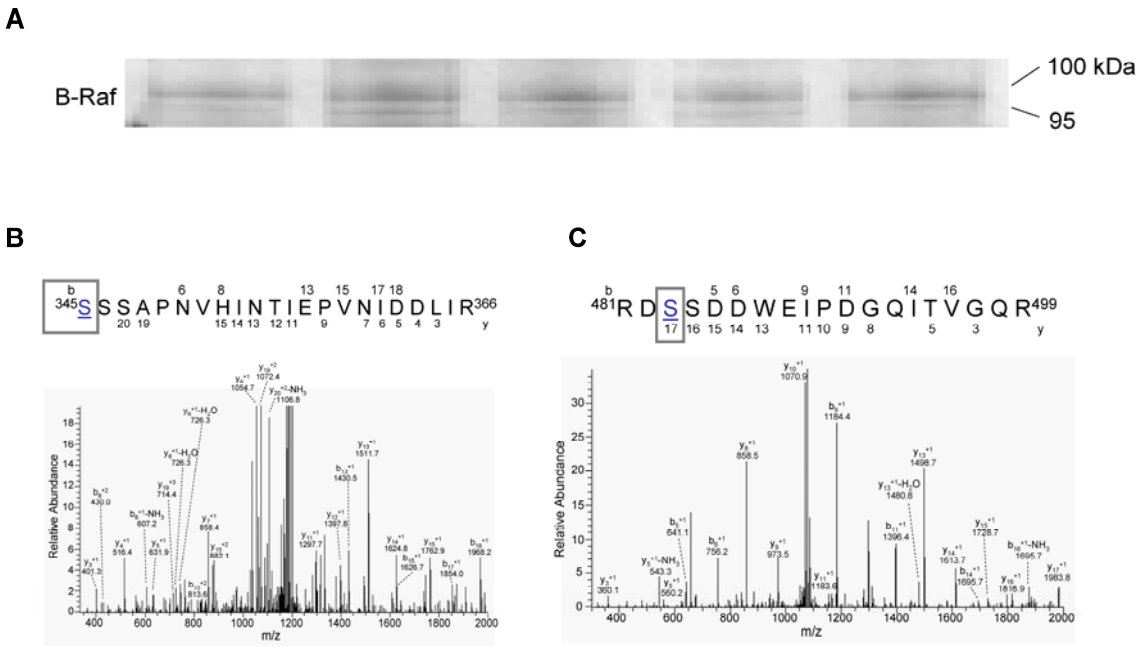

Figure A.1. B-Raf is constitutively phosphorylated at serine residues S345 and S483 in QTRRE cells.

(A) Silver stained gel of B-Raf immunoprecipitations from QTRRE cells. Both the 100 kDa and 95 kDa species were identified as B-Raf by LC-MS/MS analysis. Both species have constitutive phosphorylations on peptides described in (B) and (C). (B) Spectrum of peptide 345-366 from B-Raf. This peptide was identified by X!Tandem from a band excised from a gel corresponding to the molecular weight of B-Raf. Serine-345 was found to have a mass addition of 80, corresponding to a phosphorylation; this finding was confirmed by manual validation. The spectrum was magnified to a maximum of 20% relative abundance to account for the proline effect seen with the y9 and b13 ions. (C) Spectrum of peptide 481-499 from B-Raf. Serine-483 was found to have a mass addition of 80, corresponding to a phosphorylation; this finding was confirmed by manual validation. The spectrum was magnified to a maximum of 30% relative abundance to account for the proline effect seen with the y10 and b9 ions.

A.3.2. Splice variants within the kinase domain of B-Raf in rats

We sequenced the kinase domain of B-Raf to determine if any splice variants exist in our rat *in vitro* and *in vivo* models. RNA was isolated from QTRRE cells, equal concentrations were used to contruct cDNA libraries, and equal concentrations of cDNA were PCR amplied within the kinase domain of B-Raf (**Figure A.2 lane 2**). Bands were excised from the gel; DNA was purified and submitted for sequencing. All three bands at 600, 500, and 400 bp were identified as B-Raf, and no point mutations were identified in any band (**Figure A.2**). RNA was isolated from the OSOM of 8-month TGHQ- or vehicle-treated *Tsc-2*$^{EK/+}$ and *Tsc-2*$^{EK/+}$ rats, as well as tumors from TGHQ treated *Tsc-2*$^{EK/+}$ rats. Samples were prepared with the identical methodology as QTRRE cells. Splice variants within the kinase domain of B-Raf were identified at the identical molecular weights as in the QTRRE cells, at 600, 500, and 400 bp (**Figure A.3)**. No point mutations were identified.

A.3.3. B-Raf/Raf-1 heterodimeriation and B-Raf/A-Raf/Raf-1 trimerization in QTRRE cells

B-Raf, Raf-1, and 14-3-3 isoforms were immunoprecipitated from QTRRE lysates. Each IP and total cell lysate (TCL) from QTRRE cells were immunoblotted for B-Raf (**Figure A.4A**), Raf-1 (**Figure A.4B**), or 14-3-3 isoforms (**Figure A.4C**) protein expression. The data suggests that B-Raf/Raf-1 form a dimer that complexes with 14-3-3 in QTRRE cells (**Figure A.4**).

B-Raf, Raf-1, A-Raf, and 14-3-3 were immunoprecipitated from QTRRE lysates. Each IP and TCL from QTRRE or HK2 cells were immunoblotted for B-Raf protein

expression. The data suggest that B-Raf/Raf-1/A-Raf form a trimeric protein complex in QTRRE cells (**Figure A.5**).

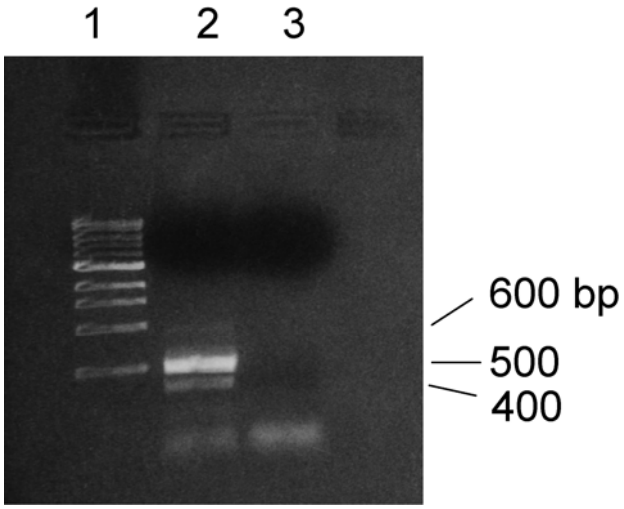

Figure A.2. Splice varients within the kinase domain of B-Raf in QTRRE cells.

RNA was isolated from QTRRE cells, equal concentrations were used to contruct cDNA libraries, and equal concentrations of cDNA were PCR amplied within the kinase domain of B-Raf. B-Raf PCR products were run on a 2% agarose gel. B-Raf species were isolated and sequencing identified each as B-Raf. Lane 1 is the ladder, lane 2 is B-Raf PCR of QTRRE cells, and lane 3 is PCR amplification control. Bands below 400 bp are primer dimmer.

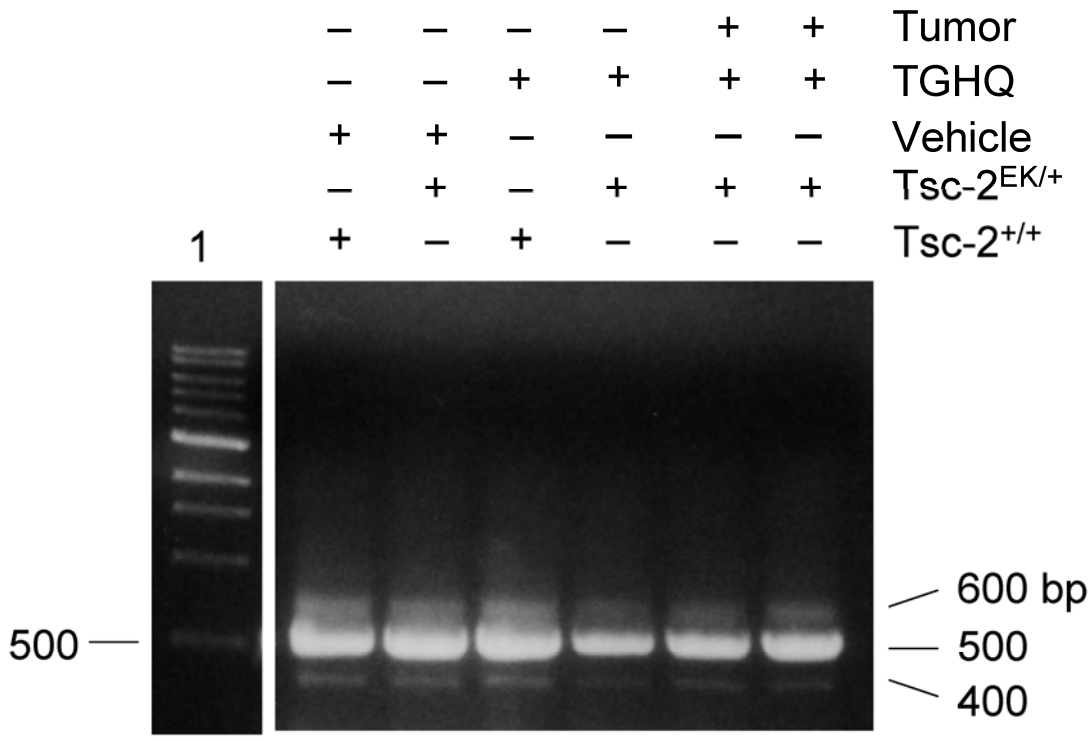

Figure A.3. Splice variants within kinase the domain of B-Raf in *Tsc-2*$^{EK/+}$ and *Tsc-2*$^{EK/+}$ TGHQ- and vehicle-treated rats.

RNA was isolated from 8-month TGHQ- or vehicle-treated *Tsc-2*$^{EK/+}$ and *Tsc-2*$^{EK/+}$ rats, equal concentrations were used to contruct cDNA libraries, and equal concentrations of cDNA were PCR amplied within the kinase domain of B-Raf. B-Raf PCR products were run on a 2% agarose gel. B-Raf species were isolated and sequencing identified each as B-Raf. Lane 1 is DNA ladder.

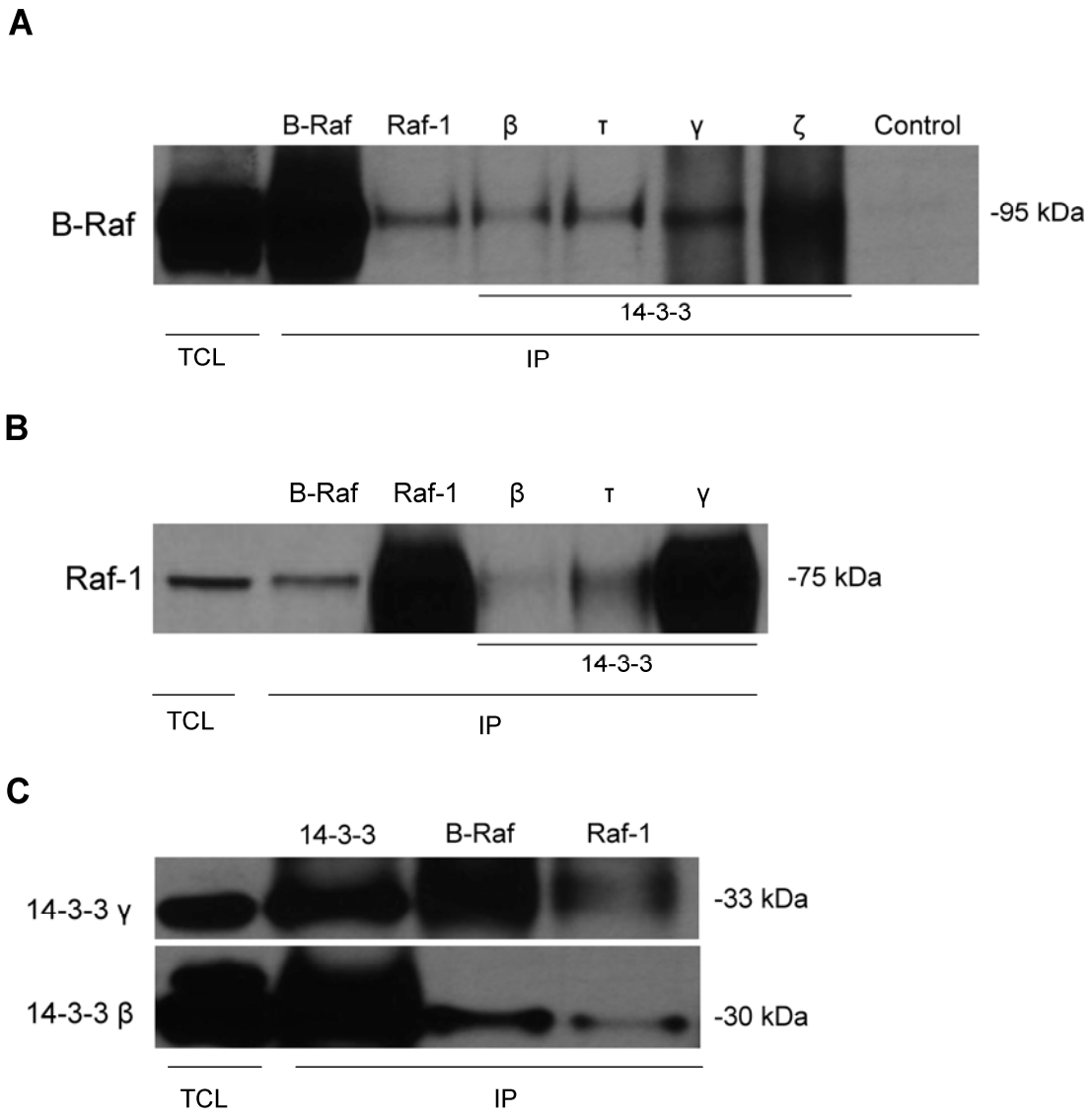

Figure A.4. B-Raf/Raf-1 heterodimerization in QTRRE cells.

B-Raf, Raf-1 and 14-3-3 isoforms were immunoprecipitated (IP) from QTRRE lysates. Each IP and total cell lysate (TCL) from QTRRE cells were immunoblotted for (*A*) B-Raf, (*B*) Raf-1 protein expression, and (*C*) 14-3-3 isoforms. QTRRE lysate was incubated with beads with no antibody (Control).

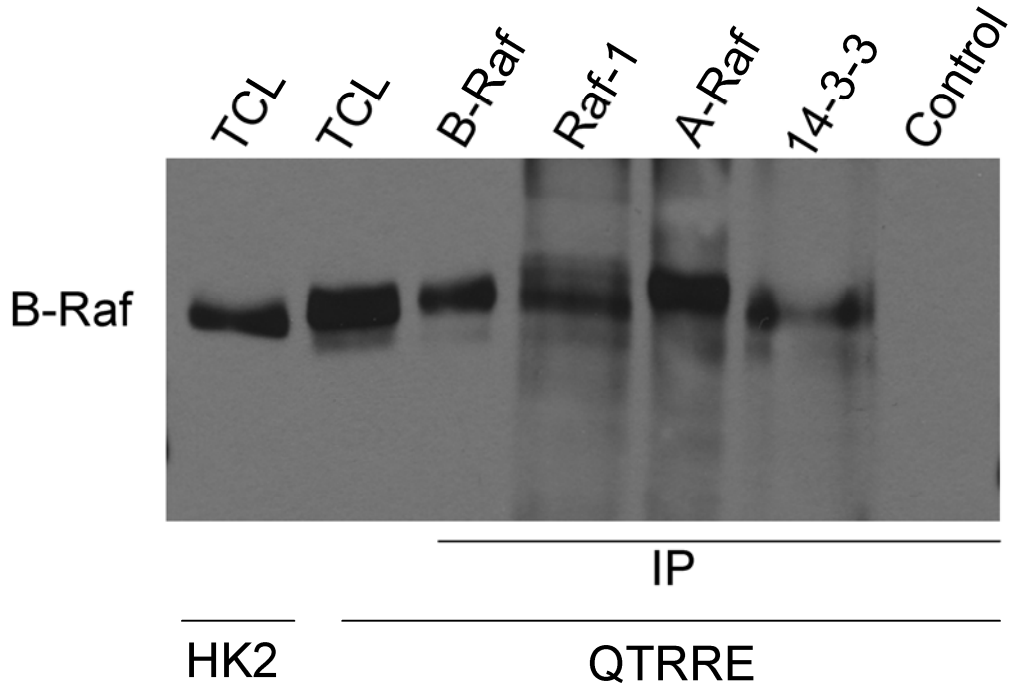

Figure A.5. B-Raf/A-Raf/Raf-1 trimerization in QTRRE cells.

B-Raf, Raf-1, A-Raf, and 14-3-3 were immunoprecipitated (IP) from QTRRE lysates. Each IP and total cell lysate (TCL) from QTRRE or HK2 cells were immunoblotted for B-Raf protein expression. QTRRE lysate was incubated with beads with no antibody (Control).

A.4. DISCUSSION

B-Raf isoforms exist between 69-75 kDa and 79-100 kDa depending on the species (Stephens et al. 1992; Barnier et al. 1995; Papin et al. 1995). Isoforms of B-Raf have frequently been found to have similar activating post translational modifications. B-Raf is constiutively expressed and activated in QTRRE cells, and with a higher level of activation than Raf-1, as determined by Raf-1 and B-Raf kinase assays (**Chapter 4**) (Yoon et al. 2004). The kinase assays confirm that B-Raf is fully activated and phosphorylated within its kinase domain at T598 and S601. We utilized LC-MS/MS to identify other constiutively phosphorylated sites on B-Raf. We identified an 80 dalton addition on S345 and S483 in both 100- and 95-kDa forms of B-Raf in QTRRE cells (**Figure A.1**). These sites correlate with human S364 and S445. B-Raf S364 is known to be phosphorylated by serum and glucocorticoid-inducible kinase (SGK) (Chong et al. 2003). Phosphorylation on this site has been associated with complex formation with 14-3-3, an adapter protein, which is thought to keep Raf in an auto-inhibited state.

Recent work in a number of different models have identified that 14-3-3 binding at the S345 site modulates B-Raf/Raf-1 heterodimerization (Garnett et al. 2005; Karbowniczek et al. 2006; Rushworth et al. 2006). In our tumorigenic QTRRE cells, we observed B-Raf/Raf-1/14-3-3 complex formation (**Figure A.4**), as well as B-Raf/Raf-1/A-Raf/14-3-3 complex formation (**Figure A.5**). This is the first data suggesting that A-Raf can complex with other Raf isoforms. A-Raf is expressed in our QTRRE cells but its biological significance and role in ERK pathway activation has yet to be determined.

In melanoma, B-Raf is commonly mutated within the kinase domain to yield a constituitively active B-Raf (Wan et al. 2004). We sought to determine if B-Raf

activation in QTRRE cells was in part due to point mutations within the kinase domain. Amplifaction of the kinase domain of B-Raf in QTRRE cells, OSOM of 8-month TGHQ- or vehicle-treated *Tsc-2*$^{EK/+}$ and *Tsc-2*$^{EK/+}$ rats, or tumors excised from 8-month TGHQ-*Tsc-2*$^{EK/+}$ rats did not reveal any point mutations within the kinase domain of B-Raf (**Figure A.2 and A.3**). Interestingly, the data revealed three possible splice variants of B-Raf within the kinase domain. The possible splice variants were around 400 and 600 bp. Both variants were diplayed in all samples, leading us to conclude that they are native to Long Evans rats and not an effect of TGHQ or loss of tuberin in TGHQ induced tuberous sclerosis renal cell carcinoma.

APPENDIX B: RECEPTOR TYROSINE KINASES AS A POTENTIAL UPSTREAM TARGET IN RENAL CELL CARCINOMA

B.1. INTRODUCTION

Tarceva is a small molecule human epidermal growth factor type 1/epidermal growth factor receptor (HER1/EGFR) inhibitor, which is approved to treat non-small cell lung cancer and pancreatic cancer. MP470 is a novel RTK inhibitor which effectively inhibits PDGFR, c-Kit and c-Met. Recently, the use of these treatments in combination has been tested in a prostate cancer model. Treatment of MP 470 in prostate LNCaP cancer cells resulted in inhibition of cell proliferation, cell growth arrest, and promotion of apoptosis (Qi et al. 2009). MP 470 in combination with tarceva drastically reduced HER family/PI3K/Akt pathway signaling, as well associated tumor growth inhibition in a LNCaP mouse xenograft model (Qi et al. 2009). This study has progressed to a phase I clinal trial.

Niether of these compounds have been tested for their efficacy in treating renal cell carcinoma. Single agent therapy with small molecule inhibitors is largely ineffective in advanced cancer treatment due to acquired mechanisms of resistance. Therefore, we are interested in determining if there is a synergistic effect of these compounds in a renal cell carcinoma model. Our proposed downstream target is the mTOR-p4EBP1 cascade, which is known to be activated by receptor tyrosine kinases (**Figure B.1**).

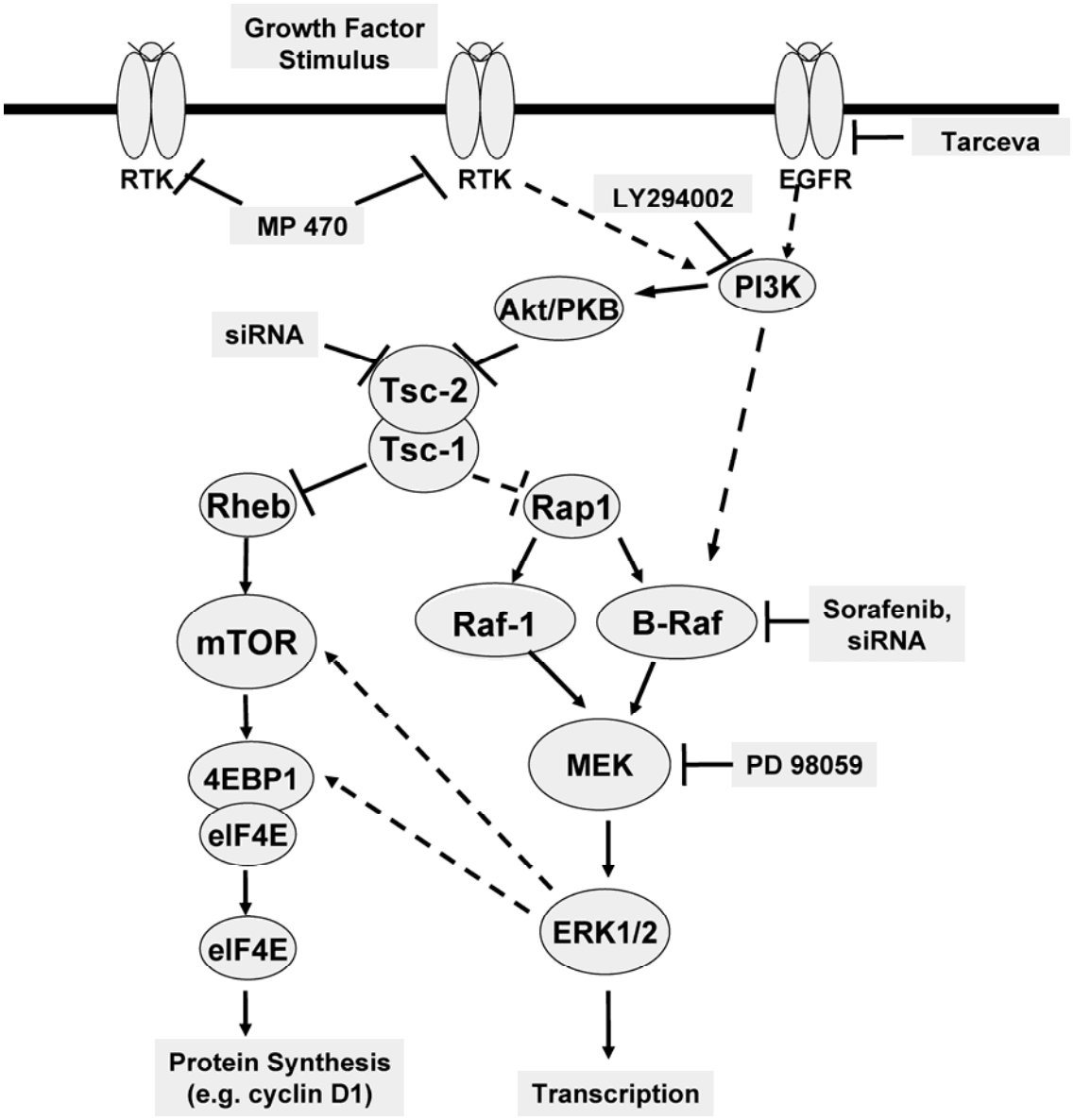

Figure B.1. Receptor tyrosine kinase pathway modulation of 4EBP1.

The proposed impact of receptor tyrosine kinase (RTK) signaling on the tuberin-mTOR-4EBP1 cascade. RTK is a known activator of PI3K. PI3K can phosphorylate AKT, which is known to phosphorylate tuberin resulting in activation of mTOR and downstream phosphorylation of 4EBP1.

B.2. MATERIALS AND METHODS

B.2.1. Cell culture

The tuberin-negative cell line QTRRE was established from primary renal epithelial cells (Yoon et al. 2001). QTRRE cells were grown in DMEM/F12 (1:1) (Invitrogen, Carlsbad, California) with 10% FBS. Cells were grown at 37°C in a humidified atmosphere of 5% CO_2.

B.2.2. MTS Proliferation Assay

QTRRE cells were seeded at 3.1×10^3 cells/well in 96-well flat-bottomed plates in DMEM/F12 with 10% FBS. At 80-90% confluency cells were treated with 10 μM or 20 μM tarceva and MP 470 in combination, in DMEM/F12 with 2% FBS for 1 or 2 h. Following single or combination drug incubations, cells were washed twice with treatment media (DMEM (-) phenol red, (-) Na pyruvate, (+) 25 mM Hepes, (+) L-glutamine) (Invitrogen) and the proliferative activity of cells was determined by MTS assay (CellTiter 96 Non-Radioactive Cell Proliferation Assay; Promega, Madison, WI), according to the manufacturer's recommendations. In metabolically active cells, MTS was bioreduced by dehydrogenase enzymes into a formazan product that was soluble in tissue culture medium. The absorbance of the formazan at 490nm was measured in a SpectraMax M2 (Molecular Devices, Sunnyvale, CA) 96-well plate reader. Values represent means ± SD (n=6).

B.2.3. Western blot analysis

QTRRE cells were treated with 20 μM tarceva, 20 μM MP470, or in combination in DMEM/F12 with 2% FBS for 30, 60, or 90 min QTRRE cells were lysed with Cell Lysis Buffer 10X (Cell Signaling Technology, Inc, Beverly, MA) containing 1 mM Pefabloc SC (Roche) and Complete protease inhibitor cocktail tablets (Roche). Protein concentration was determined with the DC Protein Assay (BioRad). Protein was subjected to 7, 10 or 12% SDS-PAGE and proteins were electrophoretically transferred to PVDF membranes. Primary antibodies used were p42/44, cyclin D1, 4EBP1, p-4EBP1 (Thr37/46), p-4EBP1 (Thr70), and p-4EBP1 (Ser65) purchased from Cell Signaling Technologies, and GAPDH (Ambion, Austin, Texas). The secondary-immunoglobulin conjugated with horseradish peroxidase (Santa Cruz Biotechnology, CA) was used at a 1:3000 dilution. The blots were visualized with Amersham ECLTM Western Blotting Detection Reagents (GE Healthcare, UK).

B.3. RESULTS

B.3.1. Tarceva and MP 470 combination treatment has minor impact on mitochondrial dehydrogenase enzyme activity in QTRRE cells

Mitochondrial dehydrogenase enzyme activity was quantified using the MTS assay, which measures dehydrogenase enzyme activity and the reduction of MTS to formazan. Treatment of QTRRE cells with a combination of 10 μM tarceva and 10 μM MP 470 did not result in a statistically significant decrease in metabolic activity at the 1 or 2 h time points (**Figure B.2**). In contrast, treatment with a combination of 20 μM tarceva and 20 μM MP 470 resulted in a maximal 30% decrease in metabolic activity at 2 h (**Figure B.2**). Therefore, we treated QTRRE cells with the 20 μM combination treatment, as there was a minimal decrease in cell viability.

B.3.2. Synergistic effect of tarceva and MP 470 combination treatment on 4EBP1 phosphorylation

TGHQ transformed QTRRE cells express constitutively phosphorylated forms of 4EBP1 (**Figure B.3 Lane 1 [DMSO]**); as well as one distinct species of 4EBP1. To examine whether receptor tyrosine kinases contribute to phosphorylation of 4EBP1 in QTRRE cells, p-4EBP1-Ser65, -Thr70, and -Thr37/46 were determined by Western analysis following treatment with tarceva (20 μM), MP 470 (20 μM), or in combination (**Figure B.3**). QTRRE cells constitutively express one visible species of 4EBP1. Treatment with tarceva exhibited a decrease in the highest molecular weight species of p-4EBP1-Ser65 and -Thr37/46, and did not result in the appearance of the lower molecular weight band. Treatment with MP 470 resulted in the appearance of the lower molecular

weight band on 4EBP1 and p-4EBP1-Thr37/46, as well as the time-dependent decrease on p-4EBP1-S65.

The most profound decrease in highest molecular weight species of p-4EBP1 was observed in the tarceva-MP 470 combination treatment time course. With the combination treatment, there was a time-dependent disappearance of the higher molecular weight band in p-4EBP1-Ser65, -Thr70, and -Thr37/46; and a parallel shift in band intensity from the higher molecular weight 4EBP1 band to the lower molecular weight band in p-4EBP1-Thr 70 and -Thr 37/46 as early as 30 min (**Figure B.3**). Maximal changes in the pattern of p4EBP1 p-4EBP1-Ser65, -Thr70, and -Thr37/46 expression occurred by 1.5 h after combination treatment. Interestingly, only the combination treatment resulted in a sustained increase in a "faster migrating" band when probed for total 4EBP1 protein (**Figure B.3**).

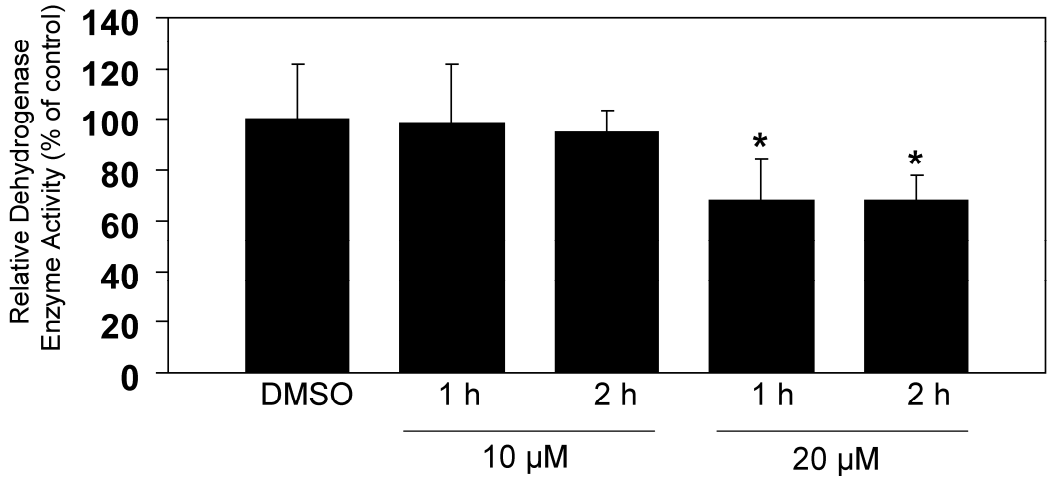

Figure B.2. Effect of Tarceva and MP 470 combination treatment on mitrochondrial dehydrogenase enzyme activity in QTRRE cells.

QTRRE cells were treated with 10 µM or 20 µM tarceva and MP470 in combination for 1 or 2 h. Control cells were treated with an equal volume of DMSO. Metabolic activity of QTRRE cells following drug treatments was quantitated using the CellTiter 96® Aqueous Non-Radioactive Cell Proliferation (MTS) Assay (Promega). Values represent the mean ± SD (n=6). A significant difference was seen between control (DMSO) and tarceva/MP 470 treated cells at * $P<0.01$.

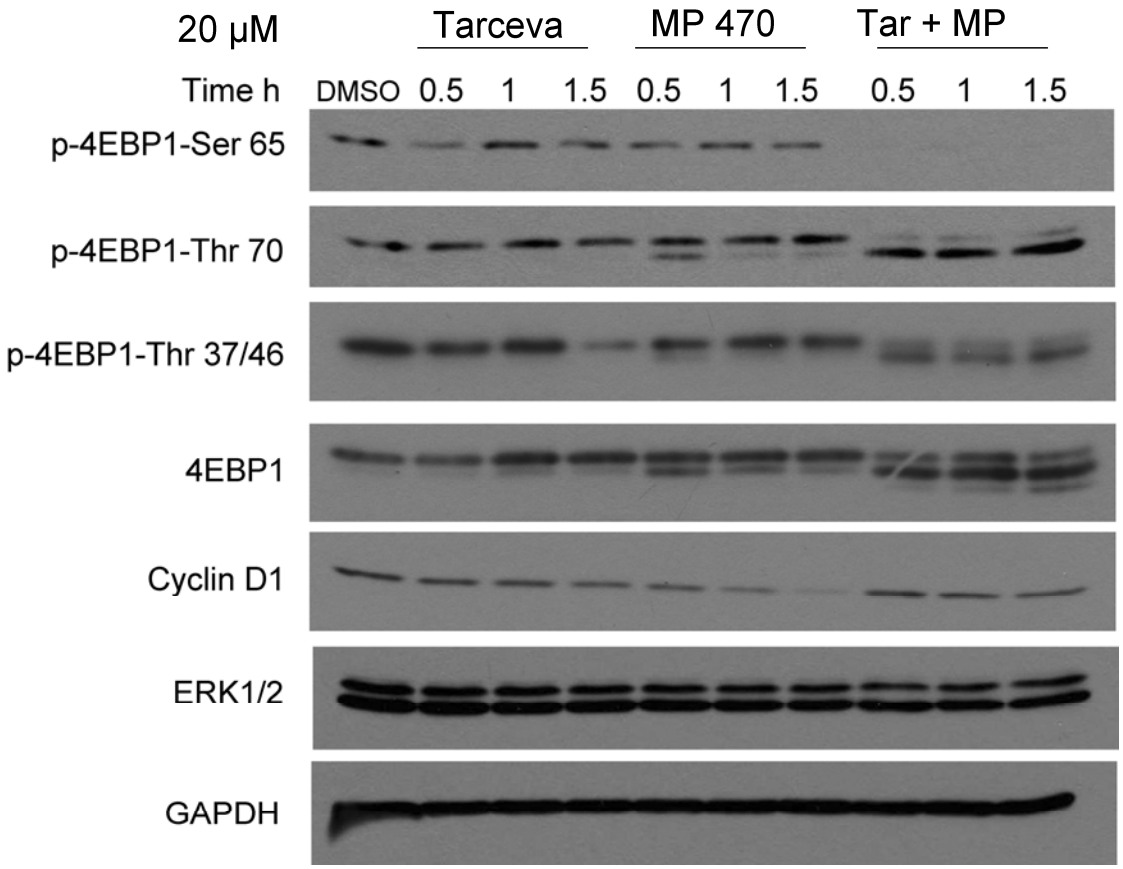

Figure B.3. Synergistic effect of tarceva and MP 470 combination treatment on 4EBP1 phosphorylation.

QTRRE cells were treated with tarveva (20 μM), MP 470 (20 μM), and in combination for 0.5, 1, and 1.5 h. Cyclin D1, ERK1/2, 4EBP1 and p-4EBP1-Ser65, -Thr70, and -Thr37/46 were visualized by Western blot analysis. GAPDH was used as a loading control.

B.4. DISCUSSION

Renal cell carcinoma is often associated with a poor prognosis, as currently available drugs have a minimal effect on overall median survival. A greater understanding of RCC tumor pathology and signal transduction needs to be determined to indicate new drug targets and possible treatment combinations. Renal carcinomas are highly vascularized, with overexpression of vascular endothelial growth factor receptors (VEGFR). The VEGF receptor is involved in angiogenesis, which is an essential event in tumor growth and metastasis. Other upregulated genes involved in progression of renal tumor development are growth factors VEGF, PDGF, bFGF, and TGF-α (van Spronsen et al. 2005).

Current treatment regimens include cytokine therapies (interleukin-2 [IL-2] and interferon-alfa [IFN-α]), VEGF and/or MAPK targeted drugs (bevacizumab, sorafenib, and sunitinib), and mTOR inhibitors (temsirolimus [CCI-779]) (Mills et al. 2009). The primary treatment for RCC is a nephrectomy because there is a generally low response to chemotherapy. Usually cytokine therapy, such as IFN-α or IL-2 is administered before or after the nephrectomy. Some chemotherapeutic drugs that are currently used to treat RCC are virblastine, 5-fluoruracil and gemcitabine (van Spronsen et al. 2005).

The MP 470-tarceva drug combination may be a promising treatment for RCC. MP 470 effectively inhibits PDGFR, which is known to be upregulated in human RCC. Furthermore, MP 470 may also bind other RCC RTK targets, as the protein binding affinities of the compound have not been fully elucidated yet. We tested these compounds in our tumorigenic QTRRE cells without any prior preliminary data suggesting activation of RTKs. Treatment with a combination of 20 μM tarceva and 20

μM MP 470 for 2h resulted in a 30% decrease in cell viability, as measured by the MTS assay (**Figure B.2**). The combination treatment effectively modulated the hierarchical phosphorylation on 4EBP1. As the tarceva-MP 470 combination proved to have a synergistic effect on the time-dependent disappearance of the higher molecular weight band in p-4EBP1-Ser65, -Thr70, and -Thr37/46; and a parallel shift in band intensity from the higher molecular weight 4EBP1 band to the lower molecular weight band in p-4EBP1-Thr 70 and -Thr 37/46 (**Figure B.3**). Just as sorafenib (**Chapter 3**) and rapamycin analogs are effective modulators of 4EBP1 phosphorylation in renal cell carcinoma, tarceva-MP 470 appears to inhibit key upstream RTK involved in modulating mTOR and/or MAPK pathways to mediate 4EBP1 phosphorylation. It may be beneficial to further explore other combination therapies, with sorafenib, rapamycin, tarceva, and MP 470, as they may prove to have effective synergistic effects on critical pathways to treat RCC.

REFERENCES

(1999). 1,4-Benzenediol. Monogr Eval Carcinog Risks Hum, International Agency for Research on Cancer (IARC). **71:** 691-719.

Alao, J. P. (2007). "The regulation of cyclin D1 degradation: roles in cancer development and the potential for therapeutic invention." Mol Cancer **6**: 24.

Alderson, N. L. and H. Hama (2009). "Fatty acid 2-hydroxylase regulates cAMP-induced cell cycle exit in D6P2T schwannoma cells." J Lipid Res **50**(6): 1203-8.

Alkarain, A., R. Jordan and J. Slingerland (2004). "p27 deregulation in breast cancer: prognostic significance and implications for therapy." J Mammary Gland Biol Neoplasia **9**(1): 67-80.

Alvarez, E., I. C. Northwood, F. A. Gonzalez, D. A. Latour, A. Seth, C. Abate, T. Curran and R. J. Davis (1991). "Pro-Leu-Ser/Thr-Pro is a consensus primary sequence for substrate protein phosphorylation. Characterization of the phosphorylation of c-myc and c-jun proteins by an epidermal growth factor receptor threonine 669 protein kinase." J Biol Chem **266**(23): 15277-85.

Ballif, B. A., P. P. Roux, S. A. Gerber, J. P. MacKeigan, J. Blenis and S. P. Gygi (2005). "Quantitative phosphorylation profiling of the ERK/p90 ribosomal S6 kinase-signaling cassette and its targets, the tuberous sclerosis tumor suppressors." Proc Natl Acad Sci U S A **102**(3): 667-72.

Balmanno, K. and S. J. Cook (1999). "Sustained MAP kinase activation is required for the expression of cyclin D1, p21Cip1 and a subset of AP-1 proteins in CCL39 cells." Oncogene **18**(20): 3085-97.

Barnes, D. M. and C. E. Gillett (1998). "Cyclin D1 in breast cancer." Breast Cancer Res Treat **52**(1-3): 1-15.

Barnier, J. V., C. Papin, A. Eychene, O. Lecoq and G. Calothy (1995). "The mouse B-raf gene encodes multiple protein isoforms with tissue-specific expression." J Biol Chem **270**(40): 23381-9.

Bartek, J., C. Lukas and J. Lukas (2004). "Checking on DNA damage in S phase." Nat Rev Mol Cell Biol **5**(10): 792-804.

Beretta, L., A. C. Gingras, Y. V. Svitkin, M. N. Hall and N. Sonenberg (1996). "Rapamycin blocks the phosphorylation of 4E-BP1 and inhibits cap-dependent initiation of translation." Embo J **15**(3): 658-64.

Bernstein, J. and T. O. Robbins (1991). "Renal involvement in tuberous sclerosis." Ann N Y Acad Sci **615**: 36-49.

Besson, A., M. Gurian-West, X. Chen, K. S. Kelly-Spratt, C. J. Kemp and J. M. Roberts (2006). "A pathway in quiescent cells that controls p27Kip1 stability, subcellular localization, and tumor suppression." Genes Dev **20**(1): 47-64.

Besson, A., M. Gurian-West, A. Schmidt, A. Hall and J. M. Roberts (2004). "p27Kip1 modulates cell migration through the regulation of RhoA activation." Genes Dev **18**(8): 862-76.

Beugnet, A., X. Wang and C. G. Proud (2003). "Target of rapamycin (TOR)-signaling and RAIP motifs play distinct roles in the mammalian TOR-dependent phosphorylation of initiation factor 4E-binding protein 1." J Biol Chem **278**(42): 40717-22.

Bhat, N. R. and P. Zhang (1999). "Hydrogen peroxide activation of multiple mitogen-activated protein kinases in an oligodendrocyte cell line: role of extracellular signal-regulated kinase in hydrogen peroxide-induced cell death." J Neurochem **72**(1): 112-9.

Bhatt, K. V., L. S. Spofford, G. Aram, M. McMullen, K. Pumiglia and A. E. Aplin (2005). "Adhesion control of cyclin D1 and p27Kip1 levels is deregulated in melanoma cells through BRAF-MEK-ERK signaling." Oncogene **24**(21): 3459-71.

Bjornsson, J., M. P. Short, D. J. Kwiatkowski and E. P. Henske (1996). "Tuberous sclerosis-associated renal cell carcinoma. Clinical, pathological, and genetic features." Am J Pathol **149**(4): 1201-8.

Blain, S. W. (2008). "Switching cyclin D-Cdk4 kinase activity on and off." Cell Cycle **7**(7): 892-8.

Blain, S. W., E. Montalvo and J. Massague (1997). "Differential interaction of the cyclin-dependent kinase (Cdk) inhibitor p27Kip1 with cyclin A-Cdk2 and cyclin D2-Cdk4." J Biol Chem **272**(41): 25863-72.

Boguski, M. S. and F. McCormick (1993). "Proteins regulating Ras and its relatives." Nature **366**(6456): 643-54.

Bond, M., Y. J. Wu, G. B. Sala-Newby and A. C. Newby (2008). "Rho GTPase, Rac1, regulates Skp2 levels, vascular smooth muscle cell proliferation, and intima formation in vitro and in vivo." Cardiovasc Res **80**(2): 290-8.

Brugarolas, J. B., F. Vazquez, A. Reddy, W. R. Sellers and W. G. Kaelin, Jr. (2003). "TSC2 regulates VEGF through mTOR-dependent and -independent pathways." Cancer Cell **4**(2): 147-58.

Bucks, D. A., J. R. McMaster, R. H. Guy and H. I. Maibach (1988). "Percutaneous absorption of hydroquinone in humans: effect of 1-dodecylazacycloheptan-2-one

(azone) and the 2-ethylhexyl ester of 4-(dimethylamino)benzoic acid (Escalol 507)." J Toxicol Environ Health **24**(3): 279-89.

Busca, R., P. Abbe, F. Mantoux, E. Aberdam, C. Peyssonnaux, A. Eychene, J. P. Ortonne and R. Ballotti (2000). "Ras mediates the cAMP-dependent activation of extracellular signal-regulated kinases (ERKs) in melanocytes." EMBO J **19**(12): 2900-10.

Cagnol, S., E. Van Obberghen-Schilling and J. C. Chambard (2006). "Prolonged activation of ERK1,2 induces FADD-independent caspase 8 activation and cell death." Apoptosis **11**(3): 337-46.

Cantin, G. T., W. Yi, B. Lu, S. K. Park, T. Xu, J. D. Lee and J. R. Yates, 3rd (2008). "Combining protein-based IMAC, peptide-based IMAC, and MudPIT for efficient phosphoproteomic analysis." J Proteome Res **7**(3): 1346-51.

Carbonara, C., L. Longa, E. Grosso, C. Borrone, M. G. Garre, M. Brisigotti and N. Migone (1994). "9q34 loss of heterozygosity in a tuberous sclerosis astrocytoma suggests a growth suppressor-like activity also for the TSC1 gene." Hum Mol Genet **3**(10): 1829-32.

Carbonara, C., L. Longa, E. Grosso, G. Mazzucco, C. Borrone, M. L. Garre, M. Brisigotti, G. Filippi, A. Scabar, A. Giannotti, P. Falzoni, G. Monga, G. Garini, M. Gabrielli, P. Riegler, C. Danesino, M. Ruggieri, G. Magro and N. Migone (1996). "Apparent preferential loss of heterozygosity at TSC2 over TSC1 chromosomal region in tuberous sclerosis hamartomas." Genes Chromosomes Cancer **15**(1): 18-25.

Cario, H., G. Janka-Schaub, G. Janssen, A. Jarisch, G. Strauss and E. Kohne (2007). "Recent developments in iron chelation therapy." Klin Padiatr **219**(3): 158-65.

Carrano, A. C., E. Eytan, A. Hershko and M. Pagano (1999). "SKP2 is required for ubiquitin-mediated degradation of the CDK inhibitor p27." Nat Cell Biol **1**(4): 193-9.

Castellvi, J., A. Garcia, F. Rojo, C. Ruiz-Marcellan, A. Gil, J. Baselga and S. Ramon y Cajal (2006). "Phosphorylated 4E binding protein 1: a hallmark of cell signaling that correlates with survival in ovarian cancer." Cancer **107**(8): 1801-11.

Cheadle, J. P., M. P. Reeve, J. R. Sampson and D. J. Kwiatkowski (2000). "Molecular genetic advances in tuberous sclerosis." Hum Genet **107**(2): 97-114.

Cheng, M., P. Olivier, J. A. Diehl, M. Fero, M. F. Roussel, J. M. Roberts and C. J. Sherr (1999). "The p21(Cip1) and p27(Kip1) CDK 'inhibitors' are essential activators of cyclin D-dependent kinases in murine fibroblasts." EMBO J **18**(6): 1571-83.

Chong, H., H. G. Vikis and K. L. Guan (2003). "Mechanisms of regulating the Raf kinase family." Cell Signal **15**(5): 463-9.

Chu, I., J. Sun, A. Arnaout, H. Kahn, W. Hanna, S. Narod, P. Sun, C. K. Tan, L. Hengst and J. Slingerland (2007). "p27 phosphorylation by Src regulates inhibition of cyclin E-Cdk2." Cell **128**(2): 281-94.

Ciaparrone, M., H. Yamamoto, Y. Yao, A. Sgambato, G. Cattoretti, N. Tomita, T. Monden, H. Rotterdam and I. B. Weinstein (1998). "Localization and expression of p27KIP1 in multistage colorectal carcinogenesis." Cancer Res **58**(1): 114-22.

Coats, S., W. M. Flanagan, J. Nourse and J. M. Roberts (1996). "Requirement of p27Kip1 for restriction point control of the fibroblast cell cycle." Science **272**(5263): 877-80.

Connor, M. K., R. Kotchetkov, S. Cariou, A. Resch, R. Lupetti, R. G. Beniston, F. Melchior, L. Hengst and J. M. Slingerland (2003). "CRM1/Ran-mediated nuclear export of p27(Kip1) involves a nuclear export signal and links p27 export and proteolysis." Mol Biol Cell **14**(1): 201-13.

Cook, S. J., B. Rubinfeld, I. Albert and F. McCormick (1993). "RapV12 antagonizes Ras-dependent activation of ERK1 and ERK2 by LPA and EGF in Rat-1 fibroblasts." Embo J **12**(9): 3475-85.

Coqueret, O. (2002). "Linking cyclins to transcriptional control." Gene **299**(1-2): 35-55.

da Silva, A. G., P. Campello-Costa, R. Linden and A. Sholl-Franco (2008). "Interleukin-4 blocks proliferation of retinal progenitor cells and increases rod photoreceptor differentiation through distinct signaling pathways." J Neuroimmunol **196**(1-2): 82-93.

Davies, H., G. R. Bignell, C. Cox, P. Stephens, S. Edkins, S. Clegg, J. Teague, H. Woffendin, M. J. Garnett, W. Bottomley, N. Davis, E. Dicks, R. Ewing, Y. Floyd, K. Gray, S. Hall, R. Hawes, J. Hughes, V. Kosmidou, A. Menzies, C. Mould, A. Parker, C. Stevens, S. Watt, S. Hooper, R. Wilson, H. Jayatilake, B. A. Gusterson, C. Cooper, J. Shipley, D. Hargrave, K. Pritchard-Jones, N. Maitland, G. Chenevix-Trench, G. J. Riggins, D. D. Bigner, G. Palmieri, A. Cossu, A. Flanagan, A. Nicholson, J. W. Ho, S. Y. Leung, S. T. Yuen, B. L. Weber, H. F. Seigler, T. L. Darrow, H. Paterson, R. Marais, C. J. Marshall, R. Wooster, M. R. Stratton and P. A. Futreal (2002). "Mutations of the BRAF gene in human cancer." Nature **417**(6892): 949-54.

Davis, R. J. (1995). "Transcriptional regulation by MAP kinases." Mol Reprod Dev **42**(4): 459-67.

DeCaprio, A. P. (1999). "The toxicology of hydroquinone--relevance to occupational and environmental exposure." Crit Rev Toxicol **29**(3): 283-330.

Deisinger, P. J., T. S. Hill and J. C. English (1996). "Human exposure to naturally occurring hydroquinone." J Toxicol Environ Health **47**(1): 31-46.

Dekant, W. (1996). "Biosynthesis and cellular effects of toxic glutathione S-conjugates." Adv Exp Med Biol **387**: 297-312.

Deng, X., S. E. Mercer, S. Shah, D. Z. Ewton and E. Friedman (2004). "The cyclin-dependent kinase inhibitor p27Kip1 is stabilized in G(0) by Mirk/dyrk1B kinase." J Biol Chem **279**(21): 22498-504.

Dephoure, N., C. Zhou, J. Villen, S. A. Beausoleil, C. E. Bakalarski, S. J. Elledge and S. P. Gygi (2008). "A quantitative atlas of mitotic phosphorylation." Proc Natl Acad Sci U S A **105**(31): 10762-7.

Dhote, R., N. Thiounn, B. Debre and G. Vidal-Trecan (2004). "Risk factors for adult renal cell carcinoma." Urol Clin North Am **31**(2): 237-47.

Divincenzo, G. D., M. L. Hamilton, R. C. Reynolds and D. A. Ziegler (1984). "Metabolic fate and disposition of [14C]hydroquinone given orally to Sprague-Dawley rats." Toxicology **33**(1): 9-18.

Duffel, M. W. and W. B. Jakoby (1982). "Cysteine S-conjugate N-acetyltransferase from rat kidney microsomes." Mol Pharmacol **21**(2): 444-8.

Dugan, L. L., J. S. Kim, Y. Zhang, R. D. Bart, Y. Sun, D. M. Holtzman and D. H. Gutmann (1999). "Differential effects of cAMP in neurons and astrocytes. Role of B-raf." J Biol Chem **274**(36): 25842-8.

Eker, R. and J. Mossige (1961). "A dominant gene for renal adenomas in the rat." Nature **189**: 858-859.

Eker, R., J. Mossige, J. V. Johannessen and H. Aars (1981). "Hereditary renal adenomas and adenocarcinomas in rats." Diagn Histopathol **4**(1): 99-110.

English, J. C., P.J. Desinger, et al. (1988). Toxicokinetics Studies with Hydroquinone in Male and Female Fischer 344 Rats: Part I." Rochester, NY, R&D Report pf Eastman Kodak Co.

Erhardt, P., E. J. Schremser and G. M. Cooper (1999). "B-Raf inhibits programmed cell death downstream of cytochrome c release from mitochondria by activating the MEK/Erk pathway." Mol Cell Biol **19**(8): 5308-15.

Everitt, J. I., T. L. Goldsworthy, D. C. Wolf and C. L. Walker (1992). "Hereditary renal cell carcinoma in the Eker rat: a rodent familial cancer syndrome." J Urol **148**(6): 1932-6.

Everitt, J. I., T. L. Goldsworthy, D. C. Wolf and C. L. Walker (1995). "Hereditary renal cell carcinoma in the Eker rat: a unique animal model for the study of cancer susceptibility." Toxicol Lett **82-83**: 621-5.

Franke, B., J. W. Akkerman and J. L. Bos (1997). "Rapid Ca2+-mediated activation of Rap1 in human platelets." EMBO J **16**(2): 252-9.

Fujita, N., S. Sato, K. Katayama and T. Tsuruo (2002). "Akt-dependent phosphorylation of p27Kip1 promotes binding to 14-3-3 and cytoplasmic localization." J Biol Chem **277**(32): 28706-13.

Fujita, N., S. Sato and T. Tsuruo (2003). "Phosphorylation of p27Kip1 at threonine 198 by p90 ribosomal protein S6 kinases promotes its binding to 14-3-3 and cytoplasmic localization." J Biol Chem **278**(49): 49254-60.

Garcia, J., J. de Gunzburg, A. Eychene, S. Gisselbrecht and F. Porteu (2001). "Thrombopoietin-mediated sustained activation of extracellular signal-regulated kinase in UT7-Mpl cells requires both Ras-Raf-1- and Rap1-B-Raf-dependent pathways." Mol Cell Biol **21**(8): 2659-70.

Garnett, M. J., S. Rana, H. Paterson, D. Barford and R. Marais (2005). "Wild-type and mutant B-RAF activate C-RAF through distinct mechanisms involving heterodimerization." Mol Cell **20**(6): 963-9.

Gevaert, K., M. Goethals, L. Martens, J. Van Damme, A. Staes, G. R. Thomas and J. Vandekerckhove (2003). "Exploring proteomes and analyzing protein processing by mass spectrometric identification of sorted N-terminal peptides." Nat Biotechnol **21**(5): 566-9.

Gingras, A. C., S. P. Gygi, B. Raught, R. D. Polakiewicz, R. T. Abraham, M. F. Hoekstra, R. Aebersold and N. Sonenberg (1999). "Regulation of 4E-BP1 phosphorylation: a novel two-step mechanism." Genes Dev **13**(11): 1422-37.

Gingras, A. C., B. Raught, S. P. Gygi, A. Niedzwiecka, M. Miron, S. K. Burley, R. D. Polakiewicz, A. Wyslouch-Cieszynska, R. Aebersold and N. Sonenberg (2001). "Hierarchical phosphorylation of the translation inhibitor 4E-BP1." Genes Dev **15**(21): 2852-64.

Gnarra, J. R., K. Tory, Y. Weng, L. Schmidt, M. H. Wei, H. Li, F. Latif, S. Liu, F. Chen, F. M. Duh and et al. (1994). "Mutations of the VHL tumour suppressor gene in renal carcinoma." Nat Genet **7**(1): 85-90.

Gnarra, J. R., J. M. Ward, F. D. Porter, J. R. Wagner, D. E. Devor, A. Grinberg, M. R. Emmert-Buck, H. Westphal, R. D. Klausner and W. M. Linehan (1997). "Defective placental vasculogenesis causes embryonic lethality in VHL-deficient mice." Proc Natl Acad Sci U S A **94**(17): 9102-7.

Gnarra, J. R., S. Zhou, M. J. Merrill, J. R. Wagner, A. Krumm, E. Papavassiliou, E. H. Oldfield, R. D. Klausner and W. M. Linehan (1996). "Post-transcriptional regulation of vascular endothelial growth factor mRNA by the product of the VHL tumor suppressor gene." Proc Natl Acad Sci U S A **93**(20): 10589-94.

Gomez, M. R. (1991). "Phenotypes of the tuberous sclerosis complex with a revision of diagnostic criteria." Ann N Y Acad Sci **615**: 1-7.

Gray-Schopfer, V. C., M. Karasarides, R. Hayward and R. Marais (2007). "Tumor necrosis factor-alpha blocks apoptosis in melanoma cells when BRAF signaling is inhibited." Cancer Res **67**(1): 122-9.

Green, A. J., P. H. Johnson and J. R. Yates (1994). "The tuberous sclerosis gene on chromosome 9q34 acts as a growth suppressor." Hum Mol Genet **3**(10): 1833-4.

Greenlee, W. F., E. A. Gross and R. D. Irons (1981). "Relationship between benzene toxicity and the disposition of 14C-labelled benzene metabolites in the rat." Chem Biol Interact **33**(2-3): 285-99.

Grewal, S. S., A. M. Horgan, R. D. York, G. S. Withers, G. A. Banker and P. J. Stork (2000). "Neuronal calcium activates a Rap1 and B-Raf signaling pathway via the cyclic adenosine monophosphate-dependent protein kinase." J Biol Chem **275**(5): 3722-8.

Grimmler, M., Y. Wang, T. Mund, Z. Cilensek, E. M. Keidel, M. B. Waddell, H. Jakel, M. Kullmann, R. W. Kriwacki and L. Hengst (2007). "Cdk-inhibitory activity and stability of p27Kip1 are directly regulated by oncogenic tyrosine kinases." Cell **128**(2): 269-80.

Haase, V. H., J. N. Glickman, M. Socolovsky and R. Jaenisch (2001). "Vascular tumors in livers with targeted inactivation of the von Hippel-Lindau tumor suppressor." Proc Natl Acad Sci U S A **98**(4): 1583-8.

Habib, S. L., M. N. Phan, S. K. Patel, D. Li, T. J. Monks and S. S. Lau (2003). "Reduced constitutive 8-oxoguanine-DNA glycosylase expression and impaired induction following oxidative DNA damage in the tuberin deficient Eker rat." Carcinogenesis **24**(3): 573-82.

Hard, G. C. (1986). "Experimental models for the sequential analysis of chemically-induced renal carcinogenesis." Toxicol Pathol **14**(1): 112-22.

Haystead, T. A., C. M. Haystead, C. Hu, T. A. Lin and J. C. Lawrence, Jr. (1994). "Phosphorylation of PHAS-I by mitogen-activated protein (MAP) kinase. Identification of a site phosphorylated by MAP kinase in vitro and in response to insulin in rat adipocytes." J Biol Chem **269**(37): 23185-91.

Hennenlotter, J., P. A. Ohneseit, P. Simon, A. S. Merseburger, J. Serth, U. Kuehs, M. Kramer, J. T. Hartmann, A. Stenzl and M. A. Kuczyk (2008). "PTEN and p27Kip1 are not downregulated in the majority of renal cell carcinomas--implications for Akt activation." Oncol Rep **19**(5): 1141-7.

Henske, E. P., H. P. Neumann, B. W. Scheithauer, E. W. Herbst, M. P. Short and D. J. Kwiatkowski (1995). "Loss of heterozygosity in the tuberous sclerosis (TSC2)

region of chromosome band 16p13 occurs in sporadic as well as TSC-associated renal angiomyolipomas." Genes Chromosomes Cancer **13**(4): 295-8.

Henske, E. P., B. W. Scheithauer, M. P. Short, R. Wollmann, J. Nahmias, N. Hornigold, M. van Slegtenhorst, C. T. Welsh and D. J. Kwiatkowski (1996). "Allelic loss is frequent in tuberous sclerosis kidney lesions but rare in brain lesions." Am J Hum Genet **59**(2): 400-6.

Herrmann, C., G. Horn, M. Spaargaren and A. Wittinghofer (1996). "Differential interaction of the ras family GTP-binding proteins H-Ras, Rap1A, and R-Ras with the putative effector molecules Raf kinase and Ral-guanine nucleotide exchange factor." J Biol Chem **271**(12): 6794-800.

Hidalgo, M. and E. K. Rowinsky (2000). "The rapamycin-sensitive signal transduction pathway as a target for cancer therapy." Oncogene **19**(56): 6680-6.

Hill, B. A., H. E. Kleiner, E. A. Ryan, D. M. Dulik, T. J. Monks and S. S. Lau (1993). "Identification of multi-S-substituted conjugates of hydroquinone by HPLC-coulometric electrode array analysis and mass spectroscopy." Chem Res Toxicol **6**(4): 459-69.

Hino, O., E. Kobayashi, Y. Hirayama, T. Kobayashi, Y. Kubo, H. Tsuchiya, Y. Kikuchi and H. Mitani (1995). "Molecular genetic basis of renal carcinogenesis in the Eker rat model of tuberous sclerosis (Tsc2)." Mol Carcinog **14**(1): 23-7.

Hochegger, H., S. Takeda and T. Hunt (2008). "Cyclin-dependent kinases and cell-cycle transitions: does one fit all?" Nat Rev Mol Cell Biol **9**(11): 910-6.

Hu, C. D., K. Kariya, G. Kotani, M. Shirouzu, S. Yokoyama and T. Kataoka (1997). "Coassociation of Rap1A and Ha-Ras with Raf-1 N-terminal region interferes with ras-dependent activation of Raf-1." J Biol Chem **272**(18): 11702-5.

Huang, J. and B. D. Manning (2008). "The TSC1-TSC2 complex: a molecular switchboard controlling cell growth." Biochem J **412**(2): 179-90.

Imami, K., N. Sugiyama, Y. Kyono, M. Tomita and Y. Ishihama (2008). "Automated phosphoproteome analysis for cultured cancer cells by two-dimensional nanoLC-MS using a calcined titania/C18 biphasic column." Anal Sci **24**(1): 161-6.

Inoki, K. and K. L. Guan (2009). "Tuberous sclerosis complex, implication from a rare genetic disease to common cancer treatment." Hum Mol Genet **18**(R1): R94-100.

Inoki, K., Y. Li, T. Xu and K. L. Guan (2003). "Rheb GTPase is a direct target of TSC2 GAP activity and regulates mTOR signaling." Genes Dev **17**(15): 1829-34.

Ishida, N., T. Hara, T. Kamura, M. Yoshida, K. Nakayama and K. I. Nakayama (2002). "Phosphorylation of p27Kip1 on serine 10 is required for its binding to CRM1 and nuclear export." J Biol Chem **277**(17): 14355-8.

Ito, N. and G. M. Rubin (1999). "gigas, a Drosophila homolog of tuberous sclerosis gene product-2, regulates the cell cycle." Cell **96**(4): 529-39.

James, M. K., A. Ray, D. Leznova and S. W. Blain (2008). "Differential modification of p27Kip1 controls its cyclin D-cdk4 inhibitory activity." Mol Cell Biol **28**(1): 498-510.

Jemal, A., R. C. Tiwari, T. Murray, A. Ghafoor, A. Samuels, E. Ward, E. J. Feuer and M. J. Thun (2004). "Cancer statistics, 2004." CA Cancer J Clin **54**(1): 8-29.

Jiang, B. H. and L. Z. Liu (2008). "Role of mTOR in anticancer drug resistance: perspectives for improved drug treatment." Drug Resist Updat **11**(3): 63-76.

Jin, M., S. Inoue, T. Umemura, J. Moriya, M. Arakawa, K. Nagashima and H. Kato (2001). "Cyclin D1, p16 and retinoblastoma gene product expression as a predictor for prognosis in non-small cell lung cancer at stages I and II." Lung Cancer **34**(2): 207-18.

Jo, S. K., W. Y. Cho, S. A. Sung, H. K. Kim and N. H. Won (2005). "MEK inhibitor, U0126, attenuates cisplatin-induced renal injury by decreasing inflammation and apoptosis." Kidney Int **67**(2): 458-66.

Jowa, L., G. Witz, R. Snyder, S. Winkle and G. F. Kalf (1990). "Synthesis and characterization of deoxyguanosine-benzoquinone adducts." J Appl Toxicol **10**(1): 47-54.

Kaldis, P. (2007). "Another piece of the p27Kip1 puzzle." Cell **128**(2): 241-4.

Kalf, G. F., R. Snyder and T. H. Rushmore (1985). "Inhibition of RNA synthesis by benzene metabolites and their covalent binding to DNA in rabbit bone marrow mitochondria in vitro." Am J Ind Med **7**(5-6): 485-92.

Kamura, T., T. Hara, M. Matsumoto, N. Ishida, F. Okumura, S. Hatakeyama, M. Yoshida, K. Nakayama and K. I. Nakayama (2004). "Cytoplasmic ubiquitin ligase KPC regulates proteolysis of p27(Kip1) at G1 phase." Nat Cell Biol **6**(12): 1229-35.

Karbowniczek, M., G. P. Robertson and E. P. Henske (2006). "Rheb inhibits C-raf activity and B-raf/C-raf heterodimerization." J Biol Chem **281**(35): 25447-56.

Kardinal, C., M. Dangers, A. Kardinal, A. Koch, D. T. Brandt, T. Tamura and K. Welte (2006). "Tyrosine phosphorylation modulates binding preference to cyclin-dependent kinases and subcellular localization of p27Kip1 in the acute promyelocytic leukemia cell line NB4." Blood **107**(3): 1133-40.

Kari, F. W., J. Bucher, S. L. Eustis, J. K. Haseman and J. E. Huff (1992). "Toxicity and carcinogenicity of hydroquinone in F344/N rats and B6C3F1 mice." Food Chem Toxicol **30**(9): 737-47.

Kida, Y., K. Yamaguchi, H. Suzuki, E. Kanda, M. Ando, K. Ohashi, N. Funata and H. Saito (2005). "Tuberous sclerosis, associated with renal cell carcinoma and angiomyolipoma, in a patient who developed endstage renal failure after nephrectomy." Clin Exp Nephrol **9**(2): 179-82.

Kikuchi, Y., E. Kobayashi, M. Nishizawa, S. Hamazaki, S. Okada and O. Hino (1995). "Cloning of the rat homologue of the von Hippel-Lindau tumor suppressor gene and its non-somatic mutation in rat renal cell carcinomas." Jpn J Cancer Res **86**(10): 905-9.

Kim, J., E. Jonasch, A. Alexander, J. D. Short, S. Cai, S. Wen, D. Tsavachidou, P. Tamboli, B. A. Czerniak, K. A. Do, K. J. Wu, L. A. Marlow, C. G. Wood, J. A. Copland and C. L. Walker (2009). "Cytoplasmic sequestration of p27 via AKT phosphorylation in renal cell carcinoma." Clin Cancer Res **15**(1): 81-90.

Kim, J. K. and J. A. Diehl (2009). "Nuclear cyclin D1: an oncogenic driver in human cancer." J Cell Physiol **220**(2): 292-6.

Klaassen, C. D. (2001). Casarett and Doull's toxicology: the basic science of poisons. New York, McGraw-Hill, Health Professions Division.

Kleiner, H. E., T. W. Jones, T. J. Monks and S. S. Lau (1998). "Immunochemical analysis of quinol-thioether-derived covalent protein adducts in rodent species sensitive and resistant to quinol-thioether-mediated nephrotoxicity." Chem Res Toxicol **11**(11): 1291-300.

Kobayashi, T., Y. Hirayama, E. Kobayashi, Y. Kubo and O. Hino (1995). "A germline insertion in the tuberous sclerosis (Tsc2) gene gives rise to the Eker rat model of dominantly inherited cancer." Nat Genet **9**(1): 70-4.

Kobayashi, T., O. Minowa, J. Kuno, H. Mitani, O. Hino and T. Noda (1999). "Renal carcinogenesis, hepatic hemangiomatosis, and embryonic lethality caused by a germ-line Tsc2 mutation in mice." Cancer Res **59**(6): 1206-11.

Kobayashi, T., S. Urakami, Y. Hirayama, T. Yamamoto, M. Nishizawa, T. Takahara, Y. Kubo and O. Hino (1997). "Intragenic Tsc2 somatic mutations as Knudson's second hit in spontaneous and chemically induced renal carcinomas in the Eker rat model." Jpn J Cancer Res **88**(3): 254-61.

Kossatz, U., J. Vervoorts, I. Nickeleit, H. A. Sundberg, J. S. Arthur, M. P. Manns and N. P. Malek (2006). "C-terminal phosphorylation controls the stability and function of p27kip1." EMBO J **25**(21): 5159-70.

Kotake, Y., K. Nakayama, N. Ishida and K. I. Nakayama (2005). "Role of serine 10 phosphorylation in p27 stabilization revealed by analysis of p27 knock-in mice harboring a serine 10 mutation." J Biol Chem **280**(2): 1095-102.

Kowalczyk, P., T. Kinjo, M. Kowalczyk, Z. Walaszek, M. Hanausek and T. J. Slaga (2009). "Effect of phosphodiesterase antagonists on glucocorticoid mediated growth inhibition in murine skin cell lines." Eur J Pharmacol **610**(1-3): 29-36.

Kremer, C. L., R. R. Klein, J. Mendelson, W. Browne, L. K. Samadzedeh, K. Vanpatten, L. Highstrom, G. A. Pestano and R. B. Nagle (2006). "Expression of mTOR signaling pathway markers in prostate cancer progression." Prostate **66**(11): 1203-12.

Krishna, M. and H. Narang (2008). "The complexity of mitogen-activated protein kinases (MAPKs) made simple." Cell Mol Life Sci **65**(22): 3525-44.

Krymskaya, V. P. (2003). "Tumour suppressors hamartin and tuberin: intracellular signalling." Cell Signal **15**(8): 729-39.

Kubo, Y., H. Mitani and O. Hino (1994). "Allelic loss at the predisposing gene locus in spontaneous and chemically induced renal cell carcinomas in the Eker rat." Cancer Res **54**(10): 2633-5.

Lau, N., E. J. Uhlmann, F. C. Von Lintig, A. Nagy, G. R. Boss, D. H. Gutmann and A. Guha (2003). "Rap1 activity is elevated in malignant astrocytomas independent of tuberous sclerosis complex-2 gene expression." Int J Oncol **22**(1): 195-200.

Lau, S. S., B. A. Hill, R. J. Highet and T. J. Monks (1988). "Sequential oxidation and glutathione addition to 1,4-benzoquinone: correlation of toxicity with increased glutathione substitution." Mol Pharmacol **34**(6): 829-36.

Lau, S. S., H. E. Kleiner and T. J. Monks (1995). "Metabolism as a determinant of species susceptibility to 2,3,5-(triglutathion-S-yl)hydroquinone-mediated nephrotoxicity. The role of N-acetylation and N-deacetylation." Drug Metab Dispos **23**(10): 1136-42.

Lau, S. S., M. G. McMenamin and T. J. Monks (1988). "Differential uptake of isomeric 2-bromohydroquinone-glutathione conjugates into kidney slices." Biochem Biophys Res Commun **152**(1): 223-30.

Lau, S. S. and T. J. Monks (1987). "Co-oxidation of 2-bromohydroquinone by renal prostaglandin synthase. Modulation of prostaglandin synthesis by 2-bromohydroquinone and glutathione." Drug Metab Dispos **15**(6): 801-7.

Lau, S. S., T. J. Monks, J. I. Everitt, E. Kleymenova and C. L. Walker (2001). "Carcinogenicity of a nephrotoxic metabolite of the "nongenotoxic" carcinogen hydroquinone." Chem Res Toxicol **14**(1): 25-33.

Lau, S. S., M. M. Peters, H. E. Kleiner, P. L. Canales and T. J. Monks (1996). "Linking the metabolism of hydroquinone to its nephrotoxicity and nephrocarcinogenicity." Adv Exp Med Biol **387**: 267-73.

Lavoie, J. N., G. L'Allemain, A. Brunet, R. Muller and J. Pouyssegur (1996). "Cyclin D1 expression is regulated positively by the p42/p44MAPK and negatively by the p38/HOGMAPK pathway." J Biol Chem **271**(34): 20608-16.

Lesuisse, C. and L. J. Martin (2002). "Immature and mature cortical neurons engage different apoptotic mechanisms involving caspase-3 and the mitogen-activated protein kinase pathway." J Cereb Blood Flow Metab **22**(8): 935-50.

Lewis, T. S., P. S. Shapiro and N. G. Ahn (1998). "Signal transduction through MAP kinase cascades." Adv Cancer Res **74**: 49-139.

Liang, J., J. Zubovitz, T. Petrocelli, R. Kotchetkov, M. K. Connor, K. Han, J. H. Lee, S. Ciarallo, C. Catzavelos, R. Beniston, E. Franssen and J. M. Slingerland (2002). "PKB/Akt phosphorylates p27, impairs nuclear import of p27 and opposes p27-mediated G1 arrest." Nat Med **8**(10): 1153-60.

Linehan, W. M., M. M. Walther and B. Zbar (2003). "The genetic basis of cancer of the kidney." J Urol **170**(6 Pt 1): 2163-72.

Liu, M. Y., L. Poellinger and C. L. Walker (2003). "Up-regulation of hypoxia-inducible factor 2alpha in renal cell carcinoma associated with loss of Tsc-2 tumor suppressor gene." Cancer Res **63**(10): 2675-80.

Long, X., Y. Lin, S. Ortiz-Vega, K. Yonezawa and J. Avruch (2005). "Rheb binds and regulates the mTOR kinase." Curr Biol **15**(8): 702-13.

M'Rabet, L., P. Coffer, F. Zwartkruis, B. Franke, A. W. Segal, L. Koenderman and J. L. Bos (1998). "Activation of the small GTPase rap1 in human neutrophils." Blood **92**(6): 2133-40.

Ma, L., Z. Chen, H. Erdjument-Bromage, P. Tempst and P. P. Pandolfi (2005). "Phosphorylation and functional inactivation of TSC2 by Erk implications for tuberous sclerosis and cancer pathogenesis." Cell **121**(2): 179-93.

Malumbres, M. and M. Barbacid (2009). "Cell cycle, CDKs and cancer: a changing paradigm." Nat Rev Cancer **9**(3): 153-66.

Marais, R., J. Wynne and R. Treisman (1993). "The SRF accessory protein Elk-1 contains a growth factor-regulated transcriptional activation domain." Cell **73**(2): 381-93.

Martin, D. E. and M. N. Hall (2005). "The expanding TOR signaling network." Curr Opin Cell Biol **17**(2): 158-66.

Masciullo, V., G. Ferrandina, B. Pucci, F. Fanfani, S. Lovergine, J. Palazzo, G. Zannoni, S. Mancuso, G. Scambia and A. Giordano (2000). "p27Kip1 expression is associated with clinical outcome in advanced epithelial ovarian cancer: multivariate analysis." Clin Cancer Res **6**(12): 4816-22.

Matsuoka, S., B. A. Ballif, A. Smogorzewska, E. R. McDonald, 3rd, K. E. Hurov, J. Luo, C. E. Bakalarski, Z. Zhao, N. Solimini, Y. Lerenthal, Y. Shiloh, S. P. Gygi and S. J. Elledge (2007). "ATM and ATR substrate analysis reveals extensive protein networks responsive to DNA damage." Science **316**(5828): 1160-6.

Maxwell, P. H., C. W. Pugh and P. J. Ratcliffe (2001). "Activation of the HIF pathway in cancer." Curr Opin Genet Dev **11**(3): 293-9.

McAllister, S. S., M. Becker-Hapak, G. Pintucci, M. Pagano and S. F. Dowdy (2003). "Novel p27(kip1) C-terminal scatter domain mediates Rac-dependent cell migration independent of cell cycle arrest functions." Mol Cell Biol **23**(1): 216-28.

Mills, E. J., B. Rachlis, C. O'Regan, L. Thabane and D. Perri (2009). "Metastatic renal cell cancer treatments: an indirect comparison meta-analysis." BMC Cancer **9**: 34.

Molina, H., D. M. Horn, N. Tang, S. Mathivanan and A. Pandey (2007). "Global proteomic profiling of phosphopeptides using electron transfer dissociation tandem mass spectrometry." Proc Natl Acad Sci U S A **104**(7): 2199-204.

Monks, T. J., R. P. Hanzlik, G. M. Cohen, D. Ross and D. G. Graham (1992). "Quinone chemistry and toxicity." Toxicol Appl Pharmacol **112**(1): 2-16.

Monks, T. J. and S. S. Lau (1992). "Toxicology of quinone-thioethers." Crit Rev Toxicol **22**(5-6): 243-70.

Monks, T. J. and S. S. Lau (1997). "Biological reactivity of polyphenolic-glutathione conjugates." Chem Res Toxicol **10**(12): 1296-313.

Monks, T. J. and S. S. Lau (1998). "The pharmacology and toxicology of polyphenolic-glutathione conjugates." Annu Rev Pharmacol Toxicol **38**: 229-55.

Morgan, D. O. (1995). "Principles of CDK regulation." Nature **374**(6518): 131-4.

Motti, M. L., D. Califano, G. Troncone, C. De Marco, I. Migliaccio, E. Palmieri, L. Pezzullo, L. Palombini, A. Fusco and G. Viglietto (2005). "Complex regulation of the cyclin-dependent kinase inhibitor p27kip1 in thyroid cancer cells by the PI3K/AKT pathway: regulation of p27kip1 expression and localization." Am J Pathol **166**(3): 737-49.

Motti, M. L., C. De Marco, D. Califano, A. Fusco and G. Viglietto (2004). "Akt-dependent T198 phosphorylation of cyclin-dependent kinase inhibitor p27kip1 in breast cancer." Cell Cycle **3**(8): 1074-80.

Nelsen, C. J., D. G. Rickheim, M. M. Tucker, L. K. Hansen and J. H. Albrecht (2003). "Evidence that cyclin D1 mediates both growth and proliferation downstream of TOR in hepatocytes." J Biol Chem **278**(6): 3656-63.

Nowak, G. (2002). "Protein kinase C-alpha and ERK1/2 mediate mitochondrial dysfunction, decreases in active Na+ transport, and cisplatin-induced apoptosis in renal cells." J Biol Chem **277**(45): 43377-88.

Okada, R. D., M. A. Platt and J. Fleishman (1982). "Chronic renal failure in patients with tuberous sclerosis. Association with renal cysts." Nephron **30**(1): 85-8.

Okada, S., M. Matsuda, M. Anafi, T. Pawson and J. E. Pessin (1998). "Insulin regulates the dynamic balance between Ras and Rap1 signaling by coordinating the assembly states of the Grb2-SOS and CrkII-C3G complexes." EMBO J **17**(9): 2554-65.

Onda, H., A. Lueck, P. W. Marks, H. B. Warren and D. J. Kwiatkowski (1999). "Tsc2(+/-) mice develop tumors in multiple sites that express gelsolin and are influenced by genetic background." J Clin Invest **104**(6): 687-95.

Onishi, T., Y. Oishi, H. Goto, S. Yanada and K. Abe (2002). "Gender as a prognostic factor in patients with renal cell carcinoma." BJU Int **90**(1): 32-6.

Osborne, J. P., A. Fryer and D. Webb (1991). "Epidemiology of tuberous sclerosis." Ann N Y Acad Sci **615**: 125-7.

Page, K., J. Li and M. B. Hershenson (1999). "Platelet-derived growth factor stimulation of mitogen-activated protein kinases and cyclin D1 promoter activity in cultured airway smooth-muscle cells. Role of Ras." Am J Respir Cell Mol Biol **20**(6): 1294-302.

Pantuck, A. J., D. B. Seligson, T. Klatte, H. Yu, J. T. Leppert, L. Moore, T. O'Toole, J. Gibbons, A. S. Belldegrun and R. A. Figlin (2007). "Prognostic relevance of the mTOR pathway in renal cell carcinoma: implications for molecular patient selection for targeted therapy." Cancer **109**(11): 2257-67.

Papin, C., A. Eychene, A. Brunet, G. Pages, J. Pouyssegur, G. Calothy and J. V. Barnier (1995). "B-Raf protein isoforms interact with and phosphorylate Mek-1 on serine residues 218 and 222." Oncogene **10**(8): 1647-51.

Paris, M., W. H. Wang, M. H. Shin, D. S. Franklin and O. M. Andrisani (2006). "Homeodomain transcription factor Phox2a, via cyclic AMP-mediated activation, induces p27Kip1 transcription, coordinating neural progenitor cell cycle exit and differentiation." Mol Cell Biol **26**(23): 8826-39.

Park, B. G., C. I. Yoo, H. T. Kim, C. H. Kwon and Y. K. Kim (2005). "Role of mitogen-activated protein kinases in hydrogen peroxide-induced cell death in osteoblastic cells." Toxicology **215**(1-2): 115-25.

Patel, S. K., N. Ma, T. J. Monks and S. S. Lau (2003). "Changes in gene expression during chemical-induced nephrocarcinogenicity in the Eker rat." Mol Carcinog **38**(3): 141-54.

Pause, A., S. Lee, K. M. Lonergan and R. D. Klausner (1998). "The von Hippel-Lindau tumor suppressor gene is required for cell cycle exit upon serum withdrawal." Proc Natl Acad Sci U S A **95**(3): 993-8.

Pavlovic, D., N. A. Andersen, T. Mandrup-Poulsen and D. L. Eizirik (2000). "Activation of extracellular signal-regulated kinase (ERK)1/2 contributes to cytokine-induced apoptosis in purified rat pancreatic beta-cells." Eur Cytokine Netw **11**(2): 267-74.

Peters, M. M., T. W. Jones, T. J. Monks and S. S. Lau (1997). "Cytotoxicity and cell-proliferation induced by the nephrocarcinogen hydroquinone and its nephrotoxic metabolite 2,3,5-(tris-glutathion-S-yl)hydroquinone." Carcinogenesis **18**(12): 2393-401.

Peyssonnaux, C. and A. Eychene (2001). "The Raf/MEK/ERK pathway: new concepts of activation." Biol Cell **93**(1-2): 53-62.

Pritchard, C. A., L. Bolin, R. Slattery, R. Murray and M. McMahon (1996). "Post-natal lethality and neurological and gastrointestinal defects in mice with targeted disruption of the A-Raf protein kinase gene." Curr Biol **6**(5): 614-7.

Pryor, W. A. (1997). "Cigarette smoke radicals and the role of free radicals in chemical carcinogenicity." Environ Health Perspect **105 Suppl 4**: 875-82.

Qi, W., L. S. Cooke, A. Stejskal, C. Riley, K. D. Croce, J. W. Saldanha, D. Bearss and D. Mahadevan (2009). "MP470, a novel receptor tyrosine kinase inhibitor, in combination with Erlotinib inhibits the HER family/PI3K/Akt pathway and tumor growth in prostate cancer." BMC Cancer **9**: 142.

Rebuzzi, L., M. Willmann, K. Sonneck, K. V. Gleixner, S. Florian, R. Kondo, M. Mayerhofer, A. Vales, A. Gruze, W. F. Pickl, J. G. Thalhammer and P. Valent (2007). "Detection of vascular endothelial growth factor (VEGF) and VEGF receptors Flt-1 and KDR in canine mastocytoma cells." Vet Immunol Immunopathol **115**(3-4): 320-33.

Recio, L., S. C. Lane, J. Ginsler and C. Walker (1991). "Analysis of ras DNA sequences in rat renal cell carcinoma." Mol Carcinog **4**(5): 350-3.

Rennebeck, G., E. V. Kleymenova, R. Anderson, R. S. Yeung, K. Artzt and C. L. Walker (1998). "Loss of function of the tuberous sclerosis 2 tumor suppressor gene results in embryonic lethality characterized by disrupted neuroepithelial growth and development." Proc Natl Acad Sci U S A **95**(26): 15629-34.

Reuther, G. W. and C. J. Der (2000). "The Ras branch of small GTPases: Ras family members don't fall far from the tree." Curr Opin Cell Biol **12**(2): 157-65.

Ridley, A. J. (2006). "Rho GTPases and actin dynamics in membrane protrusions and vesicle trafficking." Trends Cell Biol **16**(10): 522-9.

Rivard, N., G. L'Allemain, J. Bartek and J. Pouyssegur (1996). "Abrogation of p27Kip1 by cDNA antisense suppresses quiescence (G0 state) in fibroblasts." J Biol Chem **271**(31): 18337-41.

Rodier, G., A. Montagnoli, L. Di Marcotullio, P. Coulombe, G. F. Draetta, M. Pagano and S. Meloche (2001). "p27 cytoplasmic localization is regulated by phosphorylation on Ser10 and is not a prerequisite for its proteolysis." EMBO J **20**(23): 6672-82.

Rojo, F., L. Najera, J. Lirola, J. Jimenez, M. Guzman, M. D. Sabadell, J. Baselga and S. Ramon y Cajal (2007). "4E-binding protein 1, a cell signaling hallmark in breast cancer that correlates with pathologic grade and prognosis." Clin Cancer Res **13**(1): 81-9.

Rosner, M., A. Freilinger, M. Hanneder, N. Fujita, G. Lubec, T. Tsuruo and M. Hengstschlager (2007). "p27Kip1 localization depends on the tumor suppressor protein tuberin." Hum Mol Genet **16**(13): 1541-56.

Rosner, M., M. Hanneder, N. Siegel, A. Valli, C. Fuchs and M. Hengstschlager (2008). "The mTOR pathway and its role in human genetic diseases." Mutat Res **659**(3): 284-92.

Rosner, M., M. Hanneder, N. Siegel, A. Valli, C. Fuchs and M. Hengstschlager (2008). "Skp2 inversely correlates with p27 and tuberin in transformed cells." Amino Acids.

Rosner, M. and M. Hengstschlager (2004). "Tuberin binds p27 and negatively regulates its interaction with the SCF component Skp2." J Biol Chem **279**(47): 48707-15.

Roux, P. P., B. A. Ballif, R. Anjum, S. P. Gygi and J. Blenis (2004). "Tumor-promoting phorbol esters and activated Ras inactivate the tuberous sclerosis tumor suppressor complex via p90 ribosomal S6 kinase." Proc Natl Acad Sci U S A **101**(37): 13489-94.

Rushworth, L. K., A. D. Hindley, E. O'Neill and W. Kolch (2006). "Regulation and role of Raf-1/B-Raf heterodimerization." Mol Cell Biol **26**(6): 2262-72.

Sampson, J. R., S. J. Scahill, J. B. Stephenson, L. Mann and J. M. Connor (1989). "Genetic aspects of tuberous sclerosis in the west of Scotland." J Med Genet **26**(1): 28-31.

Schmitt, J. M. and P. J. Stork (2001). "Cyclic AMP-mediated inhibition of cell growth requires the small G protein Rap1." Mol Cell Biol **21**(11): 3671-83.

Schoffski, P., H. Dumez, P. Clement, A. Hoeben, H. Prenen, P. Wolter, S. Joniau, T. Roskams and H. Van Poppel (2006). "Emerging role of tyrosine kinase inhibitors in the treatment of advanced renal cell cancer: a review." Ann Oncol **17**(8): 1185-96.

Sekimoto, T., M. Fukumoto and Y. Yoneda (2004). "14-3-3 suppresses the nuclear localization of threonine 157-phosphorylated p27(Kip1)." EMBO J **23**(9): 1934-42.

Seldin, D. S., Giebisch, G. (1985). The Kidney Physiology and Pathophysiology. New York, Raven Press.

Shaw, R. J. and L. C. Cantley (2006). "Ras, PI(3)K and mTOR signalling controls tumour cell growth." Nature **441**(7092): 424-30.

Sheaff, R. J., M. Groudine, M. Gordon, J. M. Roberts and B. E. Clurman (1997). "Cyclin E-CDK2 is a regulator of p27Kip1." Genes Dev **11**(11): 1464-78.

Sherr, C. J. and J. M. Roberts (1999). "CDK inhibitors: positive and negative regulators of G1-phase progression." Genes Dev **13**(12): 1501-12.

Shiao, Y. H., B. A. Diwan, A. O. Perantoni, R. J. Calvert, B. Zbar, M. I. Lerman and J. M. Rice (1997). "Polymerase chain reaction-single-strand conformation polymorphism analysis for the VHL gene in chemically induced kidney tumors of rats using intron-derived primers." Mol Carcinog **19**(4): 230-5.

Shibata, M. A., M. Hirose, H. Tanaka, E. Asakawa, T. Shirai and N. Ito (1991). "Induction of renal cell tumors in rats and mice, and enhancement of hepatocellular tumor development in mice after long-term hydroquinone treatment." Jpn J Cancer Res **82**(11): 1211-9.

Shin, I., J. Rotty, F. Y. Wu and C. L. Arteaga (2005). "Phosphorylation of p27Kip1 at Thr-157 interferes with its association with importin alpha during G1 and prevents nuclear re-entry." J Biol Chem **280**(7): 6055-63.

Shin, I., F. M. Yakes, F. Rojo, N. Y. Shin, A. V. Bakin, J. Baselga and C. L. Arteaga (2002). "PKB/Akt mediates cell-cycle progression by phosphorylation of p27(Kip1) at threonine 157 and modulation of its cellular localization." Nat Med **8**(10): 1145-52.

Shin, M. H., N. Mavila, W. H. Wang, S. Vega Alvarez, M. C. Hall and O. M. Andrisani (2009). "Time-dependent activation of Phox2a by the cyclic AMP pathway modulates onset and duration of p27Kip1 transcription." Mol Cell Biol **29**(18): 4878-90.

Short, J. D., K. D. Houston, R. Dere, S. L. Cai, J. Kim, C. L. Johnson, R. R. Broaddus, J. Shen, S. Miyamoto, F. Tamanoi, D. Kwiatkowski, G. B. Mills and C. L. Walker (2008). "AMP-activated protein kinase signaling results in cytoplasmic sequestration of p27." Cancer Res **68**(16): 6496-506.

Shuin, T., K. Kondo, S. Torigoe, T. Kishida, Y. Kubota, M. Hosaka, Y. Nagashima, H. Kitamura, F. Latif, B. Zbar and et al. (1994). "Frequent somatic mutations and

loss of heterozygosity of the von Hippel-Lindau tumor suppressor gene in primary human renal cell carcinomas." Cancer Res **54**(11): 2852-5.

Sicinski, P., S. Zacharek and C. Kim (2007). "Duality of p27Kip1 function in tumorigenesis." Genes Dev **21**(14): 1703-6.

Siemeister, G., K. Weindel, K. Mohrs, B. Barleon, G. Martiny-Baron and D. Marme (1996). "Reversion of deregulated expression of vascular endothelial growth factor in human renal carcinoma cells by von Hippel-Lindau tumor suppressor protein." Cancer Res **56**(10): 2299-301.

Singh, S. P., J. Lipman, H. Goldman, F. H. Ellis, Jr., L. Aizenman, M. G. Cangi, S. Signoretti, D. S. Chiaur, M. Pagano and M. Loda (1998). "Loss or altered subcellular localization of p27 in Barrett's associated adenocarcinoma." Cancer Res **58**(8): 1730-5.

Soos, T. J., H. Kiyokawa, J. S. Yan, M. S. Rubin, A. Giordano, A. DeBlasio, S. Bottega, B. Wong, J. Mendelsohn and A. Koff (1996). "Formation of p27-CDK complexes during the human mitotic cell cycle." Cell Growth Differ **7**(2): 135-46.

Soucek, T., O. Pusch, R. Wienecke, J. E. DeClue and M. Hengstschlager (1997). "Role of the tuberous sclerosis gene-2 product in cell cycle control. Loss of the tuberous sclerosis gene-2 induces quiescent cells to enter S phase." J Biol Chem **272**(46): 29301-8.

Soucek, T., R. S. Yeung and M. Hengstschlager (1998). "Inactivation of the cyclin-dependent kinase inhibitor p27 upon loss of the tuberous sclerosis complex gene-2." Proc Natl Acad Sci U S A **95**(26): 15653-8.

Stephens, R. M., G. Sithanandam, T. D. Copeland, D. R. Kaplan, U. R. Rapp and D. K. Morrison (1992). "95-kilodalton B-Raf serine/threonine kinase: identification of the protein and its major autophosphorylation site." Mol Cell Biol **12**(9): 3733-42.

Stillwell, T. J., M. R. Gomez and P. P. Kelalis (1987). "Renal lesions in tuberous sclerosis." J Urol **138**(3): 477-81.

Storm, S. M., J. L. Cleveland and U. R. Rapp (1990). "Expression of raf family proto-oncogenes in normal mouse tissues." Oncogene **5**(3): 345-51.

Sturgill, T. W., L. B. Ray, E. Erikson and J. L. Maller (1988). "Insulin-stimulated MAP-2 kinase phosphorylates and activates ribosomal protein S6 kinase II." Nature **334**(6184): 715-8.

Subrahmanyam, V. V., P. Doane-Setzer, K. L. Steinmetz, D. Ross and M. T. Smith (1990). "Phenol-induced stimulation of hydroquinone bioactivation in mouse bone marrow in vivo: possible implications in benzene myelotoxicity." Toxicology **62**(1): 107-16.

Sutterluty, H., E. Chatelain, A. Marti, C. Wirbelauer, M. Senften, U. Muller and W. Krek (1999). "p45SKP2 promotes p27Kip1 degradation and induces S phase in quiescent cells." Nat Cell Biol **1**(4): 207-14.

Talarmin, H., C. Rescan, S. Cariou, D. Glaise, G. Zanninelli, M. Bilodeau, P. Loyer, C. Guguen-Guillouzo and G. Baffet (1999). "The mitogen-activated protein kinase kinase/extracellular signal-regulated kinase cascade activation is a key signalling pathway involved in the regulation of G(1) phase progression in proliferating hepatocytes." Mol Cell Biol **19**(9): 6003-11.

Tashiro, E., A. Tsuchiya and M. Imoto (2007). "Functions of cyclin D1 as an oncogene and regulation of cyclin D1 expression." Cancer Sci **98**(5): 629-35.

Tee, A. R., B. D. Manning, P. P. Roux, L. C. Cantley and J. Blenis (2003). "Tuberous sclerosis complex gene products, Tuberin and Hamartin, control mTOR signaling by acting as a GTPase-activating protein complex toward Rheb." Curr Biol **13**(15): 1259-68.

Tsutsui, T., N. Hayashi, H. Maizumi, J. Huff and J. C. Barrett (1997). "Benzene-, catechol-, hydroquinone- and phenol-induced cell transformation, gene mutations, chromosome aberrations, aneuploidy, sister chromatid exchanges and unscheduled DNA synthesis in Syrian hamster embryo cells." Mutat Res **373**(1): 113-23.

Uhlik, M. T., A. N. Abell, B. D. Cuevas, K. Nakamura and G. L. Johnson (2004). "Wiring diagrams of MAPK regulation by MEKK1, 2, and 3." Biochem Cell Biol **82**(6): 658-63.

Urakami, S., R. Tokuzen, H. Tsuda, M. Igawa and O. Hino (1997). "Somatic mutation of the tuberous sclerosis (Tsc2) tumor suppressor gene in chemically induced rat renal carcinoma cell." J Urol **158**(1): 275-8.

van Leuken, R., L. Clijsters and R. Wolthuis (2008). "To cell cycle, swing the APC/C." Biochim Biophys Acta **1786**(1): 49-59.

van Spronsen, D. J., P. F. Mulders and P. H. De Mulder (2005). "Novel treatments for metastatic renal cell carcinoma." Crit Rev Oncol Hematol **55**(3): 177-91.

van Triest, M. and J. L. Bos (2004). "Pull-down assays for guanoside 5'-triphosphate-bound Ras-like guanosine 5'-triphosphatases." Methods Mol Biol **250**: 97-102.

Vervoorts, J. and B. Luscher (2008). "Post-translational regulation of the tumor suppressor p27(KIP1)." Cell Mol Life Sci **65**(20): 3255-64.

Viglietto, G., M. L. Motti, P. Bruni, R. M. Melillo, A. D'Alessio, D. Califano, F. Vinci, G. Chiappetta, P. Tsichlis, A. Bellacosa, A. Fusco and M. Santoro (2002). "Cytoplasmic relocalization and inhibition of the cyclin-dependent kinase

inhibitor p27(Kip1) by PKB/Akt-mediated phosphorylation in breast cancer." Nat Med **8**(10): 1136-44.

Villanueva, J., Y. Yung, J. L. Walker and R. K. Assoian (2007). "ERK activity and G1 phase progression: identifying dispensable versus essential activities and primary versus secondary targets." Mol Biol Cell **18**(4): 1457-63.

Vlach, J., S. Hennecke and B. Amati (1997). "Phosphorylation-dependent degradation of the cyclin-dependent kinase inhibitor p27." EMBO J **16**(17): 5334-44.

Vossler, M. R., H. Yao, R. D. York, M. G. Pan, C. S. Rim and P. J. Stork (1997). "cAMP activates MAP kinase and Elk-1 through a B-Raf- and Rap1-dependent pathway." Cell **89**(1): 73-82.

Wagner, J. R. and W. M. Linehan (1996). "Molecular genetics of renal cell carcinoma." Semin Urol Oncol **14**(4): 244-9.

Walker, C. (1998). "Molecular genetics of renal carcinogenesis." Toxicol Pathol **26**(1): 113-20.

Walker, C., Y. T. Ahn, J. Everitt and X. Yuan (1996). "Renal cell carcinoma development in the rat independent of alterations at the VHL gene locus." Mol Carcinog **15**(2): 154-61.

Walker, C., J. Everitt, J. J. Freed, A. G. Knudson, Jr. and L. O. Whiteley (1991). "Altered expression of transforming growth factor-alpha in hereditary rat renal cell carcinoma." Cancer Res **51**(11): 2973-8.

Walker, C., T. L. Goldsworthy, D. C. Wolf and J. Everitt (1992). "Predisposition to renal cell carcinoma due to alteration of a cancer susceptibility gene." Science **255**(5052): 1693-5.

Walles, S. A. (1992). "Mechanisms of DNA damage induced in rat hepatocytes by quinones." Cancer Lett **63**(1): 47-52.

Wan, P. T., M. J. Garnett, S. M. Roe, S. Lee, D. Niculescu-Duvaz, V. M. Good, C. M. Jones, C. J. Marshall, C. J. Springer, D. Barford and R. Marais (2004). "Mechanism of activation of the RAF-ERK signaling pathway by oncogenic mutations of B-RAF." Cell **116**(6): 855-67.

Wang, X., J. L. Martindale and N. J. Holbrook (2000). "Requirement for ERK activation in cisplatin-induced apoptosis." J Biol Chem **275**(50): 39435-43.

Watanabe, G., A. Howe, R. J. Lee, C. Albanese, I. W. Shu, A. N. Karnezis, L. Zon, J. Kyriakis, K. Rundell and R. G. Pestell (1996). "Induction of cyclin D1 by simian virus 40 small tumor antigen." Proc Natl Acad Sci U S A **93**(23): 12861-6.

Weber, J. D., D. M. Raben, P. J. Phillips and J. J. Baldassare (1997). "Sustained activation of extracellular-signal-regulated kinase 1 (ERK1) is required for the continued expression of cyclin D1 in G1 phase." Biochem J **326 (Pt 1)**: 61-8.

Wellbrock, C., M. Karasarides and R. Marais (2004). "The RAF proteins take centre stage." Nat Rev Mol Cell Biol **5**(11): 875-85.

Westerhof, W. and T. J. Kooyers (2005). "Hydroquinone and its analogues in dermatology - a potential health risk." J Cosmet Dermatol **4**(2): 55-9.

Whysner, J., L. Verna, J. C. English and G. M. Williams (1995). "Analysis of studies related to tumorigenicity induced by hydroquinone." Regul Toxicol Pharmacol **21**(1): 158-76.

Wienecke, R., A. Konig and J. E. DeClue (1995). "Identification of tuberin, the tuberous sclerosis-2 product. Tuberin possesses specific Rap1GAP activity." J Biol Chem **270**(27): 16409-14.

Wienecke, R., J. C. Maize, Jr., F. Shoarinejad, W. C. Vass, J. Reed, J. S. Bonifacino, J. H. Resau, J. de Gunzburg, R. S. Yeung and J. E. DeClue (1996). "Co-localization of the TSC2 product tuberin with its target Rap1 in the Golgi apparatus." Oncogene **13**(5): 913-23.

Wilhelm, S. M., C. Carter, L. Tang, D. Wilkie, A. McNabola, H. Rong, C. Chen, X. Zhang, P. Vincent, M. McHugh, Y. Cao, J. Shujath, S. Gawlak, D. Eveleigh, B. Rowley, L. Liu, L. Adnane, M. Lynch, D. Auclair, I. Taylor, R. Gedrich, A. Voznesensky, B. Riedl, L. E. Post, G. Bollag and P. A. Trail (2004). "BAY 43-9006 exhibits broad spectrum oral antitumor activity and targets the RAF/MEK/ERK pathway and receptor tyrosine kinases involved in tumor progression and angiogenesis." Cancer Res **64**(19): 7099-109.

Wu, Z., L. J. Wu, S. Tashiro, S. Onodera and T. Ikejima (2005). "Phosphorylated extracellular signal-regulated kinase up-regulated p53 expression in shikonin-induced HeLa cell apoptosis." Chin Med J (Engl) **118**(8): 671-7.

Yeung, R. S. (2003). "Multiple roles of the tuberous sclerosis complex genes." Genes Chromosomes Cancer **38**(4): 368-75.

Yeung, R. S., K. H. Buetow, J. R. Testa and A. G. Knudson, Jr. (1993). "Susceptibility to renal carcinoma in the Eker rat involves a tumor suppressor gene on chromosome 10." Proc Natl Acad Sci U S A **90**(17): 8038-42.

Yeung, R. S., G. H. Xiao, J. I. Everitt, F. Jin and C. L. Walker (1995). "Allelic loss at the tuberous sclerosis 2 locus in spontaneous tumors in the Eker rat." Mol Carcinog **14**(1): 28-36.

Yeung, R. S., G. H. Xiao, F. Jin, W. C. Lee, J. R. Testa and A. G. Knudson (1994). "Predisposition to renal carcinoma in the Eker rat is determined by germ-line

mutation of the tuberous sclerosis 2 (TSC2) gene." Proc Natl Acad Sci U S A **91**(24): 11413-6.

Yoon, H. S., T. J. Monks, J. I. Everitt, C. L. Walker and S. S. Lau (2002). "Cell proliferation is insufficient, but loss of tuberin is necessary, for chemically induced nephrocarcinogenicity." Am J Physiol Renal Physiol **283**(2): F262-70.

Yoon, H. S., T. J. Monks, C. L. Walker and S. S. Lau (2001). "Transformation of kidney epithelial cells by a quinol thioether via inactivation of the tuberous sclerosis-2 tumor suppressor gene." Mol Carcinog **31**(1): 37-45.

Yoon, H. S., S. Ramachandiran, M. A. Chacko, T. J. Monks and S. S. Lau (2004). "Tuberous sclerosis-2 tumor suppressor modulates ERK and B-Raf activity in transformed renal epithelial cells." Am J Physiol Renal Physiol **286**(2): F417-24.

Yoon, S. and R. Seger (2006). "The extracellular signal-regulated kinase: multiple substrates regulate diverse cellular functions." Growth Factors **24**(1): 21-44.

Yu, M. C., T. M. Mack, R. Hanisch, C. Cicioni and B. E. Henderson (1986). "Cigarette smoking, obesity, diuretic use, and coffee consumption as risk factors for renal cell carcinoma." J Natl Cancer Inst **77**(2): 351-6.

Zhao, Y., C. Bjorbaek and D. E. Moller (1996). "Regulation and interaction of pp90(rsk) isoforms with mitogen-activated protein kinases." J Biol Chem **271**(47): 29773-9.